DEVELOPMENT OF A GLUTATHIONE S-TRANSFERASE-BASED BIOSENSOR FOR THE DETECTION OF HEAVY METALS

A THESIS SUBMITTED TO
THE GRADUATE SCHOOL OF NATURAL AND APPLIED SCIENCES
OF
THE MIDDLE EAST TECHNICAL UNIVERSITY

BY

EBRU SAATÇİ

IN PARTIAL FULFILLMENT OF THE REQUIREMENTS
FOR
THE DEGREE OF DOCTOR OF PHILOSOPHY
IN
BIOCHEMISTRY

AUGUST, 2005

Approval of the Graduate School of Natural and Applied Sciences.

_____

Prof. Dr. Canan Özgen

Director

I certify that this thesis satisfies all the requirements as a thesis for the degree of Doctor of Philosophy.

_____

Prof. Dr. Orhan Adalı

Head of the Department

This is to certify that we have read this thesis and that in our opinion it is fully adequate, in scope and quality, as a thesis for the degree of Doctor of Philosophy.

_____

Prof. Dr. Mesude İşcan

Supervisor

Examining Committee Members:

Prof. Dr. Nazmi ÖZER (HU, BCH) _____

Prof. Dr. Mesude İŞCAN (METU, BIO) _____

Prof. Dr. Vasıf HASIRCI (METU, BIO) _____

Prof. Dr. Tayfun AKIN ((METU, EE) _____

Prof. Dr. Tülin GÜRAY (METU, BIO) _____

I hereby declare that all information in this document has been obtained and presented in accordance with academic rules and ethical conduct. I also declare that, as required by these rules and conduct, I have fully cited and referenced all material and results that are not original to this work.

Name, Last name: **EBRU SAATÇİ**

Signature:

ABSTRACT

DEVELOPMENT OF A GLUTATHIONE S-TRANSFERASE-BASED BIOSENSOR FOR THE DETECTION OF HEAVY METALS

SAATÇİ, Ebru

PhD., Department of Biochemistry

Supervisor: Prof. Dr. Mesude İŞCAN

August 2005, 164 pages

In the recent years, environmental pollution becomes a health threatening issue for human beings. Technological developments introduce industrial wastes and heavy metals, and developments in agriculture introduce pesticides into the world that we live. All these toxic wastes accumulate in drinking water and food consumed by humans. Therefore, detection of toxic wastes in all kinds of environmental samples, and development of new detection techniques become an important issue.

In this study, a glutathione S-transferase (GST-$(His)_6$) -based biosensor for detection of heavy metals in environmental samples was developed. Recombinant GST-$(His)_6$ was expressed in *E.Coli* BL21 (DE3) expression system and purified with Glutathione Sepharose 4B affinity column and Ni-NTA spin kit. The protein expression was tested by SDS-PAGE and Western blot analysis. GST activities were determined using the GST substrate 1-chloro-2,4-dinitrobenzene (CDNB). Product formation increased up linearly to 1 mM CDNB, 1.5 mM GSH, 1.7 µg proteins in 0.05 M, pH 6.9 phosphate buffer in the final volume of 1.0 ml at 25°C.

The Vmax and Km values for GST-$(His)_6$ towards CDNB and GSH were calculated with Lineweaver-Burk as CDNB Vmax; 5.34 µmol/min/mg, Km; 0.23 mM, and as GSH Vmax; 6.63 µmol/min/mg, Km; 0.27 mM, respectively.

The biosensor working electrode was prepared by immobilizing the GST-$(His)_6$ by 1-(3-dimethylaminopropyl)-3-ethyl-carbodiimide hydrochloride (EDC) coupling on the gold surface. The electrode preparation was confirmed by cyclic voltammetry measurements. The biosensor was inserted as the working electrode in the constructed four-electrode flow cell. The conformational change was determined resulting from the binding of the metal ions to the recombinant protein causing a capacitance change proportional to the concentration of the metal ions. The working electrode is standardized and calibrated by using the standard heavy metal solutions (Cu^{2+}, Zn^{2+}, Cd^{2+}, Hg^{2+}).

The buffer system of the biosensor is optimized as 0.1 M Tris-tricine buffer at pH 8.6. The GST-$(His)_6$ biosensor has a large operational range between 1 fM and 10 mM and a storage stability of approximately 2 weeks. The sensitivity range of the biosensor is 100 nM-1 fM for Cu^{2+}; 10 µM-1 fM for Zn^{2+}; 10 µM-1 fM for Cd^{2+}; 10 mM-1 fM for Hg^{2+}.

Key words: GST-$(His)_6$, Biosensor, Heavy metals, Cyclic voltammetry, Capacitance measurements.

ÖZ

AĞIR METAL TAYİNİ İÇİN GLUTATYON S-TRANSFERASE TEMELLİ BİYOSENSÖR GELİŞTİRİLMESİ

SAATÇİ, Ebru

Doktora, Biyokimya Bölümü

Tez Danışmanı: Prof. Dr. Mesude İŞCAN

Ağustos 2005, 164 sayfa

Çevre kirliliği insan sağlığını etkileyen en önemli faktörlerden birisidir. Özellikle son yıllarda, teknolojinin gelişmiyle birlikte endüstriyel atıklar, pestisitler ve ağır metaller yaşadığımız hayata dahil olmuşlardır. Bütün bu toksik atıklar, içtiğimiz sularda, aldığımız besinlerde birikmektedir ve insan sağlığını ciddi ölçülerde tehdit etmektedir. Bu yüzden, bu toksik maddelerin her türlü çevresel örneklerde yol açtığı kirliliği hassas olarak ölçmek günümüzde oldukça önem kazanmakta ve yöntemler geliştirilmektedir.

Bu çalışmada, *E.coli* BL21(DE3) ekspresyon sistemi içinde, glutatyon-S-transferaz rekombinant proteini elde edilerek, çok düşük konsantrasyonlardaki ağır metallerin tayininde kullanılmak üzere, protein kaynaklı bir biyosensör yapımı tamamlanmıştır. Rekombinant GST proteini *E.coli* BL21(DE3) ekspresyon sistemi içinde eksprese edilerek, Glutatyon Sepharose 4B afinite kolonu ve Ni-NTA spin kit kullanılarak saflaştırılmıştır. Proteinin ekspresyonu SDS-PAGE ve Western blot analizleri ile tesbit edildi. Rekombinant GST'nin aktivitesi ve kinetik

özellikleri, substratı 1-kloro-2,4-dinitrobenzen (CDNB) kullanılarak belirlenmiştir. Ürün oluşumu, 0.05 M ve pH'sı 6.9 fosfat tamponunda izlendi. Ortamdaki CDNB, GSH ve protein miktarı sırasıyla, 1 mM, 1.5 mM ve 1.7 µg'a kadar, 25^{o}C'de doğrusal olarak arttı. GST enzimi'nin, substratı olan CDNB ve kofaktörü GSH için Km ve Vmax değerleri Lineweaver-Burke grafiğiyle hesaplandı. CDNB için Vmax; 5.34 µmol/dk/mg, Km; 0.23 mM, olarak hesaplandı. GSH için Vmax; 6.63 µmol/dk/mg, Km; 0.27 mM olarak hesaplandı.

Biyosensör, rekombinant protein, 1-(3-dimetilaminopropil)-3-etil-karbodiimide (EDC) açilleme reaksiyonu ile altın elektrot üzerine kovalent olarak bağlandı. Elektrodun hazırlanması dönüşümlü voltametri ölçümleri ile takip edildi. Biyosensör çalışma elektrodu, dörtlü elektrot sisteminde ölçümü yapan elektrot olarak kullanıldı. Metal iyonunun rekombinant proteine bağlanmasıyla meydana gelen konformasyonel değişiklik sonucunda ortaya çıkan ve metal iyonlarının konsantrasyonu ile doğru orantılı olan kapasitans değişiklikleri ölçüldü. Çalışma elektrodu, standart ağır metal solüsyonları (Cu^{2+}, Zn^{2+}, Cd^{2+}, Hg^{2+}) ile satandardize edilerek kalibrasyonu yapıldı.

Biyosensörün çalışma tamponu, pH'sı 8.6 olan 0.1 M Tris-tricine tamponu olarak optimize edildi. GST-$(His)_6$ biyosensörünün ölçüm aralığı, 10 mM ile 1 fM arasında tesbit edildi ve kullanım ömrü yaklaşık iki hafta olarak bulundu. Biyosensörün sensitivitesi Cu^{2+} için, 100 nM-1 fM; Zn^{2+} için 10 µM-1 fM; Cd^{2+} için, 10 µM-1 fM ve Hg^{2+} için 10 mM-1 fM olarak bulundu.

Anahtar kelimeler: GST-$(His)_6$, Biyosensör, Ağır metaller, Dönüşümlü Voltametry, Kapasitans ölçümleri.

TO MY FATHER, MOTHER, AND SISTER……

ACKNOWLEDGEMENTS

I would like to express my gratitude to Prof. Dr. Mesude İşcan for her encouragement, valuable advices and continued guidance throughout this study.

I wish to express my thanks to Prof. Dr. Nazmi Özer, Prof. Dr. Vasıf Hasırcı, Prof. Dr. Tayfun Akın, Prof. Dr. Tülin Güray, Prof. Dr. Levent Toppare for their valuable suggestions and corrections.

I also wish to thank to Prof. Dr. Leyla Açık for her great help and advice in the recombinant protein expression studies.

I am grateful to Dr. Elisabeth Csoregi and the biosensor group, Mihaela Nistor and Szilzvester Gaspar in Kemicentrum, Analytical Chemistry Department, Lund University, Sweden for their support and contributions to this work by helping me in capacitance measurements.

I am also extremely grateful to Prof. Dr. Canan Özgen and Prof. Dr. Fatoş Yarman Vural for their support in this work in the framework of the Faculty Development Program.

I wish to specially thank my friends' Senem Yaşasın Geylan Su, Metin Konuş, Pembegül Uyar and Gökhan Sadi for their friendship, encouragement and support.

Finally, I would like to express my sincere gratitude to my father, my mother, my sister and my fiancée for their great support, patience and encouragement during the long period of my study.

TABLE OF CONTENTS

PLAGIARISM……..…….....iii
ABSTRACT…….....iv
ÖZ……..….....vi
ACKNOWLEDGEMENTS…….....ix
TABLE OF CONTENTS……..….....x
LIST OF TABLE…….....xv
LIST OF FIGURES……..…...xvii
LIST OF ABREVIATIONS.……..……xxii
CHAPTERS
1. INTRODUCTION 1
1.1. Biosensors 2
1.2. Electrochemical Biosensors 4
1.2.1. Receptor: Biological Recognition Element..... 7
1.2.1.1. Biocatalytic Recognition Element..... 7
1.2.1.2. Biocomplexing or Bioaffinity Recognition Element 8
1.2.2. Electrochemical Transducers 9
1.2.2.1. Potentiometric 9
1.2.2.2. Amperometric 10
1.2.2.3. Voltammetric..... 10
1.2.2.4. Surface Charge Using Field-Effect Transistors (FETs)..... 10
1.2.2.5. Conductometric..... 10
1.2.3. Electrodes..... 11
1.2.3.1. Redox Electrodes 11
1.2.3.2. Ion-selective Membrane Electrodes..... 12
1.2.4. Immobilization Procedures 13
1.2.4.1. Adsorption..... 13
1.2.4.2. Microencapsulation..... 13
1.2.4.3. Entrapment..... 13
1.2.4.4. Cross-linking..... 14
1.2.4.5. Covalent bonding 14

1.2.5. Performance Factors 15
1.2.5.1. Selectivity and Reliability 15
1.2.5.2. Calibration 16
1.2.5.3. Steady-State and Transient Response Times, Sample Throughput 16
1.2.5.4. Reproducibility, Stability and Lifetime 17
1.3. Heavy Metals 18
1.4. Capacitance Measurement 18
1.4.1. The Electrical Double Layer 20
1.4.2. Measurement Principle 23
1.4.2.1. Step Measurements 24
1.5. Chemically Modified Electrodes (CMEs) 24
1.5.1. Self-assembled Monolayers (SAMs) with Metal Electrodes 25
1.5.2. SAMs of Thiols, Sulfides and Disulfides on Gold 26
1.5.3. Pretreatment of the Gold Surface 26
1.5.3.1. Mechanical Polishing 27
1.5.3.2. Oxygen Plasma Cleaning 28
1.5.4. Stability of SAMs 29
1.5.5. Insulating Properties of SAMs 31
1.5.6. Molecular Recognition at SAMs 33
1.6. Capacitive Biosensors for the Heavy Metals 34
1.6.1. Detection Strategy 34
1.6.2. Proteins as Recognition Element 35
1.6.2.1. SmtA 35
1.6.2.2. Phytochelatins 35
1.6.2.3. MerP 35
1.6.3. Metallopeptides 36
1.6.3.1. Complexes of Metal Ions with Peptides 36
1.6.3.2. Coordination of Cu(II) and Ni(II) to Histidine Peptides 38
1.7. Glutathione S-Transferase Enzyme Family 42
1.7.1. Nomenculature and Classification of Glutathione-S-Transferases 45
1.7.2. Functions and Structure of GSTs 48
1.7.2.1. Catalytic Activities of GSTs 48

1.7.2.2. Structure of the GSTs 50
1.7.3. GSTs Catalyzed Reactions and Substrates 57
1.7.3.1. Glutathione Conjugation and Detoxification 57
1.7.3.2. Model Substrates for the Characterization of GST Isoenzymes ... 59
1.7.4. Chromosomal location and Evolution of GSTs in Mammals 59
1.7.4.1. Chromosomal Location 59
1.8. Protein Engineering 63
1.8.1. Design 63
1.8.2. Engineering of Natural Proteins 64
1.8.2.1. Alteration of Natural Proteins Properties 64
1.8.2.2. Properties of Recombinant Proteins……..……65
1.8.3. Recombinant Protein Expression 67
1.8.4. Recombinant Proteins with 6xHis Tag and Purification on Ni-NTA Resin 68
1.8.5. pET System (Glutathione-S-transferase Gene Fusion System) 69
1.8.5.1. pET 42 a-c Vectors (Novagen) 71
1.9. Scope of the Work…….....……75

2. MATERIALS AND METHODS 77
2.1 Materials 77
2.2 Methods 78
2.2.1. Preparation of Competent Cells 78
2.2.2. Transformation of Competent Cells with pET42a DNA 79
2.2.3. Plasmid Isolation 79
2.2.4. Induction 80
2.2.4.1. For Small Amount of Bacterial Culture 80
2.2.4.2. For Large Amount of Bacterial Culture 81
2.2.5. Sonication 82
2.2.6. Protein Determinations 82
2.2.7. GST Activity Assay with CDNB 83
2.2.8. Thrombin Cleavage Standardization 84
2.3. Glutathione Sepharose 4B Affinity Column Purification 85

2.3.1. Batch Purification of GST-$(His)_6$ Using Bulk Glutathione Sepharose 4B 85
2.3.1.1. Preparation of Glutathione Sepharose 4B 85
2.3.1.2. Batch Binding 85
2.3.1.3. Elution of Recombinant Protein 86
2.3.2. Column Purification of Fusion Proteins Using Glutathione Sepharose 4B 87
2.3.2.1. Column Preparation 87
2.3.2.2. Column Binding 87
2.3.2.3. Column Elution 87
2.4. Ni-NTA Column Purification of GST-$(His)_6$ 88
2.4.1. Recombinant Protein Purification under Native Conditions 88
2.5. SDS-Polyacylamide Gel Electrophoresis 89
2.5.1. Preparation of Reagents 90
2.5.2. Electrophoresis Procedure 91
2.6. Silver staining of SDS-PAGE gel 93
2.7. Electroblotting of the Gels from SDS-PAGE 94
2.7.1. Immunostaining of the PVDF Membranes 97
2.8. Working Electrode Preparation 98
2.8.1. Gold Bar Pre-treatment 98
2.8.2. Thioctic Acid Deposition 98
2.8.3. Protein Coupling 98
2.8.4. Dodecanthiol Treatment 99
2.9. Capacitance Measurements 100
2.10. Cyclic Voltammetry Measurements 101

3. RESULTS 102
3.1. Transformation of Competent Cells with pET42a DNA 102
3.2. Plasmid Isolation 102
3.3. GST-$(His)_6$ Activity 105
3.3.1. Reaction Time Course of GST-$(His)_6$ 105
3.3.2. Effect of Enzyme Amount on GST-$(His)_6$ Activity 105

3.4. Thrombin Cleavage Standardization 107
3.5. GST-$(His)_6$ Purification 111
3.6. Characterization of GST-$(His)_6$ Activity 113
3.6.1. Effect of pH on GST-$(His)_6$ Activity 113
3.6.2. Effect of Substrate (CDNB) Concentration on GST-$(His)_6$ Activity 114
3.6.3. Effect of Cofactor Reduced Glutathione (GSH) Concentration on GST-$(His)_6$ Activity 115
3.6.4. Imidazole Effect on GST-$(His)_6$ Activity 117
3.7. SDS-PAGE and Western Blotting Analysis of the Purified GST-$(His)_6$ Protein 118
3.8. Preparation of Working Electrode 122
3.8.1. Cyclic Voltammograms 122
3.9. Capacitance Measurements 123

4. DISCUSSION 131
5. CONCLUSIONS 137
REFERENCES 139
APPENDIX A: CurriculumVitae 164

LIST OF TABLES

Tables

Table 1.1. Types of Receptors Used in Biosensors and the Electrochemical Measurement Techniques, Linked to Them, Which Recognize Specific Species 6

Table 1.2. Types of Electrochemical Transducers for Classified Type of Measurements, with Corresponding Analytes to be Measured.....7

Table 1.3. Metals with Biological Influence on Living Cells and Their Oxidation Forms.....19

Table 1.4. Classification of Cytosolic GSTs From Rat and Man According to the Old Nomenclature System.....47

Table 1.5. Classification of Cytosolic GSTs from Rat and Man According to the New Nomenclature System.....49

Table 1.6. Examples of GSTs Substrates from Different Compound Categories 58

Table 2.1. The Constituents of the Incubation Mixture for Recombinant GST Enzyme Assay with CDNB as Substrate.....83

Table 2.2. The Constituents of the Incubation Mixture for Cleavage of Recombinant GST from S-protein.....84

Table 2.3. Reagent Volume Requirements for Different Protein Yields…….....86

Table 2.4. Formulations for SDS-PAGE Separating and Stacking gels.....92

Table 2.5. Procedure for Rapid Silver Staining of Proteins in Polyacrylamide Gels.....96

Table 3.1. Column Purification Table of GST-$(His)_6$ from Transformed Bacterial Cell Culture.....112

Table 4.1. Comparison Table of Four Different Protein Electrodes for the Detection of Heavy Metal Ions.....136

LIST OF FIGURES

Figures

Figure 1.1. Schematic setup of a (bio)chemical sensor…….….3

Figure 1.2. Schematic diagram of possible biosensor analyte recognition cascade ……..…….....……..4

Figure 1.3. Mechanism of activation of carboxylic groups by EDC and further reaction with amines resulting in the amide bond……..15

Figure 1.4. Schematic representation of (a) double layer region, (b) potential profile across the double layer and (c) the differential capacitances in series…...21

Figure 1.5. Schematic drawing of the experiment set-up……..22

Figure 1.6. Schematic representation of the protein-immobilized capacitive biosensor…….23

Figure 1.7. Potential step technique principle: (a) applied potential pulse and (b) resulting current response……..….24

Figure 1.8. Bar electrodes (3 mm diameter) under optical microscopy after polishing with (a) 0.1 μm alumina suspension, and with (b) 0.05 μm alumina suspensions……..…...27

Figure 1.9. SEM images (1000 times magnification) of gold bars polished with alumina suspension (a) 0.1 μm and (b) 0.05 μm ……..28

Figure 1.10. Schematic of self-assembled monolayers of alkanethiols on gold electrodes: (a) a pure monolayer and (b) a mixed monolayer……30

Figure 1.11. Molecular structure of thioctic acid……..31

Figure 1.12. Cyclic voltammograms recorded in 5 mM $K_3[Fe(CN)_6]$ 32

Figure 1.13. Example of “two-step” immobilization of biomolecules on SAMs.....33

Figure 1.14. Protein-based capacitive biosensor scheme for measuring conformational change upon binding of heavy metal ions……34

Figure 1.15. Binding of metal ion with a single Gly.....37

Figure 1.16. Complex formation of metal ion with diglycine.....37

Figure 1.17. Coordination of metal ion with triglycine peptide.....38

Figure 1.18. Chelating abilities of histidine……..39

Figure 1.19. The proposed structure of the dimer His–His……...39

Figure 1.20. Structures of major complex species for Cu(II) complexes of histidine peptides……41

Figure 1.21. Mechanism for cellular protection by glutathione……....43

Figure 1.22. Glutathione metabolism……43

Figure 1.23. Mammalian GST structures.....51

Figure 1.24. The thioredoxin fold.....53

Figure 1.25. Domain structure of GST subunits.....55

Figure 1.26. Model substrates used for characterization of GSTs……60

Figure 1.27. The 3D structure of Schistosomal GST……...70

Figure 1.28. pET-42a vector map…….72

Figure 1.29. pET-42a(+) cloning/expression regions……...73

Figure 1.30. FASTA format of recombinant glutathione S-transferase-$(His)_6$....74

Figure 2.1. Home-made polishing equipment……..99

Figure 2.2. Constructed four-electrode flow cell……...…….100

Figure 3.1. Transformed colonies on a LB agar plate containing kanamycin sulfate……...……103

Figure 3.2. Agarose gel electrophoresis of isolated E. coli DNA from transformed competent cells…….104

Figure 3.3. GST-$(His)_6$ reaction time course plot.....106

Figure 3.4. Effect of enzyme amount on GST-$(His)_6$ activity…….106

Figure 3.5. SDS-PAGE stained with silver (12%), of the cleaved fractions (4µg/µl) at 4 hours and high range molecular weight markers....……108

Figure 3.6. SDS-PAGE stained with silver (12%), of the cleaved fractions (4µg/µl) at 8 hours and high range molecular weight markers ……...……109

Figure 3.7. SDS-PAGE stained with silver (12%), of the cleaved fractions (4µg/µl) at 16 hours and high range molecular weight markers.....…….110

Figure 3.8. Effect of pH on GST-$(His)_6$ activity…….……...113

Figure 3.9. Effect of CDNB concentration on GST-$(His)_6$ activity at pH 6.9 ……...……...114

Figure 3.10. Lineweaver-Burk plot of GST-$(His)_6$ activity against substrate (CDNB).....115

Figure 3.11. Effect of GSH concentration on GST-$(His)_6$ activity at pH 6.9…116

Figure 3.12. Lineweaver-Burk plot of GST-$(His)_6$ activity against cofactor (GSH) at pH 6.9……...116

Figure 3.13. The inhibition effect of imidazole concentration on GST-$(His)_6$ activity at pH 6.9……..117

Figure 3.14. SDS-PAGE stained with silver (12%), of the protein fractions (each well containing 5 µg of protein) obtained from the each purification step and low range molecular weight markers.....…….119

Figure 3.15. Western blotting of monoclonal Anti-GST antibody immunostained purification step fractions (each well containing 5 µg of protein) (PVDF membrane immunostained with monoclonal anti-GST) and biotinylated low range molecular weight marker.....…….120

Figure 3.16. Western blotting of monoclonal RGS-His antibody immunostained Ni-NTA elution fractions (each well containing 5 µg of protein)……121

Figure 3.17. Cyclic voltammograms…….....122

Figure 3.18. Capacitance changes of the GST-$(His)_6$ electrode to 1 nM Cd^{+2} and 1 nM Hg^{+2} at different buffer compositions and pH values……124

Figure 3.19. Regeneration graphic for the GST-$(His)_6$ electrode under O.1 M Borate buffer pH 8.75, 0.25 ml/min, injection of 250 µl Cd^{+2} standard solution ……..124

Figure 3.20. Regeneration graphic for the GST-$(His)_6$ electrode under O.1 M Tris-tricine buffer pH 8.6, 0.25 ml/min, injection of 250 µl 100 Cd^{+2} standard solution.....125

Figure 3.21. Calibration curve under 0.1 M Tris-tricine buffer pH 8.3, 0.25 ml/min, injection of 250 µL Cd^{+2} standard solutions.....126

Figure 3.22. Capacitance changes of GST-$(His)_6$ electrode at pH 8.1-8.9 under 0.1 M Tris-tricine buffer, 0.25 ml/min, injection of 250 µl 100 µM Cd^{+2} standard solutions.....126

Figure 3.23. Storage Stability of the GST-$(His)_6$ electrode injection of 100 µM Cd^{2+} after regeneration with 20 mM EDTA, O.1 M Tris-tricine buffer pH 8.6, 0.25 ml/min.....127

Figure 3.24. Calibration curves for Cd^{+2} recorded with two different biosensors prepared at different times under the same conditions reproducibility.....128

Figure 3.25. Calibration curves obtained for Cd^{+2}, Zn^{+2}, Cu^{+2} and Hg^{+2}, with the GST-$(His)_6$ electrode under 0.1 M Tris-tricine buffer, pH 8.6, 0.25 mL/min flowrate, injection of 250 µL standard solutions.....129

Figure 3.26. Calibration curves obtained for Cd^{+2}, Zn^{+2}, Cu^{+2} and Hg^{+2}, with the GST-(His)6 electrode at low concentrations of heavy metals under 0.1 M Tris-tricine buffer, pH 8.6, 0.25 mL/min flowrate, injection of 250 µL standard solutions.....129

Figure 3.27. Control experiment graphics. Measurements were done by Porcine Pancreatic Elastase (PPE): MW 25900 Da (Serva) and GST-$(His)_6$: MW 26500 Da under 0.1 M Tris-tricine buffer, pH 8.6, 0.25 mL/min flowrate, injection of 250 µL to Cd^{+2} and Zn^{+2} standard solutions.....130

LIST OF ABREVATIONS

AP	Alkaline phosphatase
APS	Ammonium persulfate
AS	Ammonium sulfate
BCIP	5-Bromo-4-chloro-3-indolyl phosphate
Bis	N,N′-methylene bisacrylamide
BSA	Bovine serum albumin
CDNB	1-Chloro-2,4-dinitrobenzene
CME	Chemically modified electrodes
CLECs	Cross-linked Enzyme Crystals
DCM	Dichloromethane or Methylene chloride
DCNB	1,2-Dichloro-4-nitrobenzene
EDC	1-(3-dimethylaminopropyl)-3-ethyl-carbodiimide hydrochloride
EDTA	Ethylenediaminetetraacetic acid
EIS	Electrolyte insulator semiconductor
ENFET	Enzyme field effect transistor
EO	Ethylene oxide
EPNP	1,2-Epoxy-3-(*p*-nitrophenoxy)propane
FET	Field effect transistor
FIA	Flow injection analysis
GSH	Reduced Glutathione
GSSG	Oxidized Glutathione
GST	Glutathione-S-transferase
IAA	Iminoacetic acid
IMAC	Immobilized metal-ion affinity chromatography
IMFET	Immunological field effect transistor
ISFET	Ion-sensitive field effect transistor
IPTG	Isopropyl β-D- thiogalactoside
LB	Luria Broth
4-NBC	4-Nitrobenzyl chloride

NBT	Nitro blue tetrazolium
NTA	Nitrilotriacetic acid
PBS	Phosphate buffer saline
PTFE	Polytetrafluoroethylene
PVDF	Polyvinylidene difluoride
SDS	Sodium dodecyl sulfate
SPR	Surface Plasmon Resonance
TBS	Tris-buffered saline
TE	Tris-EDTA
TEMED	N,N,N′,N′-tetramethylenediamine
Tris	Tris(hydroxymethyl) aminomethane
TTBS	Tris-buffered saline containing Tween-20

CHAPTER I

INTRODUCTION

Identification of biomolecules in complex mixtures represents one of the most difficult challenges of biological and medical researchs (Kress-Rogers, 1997, Kubo *et al*., 1991). Powerful methods for detecting biomolecules in these mixtures include the use of biosensors, chemical separations, mass spectrometry, bioassays, and immunoassays. Advances in molecular biology and combinatorial chemical synthesis have allowed researchers to generate new molecular targets, important markers for disease processes, and pharmaceutical products and drugs rapidly increase. Such progress demands new detection methodologies with enhanced throughput power, speed, sensitivity, and selectivity. Moreover, ultralow volume reactors for chemical synthesis (e.g. microreaction beads in 96-well plates) and ultrasmall biological samples (e.g. rare stem cells) demand analytical methods that have superior sample handling capabilities and can perform analyses with minimal sample manipulation (Kennedy *et al*., 1989).

Most analytical methods require one or more preliminary steps to eliminate the effects of interference (Skoog *et al*., 1991). The synergistic combination of selective detectors with a prior separation step offers such opportunities. For example, the combination of separations (e.g. HPLC, LC, GC, CE) with mass

spectrometry (Cai and Henion, 1995), NMR (Wu *et al*., 1994), and other types of molecular spectroscopy and electrochemical methods have made possible the identification of corresponding effluents based on physical properties of the molecule (e.g. mass, charge, and chemical structure). The separation identifies compounds by retention times, and spectroscopic or electrochemical features provide a second dimension to distinguish individual peaks. Many biomolecules can still evade these sensitive detection methods, and consequently, new detectors that can identify biomolecules by other mechanisms are needed. Coupling chemical separations with biosensor detection provides a new way to analyze analytes based on molecular recognition rather than on physical properties alone. Molecular recognition involves forming a complex between two molecules that is both specific and relatively permanent on the timescale of detection. Biomolecular interactions such as enzyme–substrate, antigen–antibody, and cell–cell interactions are central to biological phenomena in living organisms. The advantage of a separation/biosensor system is that individual components within a complex mixture are first purified and then detected by selective interactions (Fishman *et al*., 1998)

1.1. Biosensors

Chemical sensing is a process by which selected information about chemical composition is obtained in real time. The species is detected pass through a filter and hit the chemically sensitive layer. The interaction between the analyte molecules and this layer causes a change in the physico-chemical properties of the layer (e.g. changed mass, optical properties, etc). These changed properties are converted by the transducer to an electronic signal, which can be analyzed (Figure 1.1) (Zeigler and Göpel, 1998).

Biosensors are chemical sensors in which the recognition system utilizes a biochemical mechanism. They have an interface between biological layer (biocomponent) and the transducer, and where the biological layer surface is touched by an analyte solution (Figure 1.2) (Vadgama *et al*., 1992). For this

reason, stability, selectivity and sensitivity can be obtained in the recognition of biological components (Ziegler and Göpel, 1998).

Application areas where biosensors are set to make a significant impact reach well beyond the established needs of medicine and veterinary science and additional areas include environmental monitoring and control, food processing, agriculture, pharmaceuticals, and even defense and the petrochemical industry (Vadgama *et al*., 1992). They are adopted for practical applications such as the measurement of blood glucose (Cass *et al*., 1984), penicillin (Kulp *et al*., 1987), urea (Walcerz *et al*., 1995), lactate (Montagne *et al*., 1995), pesticides and carbamates (Campanella *et al*., 1999) and heavy metals (Bontidean *et al*., 1998, Bontidean *et al*., 2000).

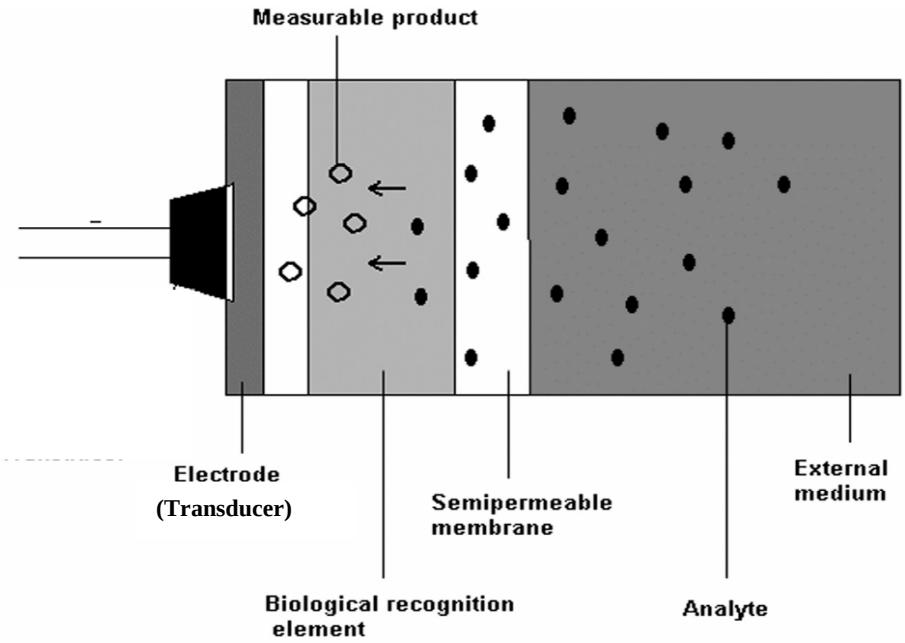

Figure 1.1. Schematic setup of a (bio)chemical sensor (Zeigler and Göpel, 1998).

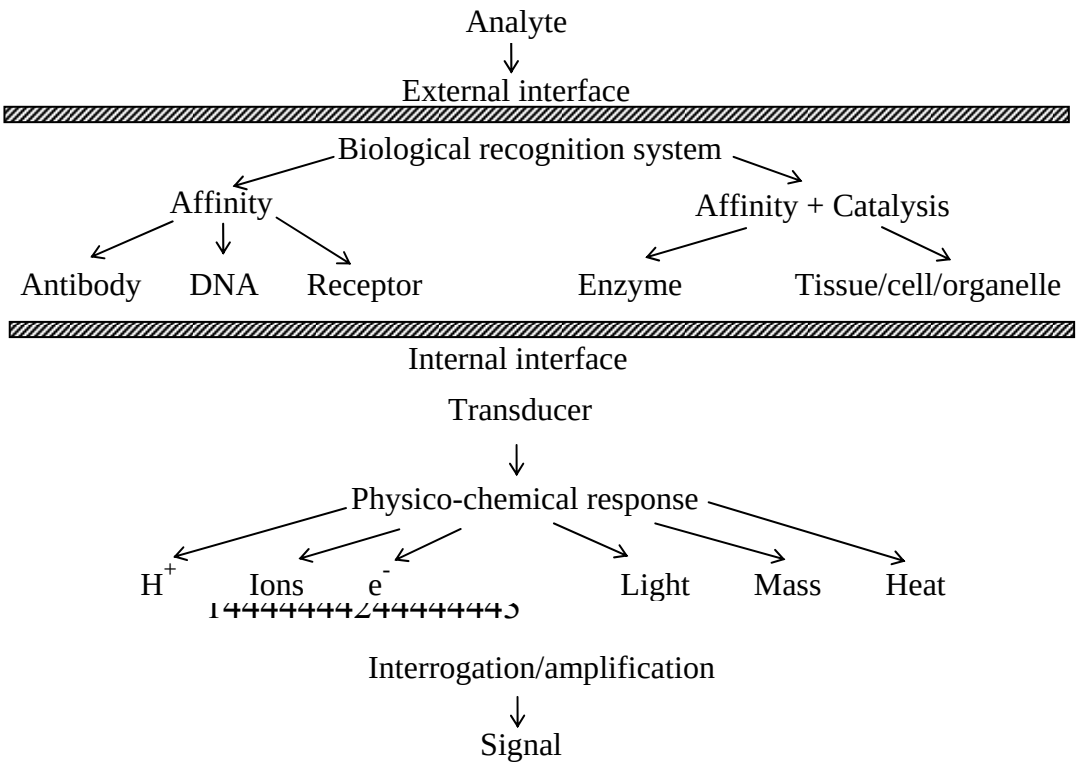

Figure 1.2. Schematic diagram of possible biosensor analyte recognition cascade (Vadgama *et al*., 1992).

1.2. Electrochemical Biosensors

An electrochemical biosensor is a self-contained integrated device, which is capable of providing specific quantitative or semi-quantitative analytical information using a biological recognition element which is retained in direct spatial contact with an electrochemical transduction element. Because of their ability to be repeatedly calibrated, it is recommended that a biosensor should be clearly distinguished from a bioanalytical system, which requires additional processing steps, such as reagent addition. (Thevenot *et al*., 2001)

The biological recognition system translates information from the biochemical domain, usually an analyte concentration, into a signal with a defined sensitivity. The main purpose of the recognition system is to provide the sensor with a high degree of selectivity for the analyte to be measured. While all biosensors are more or less sensitive (non-specific) for a particular analyte, some are, by design and construction, only class-specific, since they use class enzymes, *e.g.*, phenolic compound biosensors, or whole cells, *e.g.*, used to measure biological oxygen demand. Because in sensing systems, such as olfaction, and taste, as well as neurotransmission pathways, the actual recognition is performed by cell receptor, the word receptor or bioreceptor is also often used for the recognition system of a chemical biosensor. Examples of single multiple signal transfer are listed in Table 1.1 (Thevenot *et al*., 2001).

The transducer part of the sensor serves to transfer the signal from the output domain of the recognition system to, mostly, the electrical domain. A transducer provides bidirectional signal transfer (non-electrical to electrical and vice versa); the transducer part of a sensor is also called a detector, sensor or electrode. Examples of electrochemical transducers, often used for the listed types of measurement in Table 1.1, are given in Table 1.2, together with examples of analytes which have been measured. Transducers are classified by recognition element type (Table 1.1) or by electrochemical transducer mode (Table 1.2) (Thevenot *et al*., 2001).

Biosensors may be classified according to the biological specificity conferring mechanism, or to the mode of signal transduction or, alternatively, a combination of two (Roe, 1992).

Table 1.1. Types of Receptors Used in Biosensors and the Electrochemical Measurement Techniques, Linked to Them, Which Recognize Specific Species (Thevenot *et al*., 2001).

Analytes	**Receptor/Chemical Recognition System**	**Measurement Technique/ Transduction Mode**
1. ions	mixed valence metal oxides; perm selective, ion-conductive inorganic crystals; trapped mobile synthetic or biological ionophores; ion exchange glasses enzyme(s)	potentiometric, voltammetric, conductometric
2. dissolved gases, vapors, odors	bilayer lipid or hydrophobic membrane; inert metal electrode; enzyme(s) antibody, receptor	In series with 1; amperometric; amperometric or potentiometric amperometric, potentiometric or impedance, piezoelectric, optical;
3. substrates	enzyme(s) whole cells membrane receptors plant or animal tissue	amperometric or potentiometric; in series with 1. or 2. or metal or carbon electrode, conductometric piezoelectric, optical, calorimetric; as above as above as above
4. antibody/ antigen	antigen/antibody oligonucleotide duplex, aptamer enzyme labelled chemiluminescent or fluorescent labeled	amperometric, potentiometric or impedimetric,piezoelectric,optical, surface plasmon resonance; in series with 3.; optical
5. various proteins and low molecular weight substrates, ions	specific ligands: protein receptors and channels; enzyme labelled fluorescent labelled	as 4.

Table 1.2. Types of Electrochemical Transducers for Classified Type of Measurements, with Corresponding Analytes to be Measured (Thevenot *et al*., 2001).

Measurement Type	Transducer	Transducer Analyte
1. Potentiometric	ion-selective electrode (ISE), glass electrode, gas electrode, metal electrode	K^+, Cl^-, Ca^{2+}, F^- H^+, Na^+... CO_2, NH_3 redox species
2. Amperometric	metal or carbon electrode, chemically modified electrodes (CME)	O_2, sugars, alcohols... sugars, alcohols, phenols, oligonucleotides...
3. Conductometric, Impedimetric	interdigitated electrodes, metal electrode	urea, metal ions, oligonucleotides...
4. Ion charge or Field Effect	ion-sensitive field effect transistor (ISFET), enzyme FET (ENFET)	H^+, K^+...

1.2.1. Receptor: Biological Recognition Element

1.2.1.1. Biocatalytic Recognition Element

The biosensor is based on a reaction catalyzed by macromolecules, which are present in their biological environment, have been isolated previously or have been manufactured. Thus, a continuous consumption of substrate(s) is achieved by the immobilized biocatalyst incorporated into the sensor, transient or steady-state responses are monitored by the integrated detector. Three types of biocatalysts are commonly used:

a. Enzyme (mono- or multi-enzyme), the most common and well developed recognition system,
b. Whole cells (micro-organisms, such as bacteria, fungi, eukaryotic cells or yeast) or cell organelles or particles (mitochondria, cell walls),
c. Tissue (plant or animal tissue slice).

The first biocatalytic-based biosensor is an enzyme sensor which is first described by Clark and Lyons (1962) for the determination of glucose. The biocatalytic-based biosensors are the best known and studied and have been the most applied to biological matrices. One or more analytes, substrates S and S', react in the presence of enzyme(s) and yield one or several products, P and P', according to the general reaction scheme (Thevenot *et al*., 2001):

$$S + S' \xrightarrow{\text{Biocatalyst}} P + P'$$

Then, the adjacent transducers are used for monitoring the analyte consumption or the product formation by this biocatalysed reaction.

1.2.1.2. Biocomplexing or Bioaffinity Recognition Element

The biosensor operation is based on interaction of the analyte with macromolecules or organized molecular assemblies that have either been isolated from their original biological environment or engineered (Roe, 1992).

Bioaffinity biosensors are highly versatile. In recent years, DNA biosensors (Vo-Dinh *et al*., 1998, Guiducci *et al*., 2002) are developed in this group which relies on the immobilization of a single-stranded DNA sequence (the ‘probe’) and its hybridization with the complementary (‘target’) strand to give a suitable electrical or optical signal.

Antigen-antibody (Ab-Ag) and enzyme-enzyme inhibitor sensors are used in the field of medical diagnostics. Several studies have been described involving direct monitoring of the Ab-Ag complex formation on ISFETS (Thevenot *et al*., 2001). Mass-sensitive detection by a quartz crystal microbalance is also used in these applications (Vadgama *et al*., 1992).

Surface plasmon resonance (SPR) based bioaffinity sensors are being used to define the kinetics of wide molecular interactions (Myszka, 1997, Nelson *et al*., 1999, Zybin *et al*., 2005).

For selective and sensitive detection of heavy metals (Cu^{2+}, Cd^{2+}, Hg^{2+}, Zn^{2+} and Ni^{2+}, etc.), bioaffinity sensors are designed. These are based on bioengineered proteins such as glutathione-S-transferase-SmtA and MerR (Bontidean *et al*., 1998, Corbieser *et al*., 1999) and the inhibition effect of heavy metal ions on the activity of oxidase enzymes such as alcohol oxidase, glycerol 3-P oxidase, sarcosine oxidase, used for the construction of calibration curves in flow-injection analysis (FIA) (Compagnone *et al*., 2001). The multienzyme electrochemical sensors, based on capacitance pH-sensitive electrolyte-insulator-semiconductor (EIS) with silicon nitride ion-sensitive layers, have been also developed (Kukla *et al*., 1999).

1.2.2. Electrochemical Transducers

1.2.2.1. Potentiometric

Potentiometry is the measurement of electrical potetial difference between two electrodes in an electrochemical cell. In the potentiometric type sensor, a membrane (glass, solid state, liquid) selectively extracts a charged species into the membrane phase, generating a potential difference between the internal filling solution and the sample solution. This potential is proportional to the analyte concentration following the Nerst equation (Geiger, 1997):

$e = e_o + (RT/zF) \ln a$

e : single potential
e_o : standard potential
R : gas constant
T : absolute temperature
z : charge
F : Faraday constant
a : analyte concentration

The transducer may be an ISE which is an electrochemical sensor based on thin films or selective membranes as recognition elements (Thevenot *et al*., 2001). Thick and thin film technology is used for disposable heavy metal sensor production in field analysis (Palchetti *et al*., 2001).

1.2.2.2. Amperometric

Amperometry is based on the measurement of the current resulting from the electrochemical oxidation or reduction of an electroactive species. It is usually performed by maintaining a constant potential at a Pt, Au or C based working electrode or on array of electrodes with respect to a reference electrode, which may also serve as the auxillary electrode, if currents are low (10^{-9} to 10^{-6} A). The resulting current is directly correlated to the bulk concentration of the electroactive species or its production or consumption rate within the adjacent biocatalytic layer. Such steady-state currents are usually proportional to the bulk analyte concentration (Niculescu *et al*., 2000, Niculescu *et al*., 2002).

1.2.2.3. Voltammetric

Voltammetric transducers are used to solution composition based on the current-potential relationships obtained when the potential of an electrochemical cell is varied under a control of a three-electrode potentiostat. In a three electrode system, the polarizable working electrode potential is measured potentiometrically between the working and reference electrodes, and the cell current is measured between the working and counter electrodes (Eggins, 1996).

1.2.2.4. Surface Charge Using Field-Effect Transistors (FETs)

An ion-sensitive field effect transistor (ISFET) is composed of an ion-selective membrane applied directly to the insulated gate of the FET. When such ISFETs are coupled with a biocatalytic or biocomplexing layer, they become biosensors, and are usually called either enzyme (ENFETs) or immunological (IMFETs) field-effect transistors (Thevenot *et al*., 2001).

1.2.2.5. Conductometric

Conductometry is the measurement of the current flow between two non-polarized electrodes and between which a known electrical potential is established (Eggins, 1996). In order to avoid polarization of the electrodes, an alternating potential is applied.

Conductivity is the inverse of resistance. Ohm's law gives the relationship

$E = I.R$ E = the e.m.f. of the cell
I = the current
R = the resistance (impedance)

and conductance, L: $L = 1/R$

so

$E = I/L$

Conductivity is fairly simple to measure. It is directly proportional to the concentration of ions in the solution. It varies according to the charge on the ion, the mobility of the ion and the degree of dissociation of the ion (Eggins, 1996).

The measurement of the conductance involves an alternating current, in the classical conductance bridge. This can be extended by varying the frequency of the alternating current. The quantity measured is then the admittance (=1/impedance), which not only depends on simple conductance but also on the capacitance and inductance of the system. These components can be separated as imaginary components, particularly using a frequency response analyzer (Eggins, 1996).

1.2.3. Electrodes

1.2.3.1. Redox Electrodes

Redox potentials are the result of chemical equilibrium involving electron transfer reactions (Eggins, 1996):

(1) Oxidized form (Ox) + ze^- ↔ Reduced form (Red)

(2) $Red_1 + Ox_2 \leftrightarrow Ox_1 + Red_2$

Inert metal electrodes:

Platinum and *gold* are used to record the redox potential of a redox couple dissolved in an electrolyte solution;

Hydrogen electrode is often used for pH measurements.

Metal electrodes:

Silver electrode consists of a silver wire immersed in a solution containing silver ions.

(3) $Ag^{+} + e^{-} \rightleftharpoons Ag$

Silver/silver chloride electrode consists of a silver wire that has been electrolytically coated with silver chloride. The electrode dips into a solution containing Cl^{-}.

(4) $AgCl\ (solid) + e^{-} \rightleftharpoons Ag\ (metal) + Cl^{-}$

Calomel electrode consists of mercury covered by a layer of calomel (Hg_2Cl_2), which is in contact with an electrolyte solution containing Cl^{-}.

(5) $1/2\ Hg_2Cl_2\ (solid) + e^{-} \rightleftharpoons Hg\ (metal) + Cl^{-}$

Carbon-based electrodes:

Carbon-based materials such as graphite, carbon black and carbon fiber are used to construct electrodes (Zhang *et al.*, 2000).

1.2.3.2. Ion-selective Membrane Electrodes

Membrane potentials are caused by the permeability of certain types of membranes to selected anions or cations.

Solution 1	Ion selective membrane	Solution 2	The potentials of solution 1 and 2 are recorded with any suitable reference electrode.

Glass, solid-state, gas, Liquid ion-exchange and enzyme electrodes are available in ion-sensitive membrane electrodes (Eggins, 1996).

1.2.4. Immobilization Procedures

Biological receptors, with high biological activity, can be immobilized on a thin layer at the transducer surface by using different procedures.

1.2.4.1. Adsorption

Adsorption is the simplest method. However, the bonding is weak and this method is satisfactory for short-term investigations.

Many substances adsorb biocomponents on their surfaces, e.g. alumina, charcoal, clay, cellulose, kaolin, silica gel, glass and collagen. Absorbed biocomponent is very susceptible to changes in pH, temperature, ionic strength and the substrate.

Physical adsorption occurs via the formation of van der Waals bonds, hydrogen bonds or charge transfer forces. Chemical adsorption is much stronger and involves the formation of covalent bonds (Eggins, 1996).

1.2.4.2. Microencapsulation

In this method, an inert membrane is used to trap the biomaterial on the transducer. There is a close attachment between the biocomponent and the transducer. It is very adaptable and limits contamination and degradation. This procedure performes good stability to changes in temperature, pH, ionic strength and substrate concentration.

The main types of membranes used are the followings: cellulose acetate, polycarbonate (Nucleopore), collagen, polytetrafluoroethylene (PTFE, Teflon), nafion and polyurethane (Eggins, 1996).

1.2.4.3. Entrapment

A polymeric gel (i.e. polyacrylamide, starch, nylon, silastic gels, conducting polymers such as polypyrrole) is prepared in a solution containing the biocomponent thus trapped within the gel matrix.

This method has some disadvantages. It inhibits the diffusion of the substrate; slows the reaction and the response time of the sensor. There is loss of enzyme activity through the pores in the gel (Thevenot *et al*., 2001).

1.2.4.4. Cross-linking

Bifunctional agents are used to bind the biomaterial to solid supports. Although it is a useful method to stabilize adsorbed biocomponents, it causes damage to the biocomponents and limits diffusion of the substrate. Also there is poor rigidity (Geiger, 1997).

1.2.4.5. Covalent Bonding

Some functional groups which are not essential for the catalytic activity of a biocomponent (enzyme) can be covalently bonded to the support matrix (transducer or membrane). This method uses nucleophilic groups for coupling such as -NH_3, -COOH, -OH, -SH and imidazole (Telefoncu, 1999). Figure 1.3 shows a covalent bonding reaction in which a carboxyl group on the support is reacted with a carbodiimide. This then couples with N-terminal amine group on the biocomponent to form an amide bond between the support and the enzyme. Reactions need to be under mild conditions -low temperature, low ionic strength and pH in physiological range (Eggins, 1996).

The advantage is that the enzyme will not be released during use. In order to protect the active side of the enzyme, the reaction is often carried out in the presence of the substrate (Telefoncu, 1999).

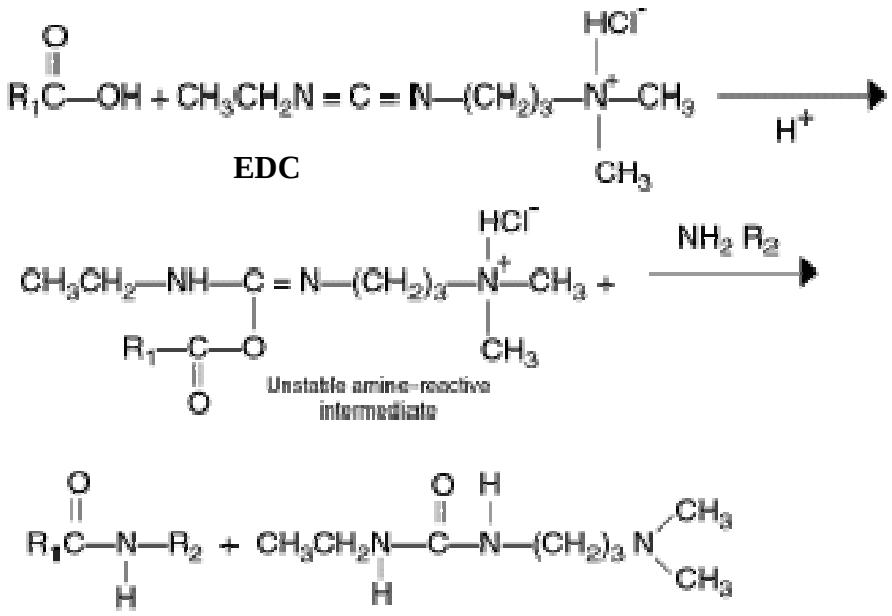

Figure 1.3. Mechanism of activation of carboxylic groups by EDC and further reaction with amines resulting in the amide bond (Eggins, 1996).

1.2.5. Performance Factors

Anyone developing a new sensor of any sort needs to have some idea of what performance requirements are needed for the particular application in mind (Eggins, 1996).

The rapid proliferation of biosensors and their diversity has led to a lack of strictness in defining performance criteria. Although each sensor can only be evaluated for a particular application, it is useful to establish standard protocols for evaluation of performance criteria, in accordance with standard IUPAC protocols or definitions. These protocols are recommended for general use and include four sets of parameters (Thevenot, 2001).

1.2.5.1. Selectivity and Reliability

This factor is established by the nature of biological material. There are effectively three distinct types: enzymes, antibodies and nucleic acids. Many enzymes are specific. Nevertheless, class (non-selective) enzymes have been used

for the development of class biosensors, used in environmental monitoring. Bacteria, yeast or tissue cultures are naturally non-specific. Whereas oxygen electrodes, pH electrodes and ISFETs show appropriate selectivity, metal electrodes are often sensitive to numerous interfering substances. This direct selectivity can be modified when these transducers are associated with receptors (Thevenot, 2001).

The reliability of biosensors for given samples depends both on their selectivity and their reproducibility. It has to be determined under actual operating conditions, i.e., in the presence of possible interfering substances (Thevenot, 2001).

1.2.5.2. Calibration

Sensor calibration is performed by adding standard solutions of the analyte and by plotting steady-state responses, possibly corrected for a blank (background) signal, versus the analyte concentration. Transient responses are important for sequential samples but are less significant for continuous monitoring: within several possibilities, they are generally defined as the maximum rates of variation of the sensor response, after addition of analyte into the measurement cell (Thevenot, 2001).

1.2.5.3. Steady-State and Transient Response Times, Sample Throughput

Steady-state response time is the time necessary to reach 90% of the steady-state response. Transient response time corresponds to the time necessary for the first derivative of the output signal to reach its maximum value following the analyte addition. Both response times depend upon the analyte, co-substrate and product transport rates through different layers or membranes. Therefore, the thickness and permeability of these layers are essential parameters. They also depend upon the activity of the recognition system. The higher this activity, the shorter is this response time.

When biosensors are used for sequential measurements, either in batch or flow through setups, the sample throughput is a measure of the number of individual samples per unit of time. This parameter takes into account the steady-state or transient response times but also includes the recovery time, i.e., the time needed for the signal to return to its base-line (Thevenot, 2001).

1.2.5.4. Reproducibility, Stability and Lifetime

Reproducibility is a measure of the scatter or drift in a series of observations or results performed over a period of time. It is generally determined for the analyte concentrations within the usable range.

The operational stability of a biosensor response is depending on the analyte concentration, the continuous or sequential contact of the biosensor with the analyte solution, temperature, pH, buffer composition, presence of organic solvents, and immobilization methods (Thevenot, 2001).

The enzyme concentration is not crucial for the operation of a biosensor, but there are limiting factors. If there is too much enzyme or if the quality of the enzyme preparation is poor, considerable material is needed to provide sufficient units of enzyme activity. The optimum pH is dependent on the electron transfer mediator being used. The excess of material can affect the diffusion of analytes to transducer.

Chemical (covalent) methods result in longer lifetimes, but can limit the response and may damage the enzyme, causing a further diminishing in response. In entrapment or adsorption methods, the rapid loss of biocomponent can affect the response and lifetime.

Working lifetime is determined by the instability of the biocomponent. It can vary from a few days to a few months. There are three aspects of lifetime; the lifetime of the biosensor in use, the lifetime of the biosensor in storage, and the lifetime of the biocomponent stored separately (Eggins, 1996).

1.3. Heavy Metals

Heavy metals and their compounds are potentially the most toxic elements for the environment. They are not biodegradable and therefore are retained indefinitely in the ecological systems and in the food chain (Palchetti *et al*., 2001). Various biological effects have been described at the molecular level they decrease the activity of certain enzymes. The effect of heavy metals seems to involve the -SH groups of proteins. Fixation of heavy metals on these thiol groups may explain their noxious effect (Compagnone *et al*., 2001).

Classical techniques, like Atomic Absorption Spectrometry, Anodic Stripping Voltammetry, and Inductive Coupled Plasma are in wide use. Enzyme assays for the identification and detection of pollutants are largely proposed in the literature (Compagnone *et al*., 2001). These methods require sophisticated instrumentation and skilled personnel, and there is a need for simple methods (Bontidean *et al*., 1998). Electrochemical biosensors represent a good alternative for a rapid and simple “in field” measurement of bioavailable heavy metal ions (e.g. Cd, Zn, Cu, Hg, Ni, Fe, Co, Mo, Pb). Some of their main properties are presented in Table 1.3 (Brown, 1994).

1.4. Capacitance Measurement

Capacitive detection has been successfully applied to preparation of immunosensors, detection of analyte binding with two-dimensional artificial receptors and in biosensors for heavy metal ions (Panasyuk *et al*., 1999).

Table 1.3. Metals with Biological Influence on Living Cells and Their Oxidation Forms (Brown, 1994)

Metal	Toxicity	Available Inorganic Ionic Forms
Cd	Toxic due to thiol binding and protein denaturation	Cd(II) in CdS
Zn	Very important physiological function, very low toxicity	only as Zn(II)
Cu	Toxicity is based on the ability of Cu to easily interact with radicals	Cu(II) and Cu(I)
Hg	Metal with strongest toxicity, no beneficial function	Hg(II) in HgS
Ni	Medium toxicity	Ni(II) and very unstable Ni(III)
Fe	Biologically most important metal, not toxic	Fe(II) and Fe(III)
Co	Co(II) has medium toxicity, but Co dust causes lung disease	Almost only Co(II), rarely Co(III)
Mo	Molybdate is the most important heavy metal oxyanion	Mo(VI) in molybdate
Pb	Toxic, acts on the nervous system	Pb(II)

1.4.1. The Electrical Double Layer

The capacitive measurements are based on the theory of the electrical double layer. When a potential is applied, double layer of charges takes place at the electrode/solution interface, due to the conducting propriety of an electrode. Helmholtz was the first to call this phenomenon the electrical double layer (Mortari *et al*., 2004).

For a given potential the metal electrode will possess a charge q_m and the solution another charge q_s, where $q_m = -q_s$ (Bontidean *et al*., 2000).

The double layer is represented in Figure 3a, where a metallic electrode having a positive charge at the interface is shown. In solution, three different theoretical layers can be distinguished (Figure 3b): *the inner Helmhotz plane* (*IHP*), *the outer Helmhotz plane* (*OHP*) and *the diffuse layer*. The *IHP* is the closest to the electrode, at distance X_1 and is constituted by molecules of the solvent. The following layer is the *OHP*, where solvated ions can approach the surface at distances X_2. The interaction between charged metal and solvated ions is governed by long-rate electrostatic forces. The next layer is the *diffuse layer*, which extends from the *OHP* to the bulk solution. The thickness of this layer depends on the total ionic concentration of the solution. These layers have different electrostatic potential (Figure 3b), which decreases linearly through the IHP and the OHP and exponentially in the diffuse layer (Mortar *et al*., 2004).

Such structure is equivalent to a parallel-plane capacitor (Figure 3c), where the capacitance (*C*) is calculated with equation 1:

$$C = \varepsilon\varepsilon_0 S/d \qquad (1)$$

where ε_0 is the permeability of free space, ε is the dielectric constant of the medium, *S* is the area and *d* the inner-plate distance (Mortari *et al*., 2004).

Capacitances in series can be identified as the capacitances C_H and C_D, meaning the capacitances due to the compact layer and the diffuse layer, respectively. The final capacitance can be calculated using equation 2:

$$\frac{1}{C} = \frac{1}{C_H} + \frac{1}{C_D} \qquad (2)$$

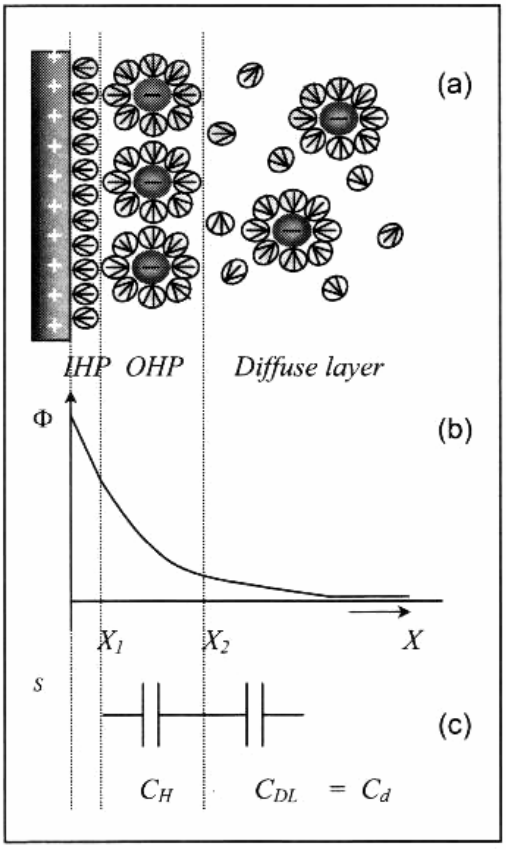

Figure 1.4. Schematic representation of (a) double layer region, (b) potential profile across the double layer and (c) the differential capacitances in series (Mortari *et al*., 2004).

The measuring cell (Figure 1.5) usually consists of three (or four) electrodes: The working electrode is a gold rod mounted in a Teflon holder, the auxiliary electrode, a disk-shaped platinum foil with a hole in the center, and the reference electrode, a platinum wire. The potential of the platinum electrode is

compared to Ag/AgCl reference electrode before the potentiostatic pulse is applied, as the platinum does not have a defined potential (Berggren *et al*., 1997).

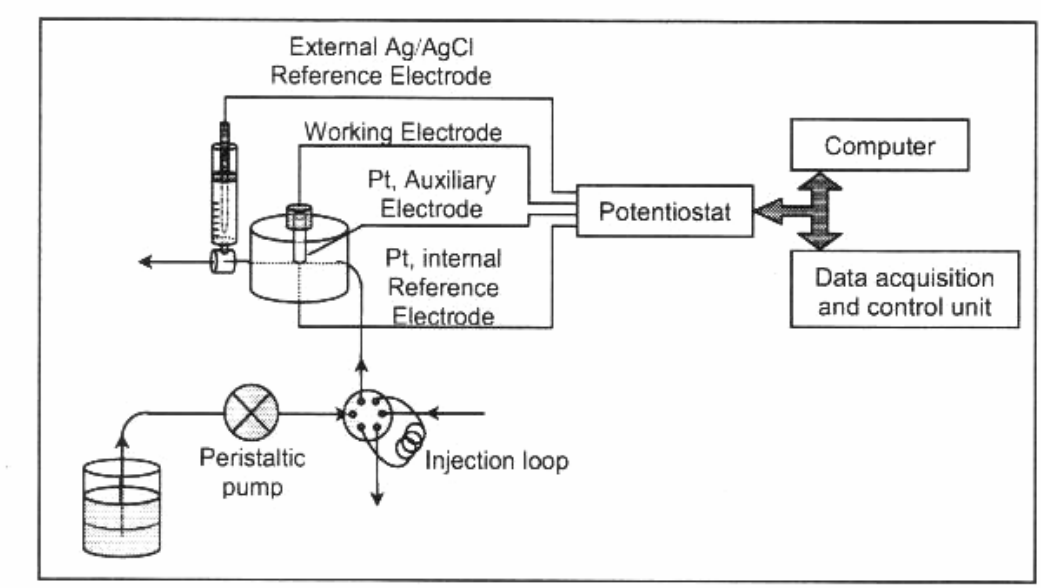

Figure 1.5. Schematic drawing of the experiment set-up (Mortari *et al*., 2004).

The capacitance of the electrode is composed of a series of capacitances of the different layers on the surface which is schematically presented in Figure 1.6. The total capacitance (C_{tot}) has three components (i) the capacitance of the self-assembled layer of thiol, C_{SAM}, (ii) the capacitance of the recognition element, C_P, and (iii) the capacitance of the diffuse layer, C_{DL}, extending out into the bulk of the solution (Bontidean *et al*., 2002).

The total capacitance is described by equation 3:

$$\frac{1}{C_{tot}} = \frac{1}{C_{SAM}} + \frac{1}{C_P} + \frac{1}{C_{DL}} \qquad (3)$$

The lowest capacitance dominates the value of total capacitance, therefore C_{SAM} and C_{DL} should be made as large as possible so that the changes of C_P caused by the binding of analyte, to be detectable (Bontidean *et al*., 2002).

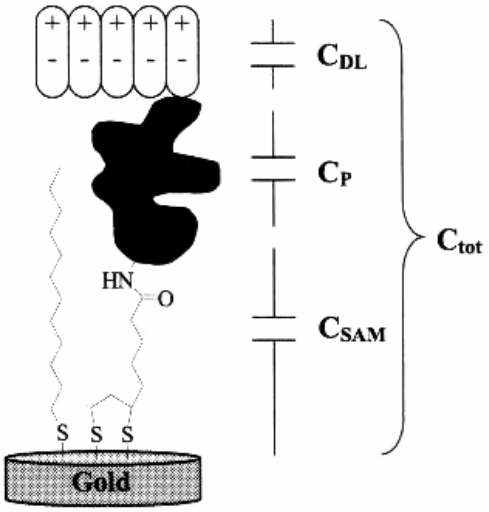

Figure 1.6. Schematic representation of the protein-immobilized capacitive biosensor (Bontidean *et al*., 2002).

1.4.2. Measurement Principle

The capacitance is determined from the current response obtained when a potentiostatic step is applied on the electrode. The resulting current decays as a logarithmic function. Evaluation can be made by assuming that the response follows a simple RC model. With this model, the current transient after a potential step will approximately follow equilibrium:

$$i\,(t) = u / R_s \exp\,(-t / R_s\, C_1)$$

where $i\,(t)$ is the current in the circuit as a function of the time, u is the applied pulse potential, R_s is the dynamic resistance of the self-assembled layer, C_1 is the capacitance measured between the electrode and the solution, and t is the time elapsed after the potentiostatic pulse was applied. The capacitive sensor relies on the measurement of changes in C_1 (Berggren *et al*., 1997).

1.4.2.1. Step Measurements

The other method to evaluate the capacitance is to perturp the system with a potential step. A potentistatic step with amplitude of 50 mV is applied (Figure 1.7a) and the current response (Figure 1.7b) is sampled at a frequency of 50 kHz and saved in a computer for evaluation.

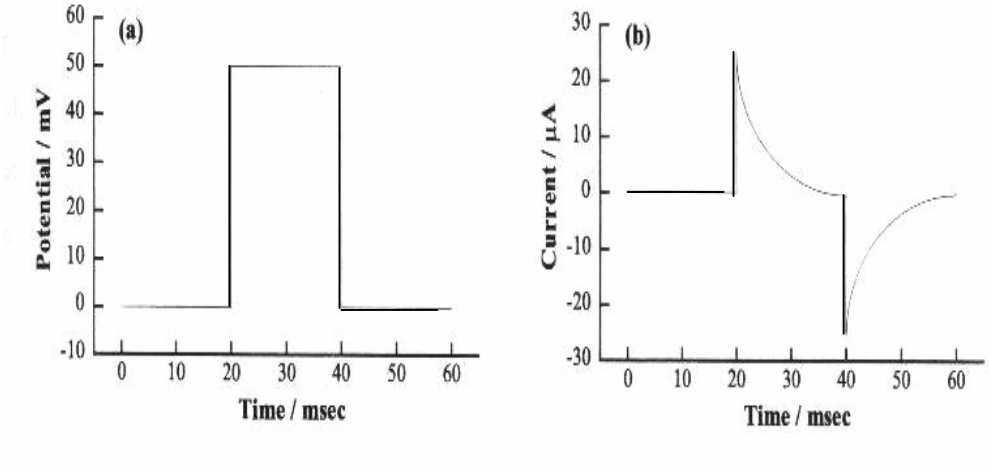

Figure 1.7. Potential step technique principle: (a) applied potential pulse and (b) resulting current response (Berggren *et al*., 1997).

1.5. Chemically Modified Electrodes (CMEs)

Chemically modified electrodes (CMEs) represent a modern approach to electrode systems. There are various ways in which CMEs can benefit analytical applications. These include acceleration of electron transfer reactions, preferential accumulation, or selective membrane permeation. Such steps can impart higher selectivity, sensitivity, or stability to electrochemical devices. These analytical applications and improvements have been extensively reviewed (Bain and Whitesides, 1988, Walczak *et al*., 1991, Scheibler *et al*., 1998, Smith *et al*., 2004).

1.5.1. Self-assembled Monolayers (SAMs) with Metal Electrodes

There is considerable interest in the synthesis and properties of well-organized mono- and multilayer molecular thin films. These films are usually formed by the Langmuir-Blodgett (LB) method of thin film transfer from solvent to substrate (Pettytt *et al*., 1992), by "self-assembly" chemisorptions, and by vapor deposition (Ulman, 1996). The self-assembly chemisorption is a process by which an oriented monolayer film forms on a surface by the spontaneous adsorption of molecules from solution. It is the most promising strategy for constructing stable, well-defined monolayer on electrode surfaces. Molecules that adsorb strongly to a surface and have shapes that pack well in two dimensions are used to form SAMs (Wink *et al*., 1997). Chemical systems that exhibit self-assembly include thiols, disulfides, and sulfides on gold (Bain and Whitesides, 1988, Gooding *et al*., 1998, Gooding and Hibbert, 1999 and Gooding *et al*., 2001), silanes on silicon dioxides (Sagiv, 1980), fatty acids on metal oxide surfaces, phosphonates on phosphonate surfaces (Lee *et al*., 1981), and isocyanides on platinum (Lee *et al*., 1991). Of all the types of self-assembled monolayers that have been studied (Lee *et al*., 1988), two systems have shown the greatest promise for providing an organic surface with a uniform chemical structure: adsorption of organosulfur compounds on noble metals such as gold (Nuzzo and Allara, 1983, Porter *et al*., 1987, Troughton *et al*., 1988, Bain *et al*., 1989), and silver and reaction of alkyltrichlorosilanes with silicon or glass (Sagiv, 1980).

Self-assembled monolayers (SAMs) are versatile model systems for studying interfacial electron transfer, biological interactions, molecular recognition, double-layer structure, adhesion, and other interfacial phenomena (Bryant and Crooks, 1993). SAMs can produce a variety of structures with different types of surface functional groups and with varied topography (Allara *et al*., 1995). Such structural flexibility suggests many future applications.

The SAMs can be divided into those that adhere to the substrate primarily via chemical reaction (chemisorption) and those that adhere primarily via long range forces (physisorption). The latter always involve cross-linked molecules for film stability and are exemplified by alkylsiloxanes (Lercel *et al*., 1994). The

chemisorbed SAMs can be divided further into those that form superlattices of the substrate structure, exemplified by alkanethiols on Au (Dubois and Nuzzo, 1992) and those that do not. The latter in turn can be divided into cases with covalent and ionic type bonding (Nuzzo and Allara, 1983).

The majority of cases studied have involved assembly of normal alkyl chain-based molecules. The primary reason for this is the ease with which alkyl chains self-organize, as is widely manifested in biological structures involving lipid molecules (Nuzzo and Allara, 1983) and amino acids (Yang *et al*., 2001).

1.5.2. SAMs of Thiols, Sulfides and Disulfides on Gold

Exposure of a gold surface to a dilute (1.0 mM) solution of an alkanethiol results in a chemisorbed monolayer that is densely packed in two dimensions and excludes ions and water from the underlying gold (Porter *et al*., 1987, Finklea and Hanshew, 1992, Chidsey and Loiacono, 1990). The thermodynamically favorable formation of the gold-thiolate bond makes the gold-thiol system ideal for monolayer self-assembly schemes, and the stability of that bond over a wide range of applied potential makes such a system suitable for electrochemical studies.

The binding formed between sulfur atom and gold is very strong and the so formed SAM is stable in air, water and ethanol at room temperature. Upon adsorption, the thiol head group looses its hydrogen and the sulfur atom is oxidized. The adsorption process occurs with an initial rapid phase followed by a slower phase, resulting in ordering of the layer. In the first phase, the molecules are adsorbed due to the strong affinity of sulfur for gold. The slower phase is due to van der Waals interactions between the hydrocarbon chains stabilizing the structure (Berggren *et al*., 1997).

1.5.3. Pretreatment of the Gold Surface

For the formation of a well ordered and packed SAM both the structure and the state of the gold surface are important (Troughton and Bain, 1988, Walczak *et al*., 1991). Many different cleaning procedures of gold surfaces prior to self-assembling

have been described, e.g. aqua regia (Cheng and Brajter-Toth, 1996), sulphochromic acid, hydrochloric acid, hydrogen peroxide, hydrochloric acid or ammonia (Bertilsson and Liedberg, 1993, Miller *et al*., 1991), often combined with ultrasonication (Finklea and Hanshew, 1992), ozonolysis (Clegg and Hutchison, 1996), oxygen plasma (Steinberg *et al*., 1995), mechanical polishing, electrochemical cleaning (Akram *et al*., 2004), and potential step (Dijksma *et al*., 2000).

1.5.3.1. Mechanical Polishing

This method is a sequential polishing treatment 'until a mirror surface is obtained'. In Figure 1.8, two optical microscopy images of the same electrode are shown: (a) polished using 0.1 μm alumina suspension and (b) after polishing using 0.05 μm alumina suspensions. Under optical microscopy, it looks like the gold surface is polished efficiently, but under scanning electron microscopy (SEM) scratches are revealed (Figure 1.9).

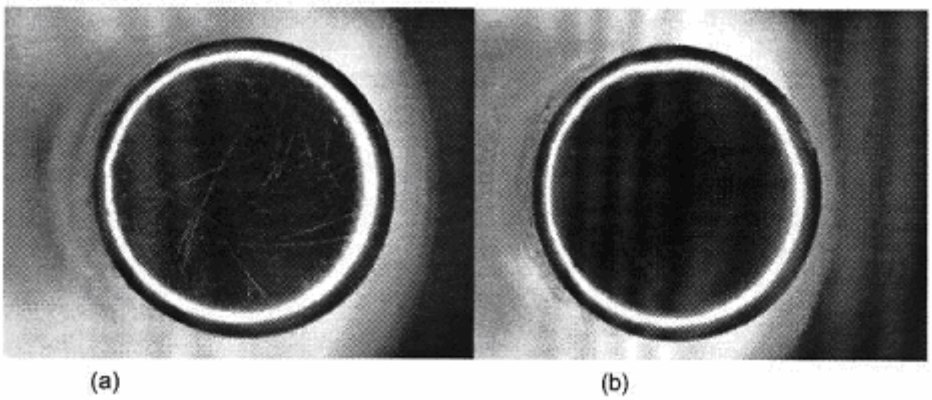

Figure 1.8. Bar electrodes (3 mm diameter) under optical microscopy after polishing with (a) 0.1 μm alumina suspension, and with (b) 0.05 μm alumina suspensions (Mortar *et al*., 2004).

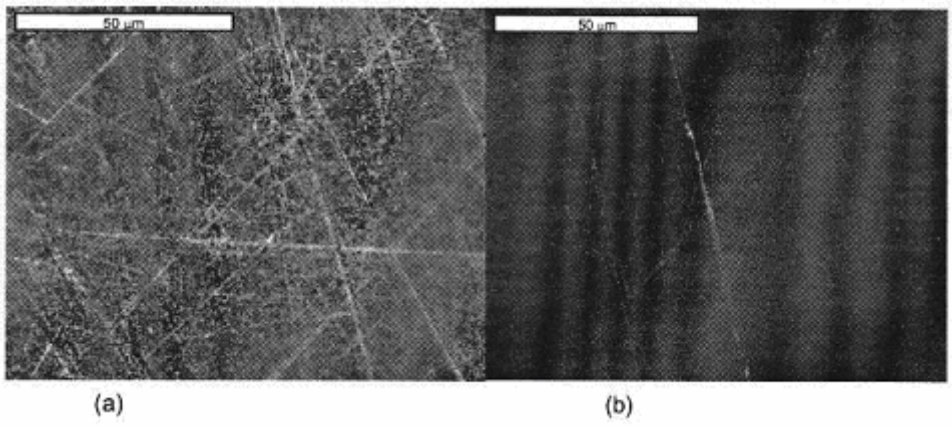

Figure 1.9. SEM images (1000 times magnification) of gold bars polished with alumina suspension 0.1 µm (a) and 0.05 µm (b) (Mortar *et al*., 2004).

1.5.3.2. Oxygen Plasma Cleaning

One such alternative method for organic removal is plasma cleaning. If an object is immersed in glow discharge plasma of a suitable gas, the bombardment of the surface with energetic ions and molecules results in the removal of surface contaminants. Commercial plasma reactors are available and are often used in manufacturing for cleaning. The plasma in these reactors is achieved by reducing the pressure to below one Torr and a flowed gas such as argon or oxygen through the system (Ward, 1990).

Plasma is a gas that becomes activated by flowing it through an area of high electrical energy. The energy will disassociate or accelerate the molecules and atoms and cause them to exist at a high energy state. This higher energy level allows these particles to be able to bond with most compounds that they come into contact with. Plasma typically comes in two types, chemical and physical. Physical plasma is one where atoms are accelerated in a straight line towards a surface in order to etch the surface. Chemical plasma is where the atoms become disassociated and highly active. In this case, the gas is then flowed over a surface, like a cloud of gas, in order to react with any impurities or oxides (Ward, 1990).

Plasma Formation

Radio frequency (RF) oscillating electric field is generated in the gas region, either through the use of capacitive plates or through magnetic induction. At sufficiently low pressures the combined effect of the electric field acceleration of electrons and elastic scattering of the electrons with neutral atoms or field lines leads to heating of the electrons. When electrons gain kinetic energy in excess of the first ionization threshold in the neutral gas species, electron-neutral collisions lead to further ionization, yielding additional free electrons that are heated in turn (Ward, 1990).

Plasma Surface Interaction

The energy of plasma electrons and ions is sufficient to ionize neutral atoms, break molecules apart to form reactive radical species, generate excited states in atoms or molecules, and locally heat the surface. Depending on the process gases and parameters, plasmas are capable of both mechanical work, through the ablative effect of kinetic transfer of electrons and ions with the surface, and chemical work, through the interaction of reactive radical species with the surface. In general, plasmas can interact with and modify a surface through several mechanisms: ablation, activation, deposition, cross-linking and grafting (Ward, 1990).

1.5.4. Stability of SAMs

The chemisorptions of alkanethiols ($CH_3(CH_2)_nSH$) on gold surface is presumably formed by deprotonation of thiol groups upon adsorption. The assumed formation of a gold-thiolate bond form sulfides and disulfides is shown as (Walczak, 1991):

$$AuS(CH_2)_nCH_3 + 2H_2O \longrightarrow Au(0) + {}^{-}O_2S(CH_2)_nCH_3 + 4H^{+} + 3e^{-} \quad (I)$$

$$AuS(CH_2)_nCH_3 + e^{-} \longrightarrow Au(0) + {}^{-}S(CH_2)_nCH_3 \quad (II)$$

The electrode reactions indicate that adsorption at gold results in the loss of the mercaptohydrogen and the formation of a gold alkanethiolate.

The stability of SAMs depends on several factors: (i) chain lengths, (ii) nature of tail group, (iii) symmetry of the alkylthiol, (iv)pH, (v) potential window, etc. Alkanethiols with long chains (n > 10) make more stable, crystalline-like monolayer, while a reduction in chain length leads to a less ordered less stable structure (Bontidean *et al.*, 2002). The order of the SAM is also adversely affected by the roughness of the gold surface. The alkane chains are all in the trans-conformation, tilted slightly from normal to the metal surface by ~20^{o}-30^{o}, resulting in the formation of a densely packed, highly ordered monolayer (Figure 1.10) (Gooding and Hibbert, 1999).

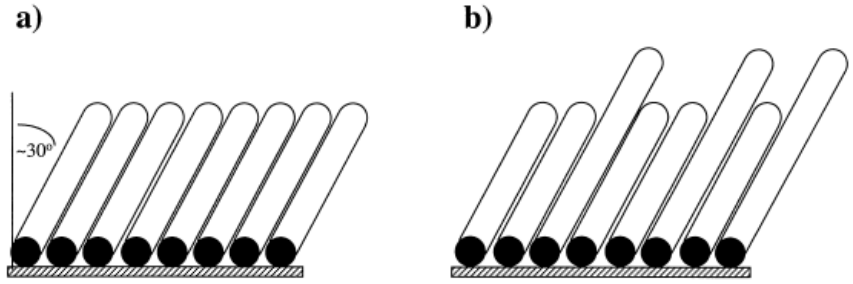

Figure 1.10. Schematic of self-assembled monolayers of alkanethiols on gold electrodes: (a) a pure monolayer and (b) a mixed monolayer (Gooding and Hibbert, 1999).

Monolayers are stable at acid and alkaline conditions in a range of pH 5-13. They are usually stable in the potential range from -400 to +1400 mV *vs* SCE in dilute sulfuric acid solutions (Bontidean *et al.*, 2002).

Thioctic acid, a cyclic disulfide containing a carboxylic acid, is used as a pH-dependent SAM. At increasingly higher pH values, the SAM becomes more negatively charged. At low pH values, carboxylic acid group is neutral. Thioctic acid serves as a basis for a ‘novel separation-free sandwich-type enzyme immunoassay’ for proteins. It combines stability, due to van der Waals interactions

and the two sulphiric bounds (Figure 1.11) to the gold surface per molecule, with a short alkanethiol chain, which confers high sensibility to the sensor. Long-chain alkanethiols have detection limit in the nanomolar range, whilst femtomolar detection has been achieved using thioctic acid as SAM (Wink *et al*., 1997, Mortari *et al*., 2004).

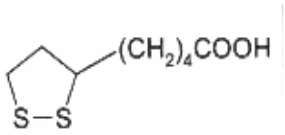

Figure 1.11. Molecular structure of thioctic acid

Some considerations to use SAMs in analytical applications include: (*a*) the (alkane)thiols form easy-to-manufacture, pinhole-free, stable monolayers from dilute solutions, ensuring a uniform immobilization surface; (*b*) SAMs shield biological substances from the sensor surface, preventing possible denaturation; (*c*) contamination of metal surfaces (non-specific adsorption altering the hydrophobic c.q. hydrophilic properties) impairs analysis and has to be avoided; and (*d*) the monolayer can be tailored with functional terminal groups for immobilization purposes (Bontiean, 2003, Smith *et al*., 2004).

1.5.5. Insulating Properties of SAMs

SAMs can either be used for studying non-electroactive properties, or for obtaining a selective electroactive surface.

To produce capacitance sensors with high sensitivity, the insulating property of the SAM is of vital importance. The quality of insulation is studied by cyclic voltammetry, with a redox couple, such as $K_3[Fe(CN)_6]$, present in the solution.

On a clean gold surface, the redox species will be oxidized and reduced, and peak currents proportional to with the total surface concentration of the redox species are obtained in Figure 1.12 (Bontidean *et al*., 1998).

Well designed surface structures are crucial to assure large capacitance changes and to prevent at the same time (i) short-circuiting caused by the electrolyte and (ii) interferences from any redox active couples. Each immobilized layer insulates the electrode surface to a certain degree but a total insulation has been achieved by a final coating with 1-dodencanthiol. The contaminant is detected by cyclic voltammetry (Figure 1.12) (Bontidean *et al.*, 2002).

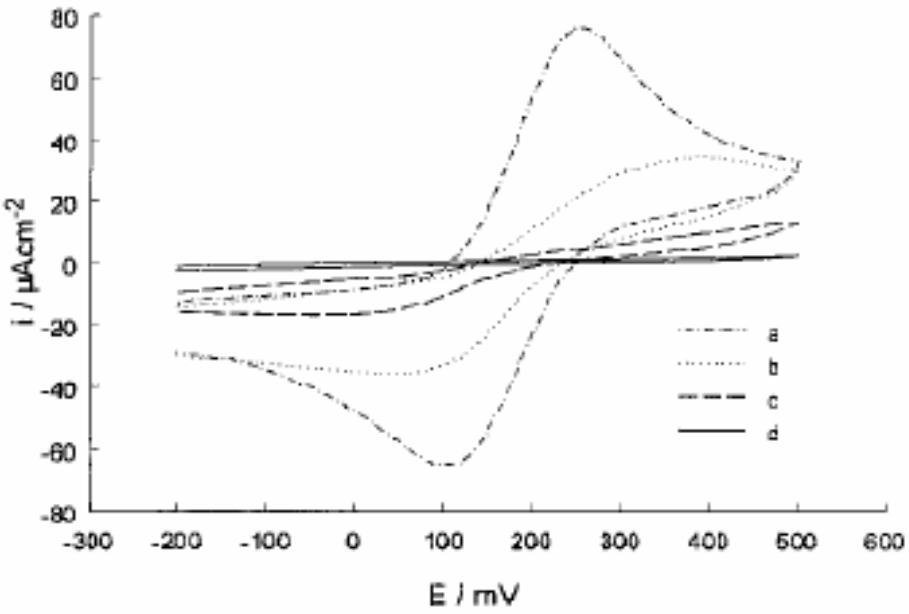

Figure 1.12. Cyclic voltammograms recorded in 5 mM $K_3[Fe(CN)_6]$ on (a) bare gold electrode, (b) thioctic acid covered gold, (c) protein coupled to the SAM, and (d) after a final treatment of electrode in 1-dodecanthiol (Bontidean *et al*., 2002).

1.5.6. Molecular Recognition at SAMs

After formation of SAMs, in a second step the recognition element is bound to the SAMs, to make selective surfaces. In this fashion, proteins have been attached to SAMs with –COOH, -SS-2-pyridine and NH_2 groups (Mrksciha and Whitesides, 1995).

Biorecognition elements can be coupled to SAMs in a single step, if the SAM is already activated, or in two steps, when the SAM is activated before the covalent coupling of the biological element, as shown in Figure 1.13.

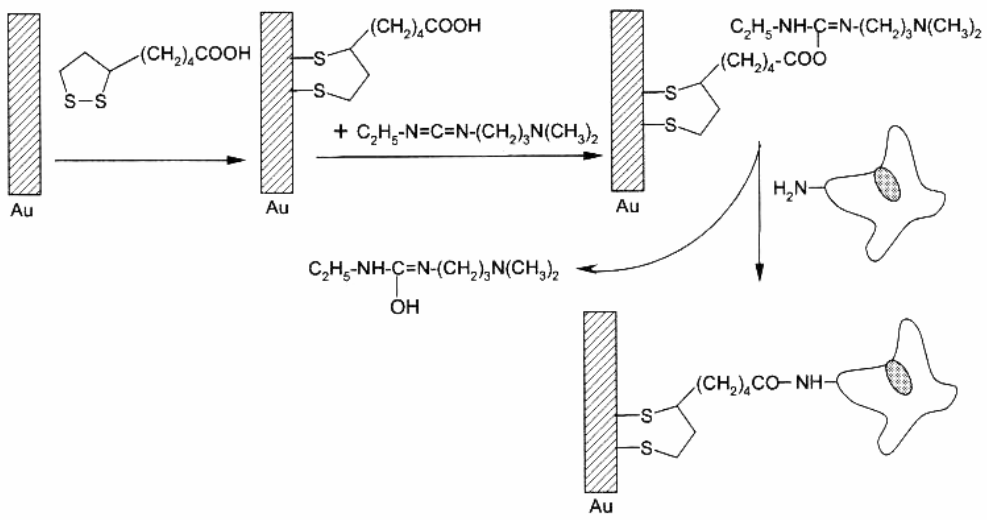

Figure 1.13. Example of "two-step" immobilization of biomolecules on SAMs. The self-assembled monolayer of thioctic acid is activated with 1-ethyl-3-(3-diamino)propyl)-carbodiimide (EDC). The protein is subsequently to the activated SAM via reaction with specific moieties present on the biomolecule surface (Bontidean *et al.*, 2002).

1.6. Capacitive Biosensors for the Heavy Metals

1.6.1. Detection Strategy

The detection principle is based on the conformational change in the structure of protein which is assumed to take place when the analyte, e.g. heavy metal ion, binds to the protein. A schematic representation of the detection principle is shown in Figure 1.14 (Bontidean *et al.*, 2002).

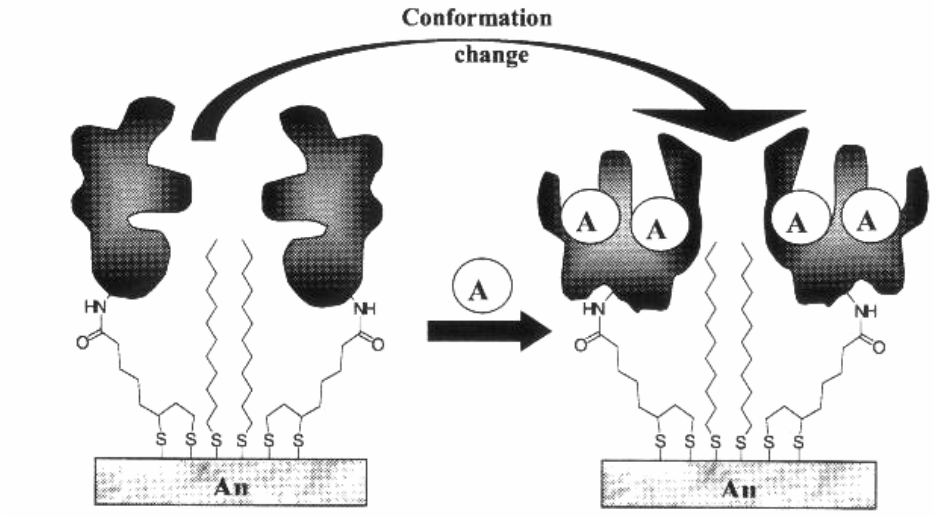

Figure 1.14. Protein-based capacitive biosensor scheme for measuring conformational change upon binding of heavy metal ions (Bontidean *et al.*, 2002).

As a result of the conformational change the thickness of the immobilized layer on the electrode surface is changed and the water molecules come closer to the electrode surface, therefore the total capacitance of the system is changed and this change is proportional to the concentration of the analyte.

1.6.2. Proteins as Recognition Element

Heavy metal ion coordinating proteins, as bio-recognition element, are highly presented in nature and they can be expressed in host cells and easily modified to increase their metal binding capacity.

Heavy metal detecting biosensors based on metal binding proteins e.g. metallothionein (SmtA), regulatory mercury proteins (MerR), and phytochelatins, coupled to the highly sensitive capacitive transducer, are first described by Bontidean *et al*., 1998, 2000 and 2002 articles.

1.6.2.1. SmtA

SmtA is a metallothionine: a low molecular weight, cysteine rich protein with high selective capacity of binding heavy metal. They involved in the detoxification process of heavy metal ions and radicals. SmtA is specifically produced in cyanobacterium *Synechococcus* for managing the zinc homeostasis (Bontidean *et al*., 1998).

1.6.2.2. Phytochelatins

Phytochelatins (PCs) are short, cysteine-rich peptides with the general structure $(\gamma Glu\text{-}Cys)_nGly$ (n = 2-11). PCs have high metal-binding capacity, on a per cysteine basis and they can incorporate high levels of inorganic sulphide that results in tremendous increases in the Cd^{2+}-binding capacity of these peptides (Bontidean *et al*., 2002).

1.6.2.3. MerP

MerP is a well-characterized mercury binding protein that participates in the mercury uptake system in mercury-resistance Gram-negative bacteria. It has common features with metallochaperons and the N-terminal binding domains of heavy-metal transporting ATPases, and contains one single heavy metal associated motif (HMA) of the type GMTCXXC. MerP is used as a model protein for studying metal selectivity (Mortari *et al*., 2004).

1.6.3. Metallopeptides

Peptides can be very effective, and often specific, ligands for a variety of metal ions. They contain a great number of potential donor atoms through the peptide backbone and amino acid side chains. The complexes formed exist in a variety of conformations that are sensitive to the pH environment of the complex. With at least 20 amino acid combinations available, some with coordinating side chains, in any particular order and length, the number of ligands that can be synthesized using simple amino acids is practically infinite. To appreciate the diversity of ligands and their selectivity's for different metals requires an introduction to the complexing of metals with peptides (Gooding *et al.*, 2001).

Peptides with non-coordinating side-chains possess amino and amide nitrogen and carboxyl oxygen as donor sites.

Conformational consequences of metal ion binding to peptide ligands may also have a critical impact on the peptide folding processes. Protein folding, and in particular hydrophobic effects, although receiving much attention, are only partly understood. The existence of a relation between the binding of metal ions to proteins and the local hydrophobicity at the binding site has been recognized only recently. Thus, detailed studies on the relations between the peptide sequence, complex structure and thermodynamical stability are instrumental for the under standing of biological functions of peptides as well as the impact of metal ions on protein folding and conformation (Kozlowsky *et al*., 1999).

1.6.3.1. Complexes of Metal Ions with Peptides

In a single amino acid, with a non-coordinating side chain, there are two donor atoms that complex the metal, the terminal amine and carbonyl oxygen or amide nitrogen as shown in Figure 1.15.

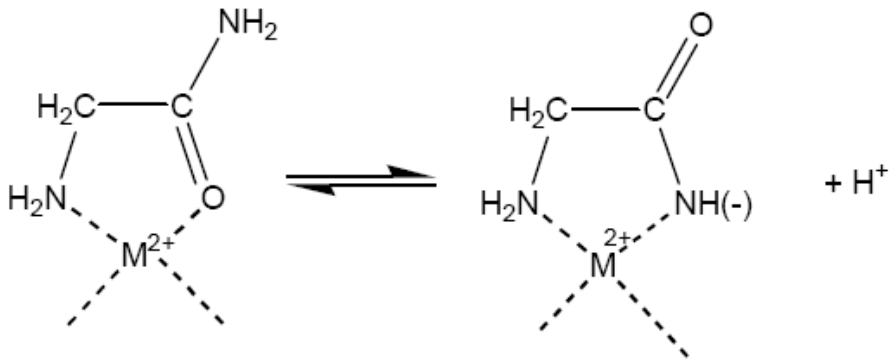

Figure 1.15. Binding of metal ion with a single Gly (Gooding *et al.*, 2001).

With a peptide the potential donor atoms is extended to the amide in the peptide backbone. Binding to metal ions involving an amide group also presents two possibilities; either the carbonyl oxygen or the amide nitrogen can be involved as shown in Figure 1.16 for diglycine.

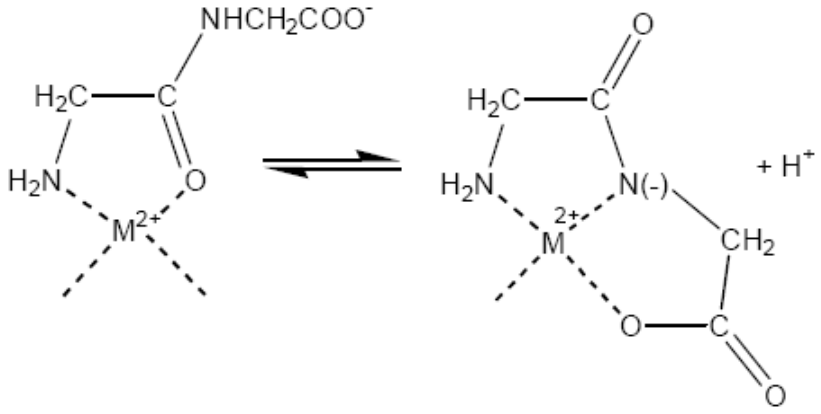

Figure 1.16. Complex formation of metal ion with diglycine (Gooding *et al.*, 2001).

Significantly stronger binding is achieved when the amide nitrogen is involved. Extending this Gly-Gly dipeptide to Gly-Gly-Gly and Gly-Gly-Gly-Gly results in tetradentate ligands with the potential to produce more stable complexes. In view of these binding modes it is clear that to coordinate strongly to the amide group the metal ions must be capable of substituting for the nitrogen bound amide hydrogen. Therefore, the number of peptide nitrogens involved in the bonding is dependent on the pH. Coordination of metal ions such as Cu^{2+} and Ni^{2+} starts at

the N-terminal amino nitrogen. The adjacent carbonyl oxygen is the second donor to complete the chelate ring. By raising the pH the metal ions are able to deprotonate successive peptide nitrogens forming M-N- bonds until eventually a 4N complex is formed around pH 9-10 (Figure 1.17). The well separated pKs for the deprotonation of the peptide nitrogens indicates that there is no cooperation in the binding process (Gooding *et al.*, 2001).

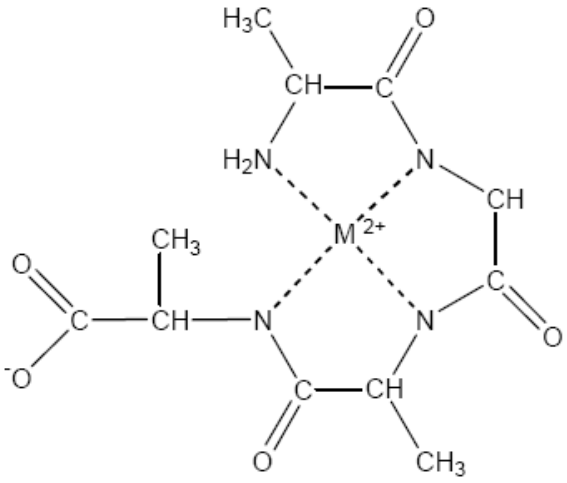

Figure 1.17. Coordination of metal ion with triglycine peptide (Gooding *et al.*, 2001).

1.6.3.2. Coordination of Cu(II) and Ni(II) to Histidine peptides

The histidine residue possesses a very efficient nitrogen donor in its side chain imidazole ring. The cooperativity of all three donor groups of this amino acid in metal binding is made possible by the formation of two fused chelate rings: the five-membered {NH_2, COO^-} (amino acid-like) and the six-membered {NH_2, N_{im}} (histamine-like). The high thermodynamic stability of five- and six-membered rings versus larger ones results in the selection of the N-1 rather the N-3 imidazole nitrogen (Figure 1.18). Such terdentate binding makes histidine a primary low molecular weight chelator in living systems. The specificity of histidine in metal ion binding is preserved in His-containing peptides. Histidine

residue provides two nitrogen donors and a six-membered chelate ring for the coordination (Kozlowsky *et al*., 1999).

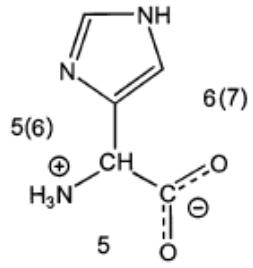

Figure 1.18. Chelating abilities of histidine. Numbers are denoting sizes of potential chelate rings (Kozlowsky *et al*., 1999).

His–His peptide coordination properties towards Cu(II) is studied. Three major coordination modes are found, depending on pH (Figure 1.19).

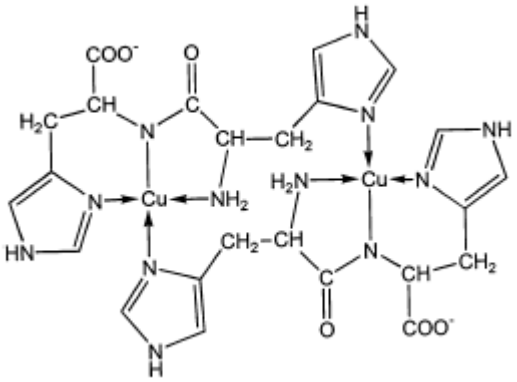

Figure 1.19. The proposed structure of the dimer His–His (Kozlowsky *et al*., 1999).

The insertion of histidine in position two of the peptide chain allows for the simultaneous participation of the amine, the imidazole and the intervened His amide nitrogens in the binding. Gly–His is the simplest peptide of this group of peptides. A very high stability of this complex results from the formation of another pair of fused chelate rings. This flat chelate system uses only three of four

equatorial coordination positions around the Cu(II) ion. The fourth position can be occupied by a second Gly–His molecule, or a molecule of another ligand (Figure 1.20a) (Kozlowsky *et al*., 1999).

The presence of the His residue in position three of the peptide chain allows for the simultaneous formation of three fused chelate rings, and thus the saturation of the coordination plane. The Cu(II) complexation reaction with the simplest representative of this class of peptides, Gly–Gly–His, proceeds cooperatively, with both amide groups deprotonating and bonding to Cu(II) (Figure 1.20b). Gly–Gly–His is ten-fold more effective in Cu(II) sequestrating than Gly–His (Kozlowsky *et al*., 1999).

Separation of the N-terminal amine and the imidazole donors by two or more intervening amino acid residues removes the possibility of concerted formation of the fused chelate system, because there are five or more potential nitrogen donors for four equatorial sites around the metal ion. A study of Cu(II) complexation by Gly–Gly–Gly–His, Ala–Gly–Gly–His, and their analogues with particular donor groups selectively blocked, provided insight into this situation [88]. For tetrapeptides with both terminal donors available, the next complex species (2N), present at neutral pH contain 15-membered macrochelate loops with the {NH2, Nim} coordination (Figure 1.20c). At higher pH amide deprotonations occur (Kozlowsky *et al*., 1999).

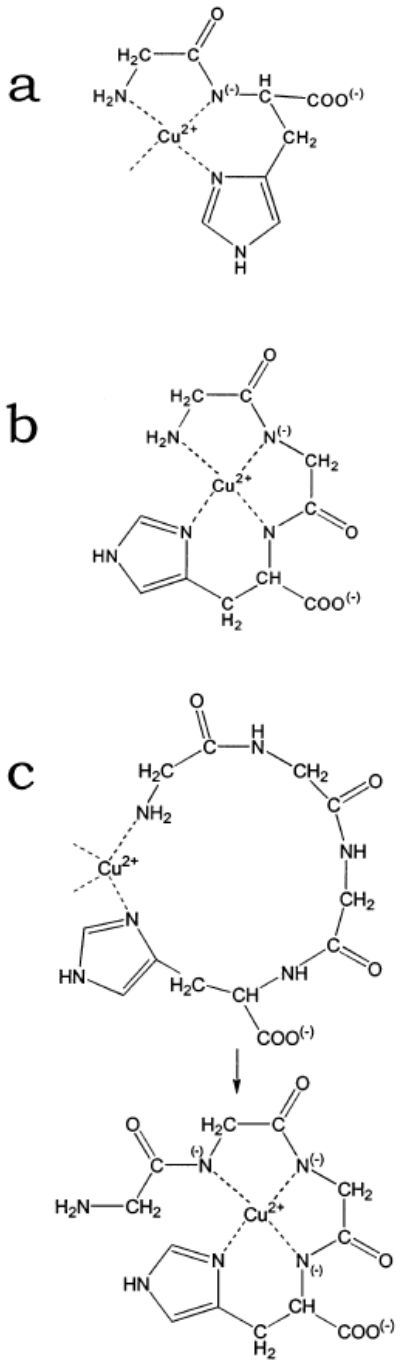

Figure 1.20. Structures of major complex species for Cu(II) complexes of histidine peptides: (a) Gly–His; (b) Gly–Gly–His; and (c) Gly–Gly–Gly–His; initial metal ion concentration 1 mmol dm^{-3} and metal-to-ligand molar ratio 1:1 (Kozlowsky *et al*., 1999).

1.7. Glutathione S-Transferase Enzyme Family

The GSTs (EC.2.5.1.18) are enzymes that participate in cellular detoxification of endogenous as well as foreign electrophilic compounds (Armstrong, 1991).

$$GSH + RX \xrightarrow{GST} GSR + HX$$

GSTs as a part of detoxification systems are evolved to protect cells against reactive oxygen metabolites by conjugating the reactive molecules to the nucleophile scavenging tripeptide glutathione (GSH, γ-glu-cys-gly) (Coles and Ketterer, 1990). With different electrophilic species, GSTs serve as transporters of potentially harmful substances out of the cell (Jemth and Mannervik, e*t al.*, 1999). Following conjugation, these generally harmless GSH adducts, or their mercapturic metabolites, are secreted into the bile or urine (Anderson *et al*., 1999).

Glutathione (GSH), first described in 1888 as philothion, is the most ubiquitous and abundant non-protein thiol in mammal cells and serves as a necessary nucleophile in a number of detoxification reactions (Tew, 1994). In addition to its role in intracellular detoxification, it participates in interconversions of arachidonic acid pathway metabolites (prostoglandins and leukotrienes) (Flatgoord, 1993) and contributes to regulation of protein and DNA synthesis (Ross, 1993) (Figure 1.21).

Maintenance of a homeostatic GSH content is achieved by both de novo synthesis and salvage synthesis and a number of interrelated pathways are also involved (Figure 1.22).

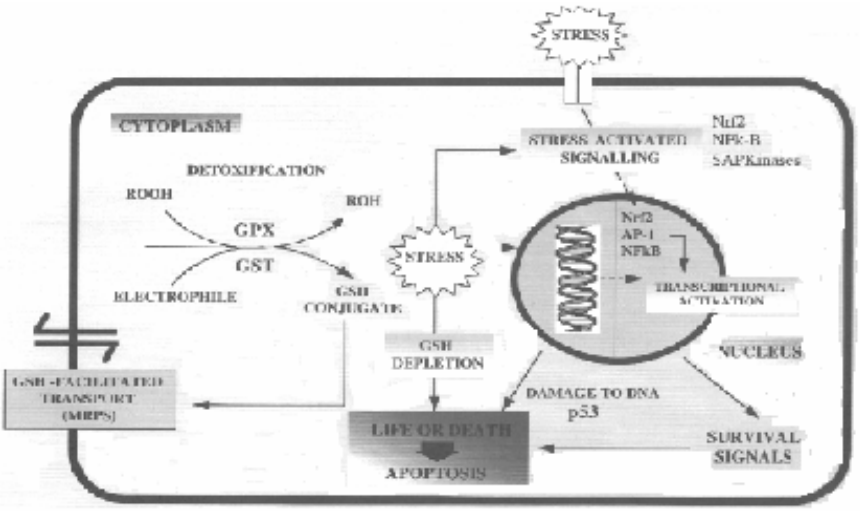

Figure 1.21. Mechanism for cellular protection by glutathione (McLellan, 1999).

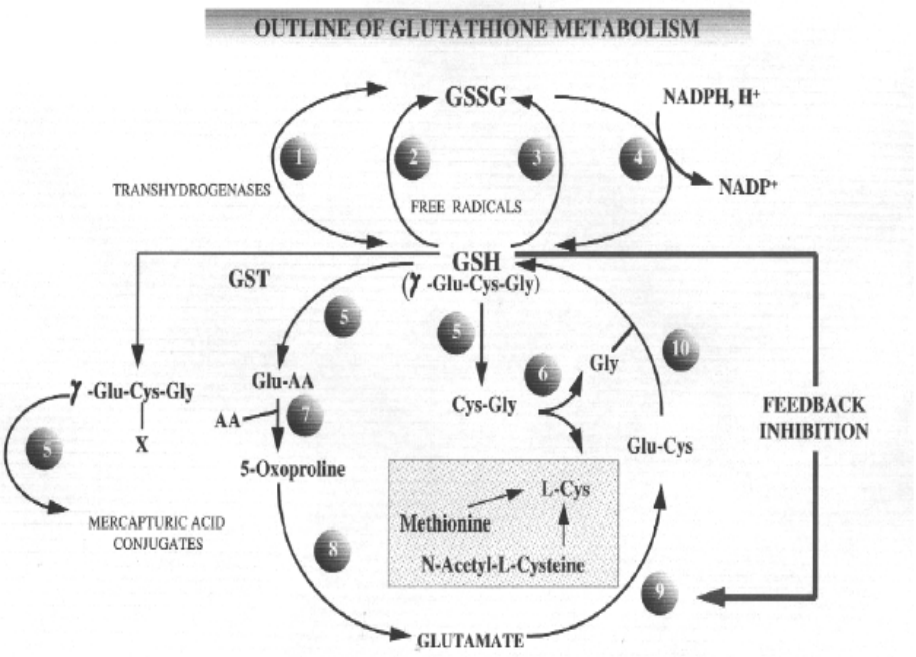

1. GSH thioltransferase; **2**. reaction of free radicals with GSH; **3**. GSH peroxidases; **4**. Glutathione disulphide reductase; **5**. γ-glutamyl transpeptidase; **6**. dipeptidases; **7**. γ-glutamyl cyclotransferase; **8**. 5-oxoprolinase; **9**. γ-glutamyl cysteine synthetase; **10**. GSH-synthetase.

Figure 1.22. Glutathione metabolism (McLellan, 1999).

All GST isozymes used reduced GSH as an acceptor species, but they differ in the specificity with which different substrates are transferred to the cysteine thiol of GSH. The GSTs are found in all eukaryotes and prokaryotic systems, in the cytoplasm, in the microsomes and in the mitochondria (Abu-Hijleh, 1999)

In those species so far investigated, soluble forms of GSTs are homo or heterodimers of different subunits with distinct substrate specificities (Mannervik and Jenssen, 1982) having molecular weight from 20000 to 26000. Sequences and the known three-dimensional structures suggest that these proteins share a common ancestry, though the precise details of their evolution remain obscure. They are expressed at high levels in mammalian liver constituting up to 4% of the total soluble proteins (Eaton,1999) and at least six distinct classes of soluble GSTs have been identified thus far: alpha (α), mu (μ), pi (π), sigma (σ), theta (θ), and zeta (δ). This classification is in accordance with the substrate specificity, chemical affinity, structure, amino acid sequence and kinetic behavior of the enzyme (Landi, 2000). The amino acid sequence identity within class is greater than 70%, whereas the interclass identity is usually less than 30% (Rossjohn *et al.*, 1998).

The GSTs in addition to their enzymatic activities, bind with high affinity a variety of hydrophobic compounds such as heme, bilirubin, hormones and drugs, which suggests that they may serve as intracellular carrier proteins for the transport of various ligands. A marked increase in GST activity has been observed in tumor cells resistant to anticancer drugs (Daniel, 1993).

In addition to the roles of GST in drug metabolism, detoxification, and resistance, there are several reports suggesting that a particular GST isozyme, GST-π for example may serve as a biochemical marker for neoplastic transformation (Shea, 1990).

The presence of GSTs was first demonstrated in rat tissues (Booth *et.al.*, 1961). The presence of a wide range of GSTs isozymes with a differential and overlapping substrate specificity has been detected in a wide variety of species, including man (Kamisaka *et al.,* 1975), rat (Pabst *et al.,* 1973; Askelof, 1975; Igarashi *et al.,* 1986), mouse (Clark *et al.,* 1973; Lee *et al.,* 1981; Igarashi *et al.,* 1986), rabbit (Igarashi *et al.,* 1986) hamster (Smith *et al.,* 1980; Igarashi *et al.,* 1986), guinea pig (Irwin *et al.,* 1980; Di Ilio *et al.,* 1982; Igarashi *et al.,* 1986; Oshino *et al.,* 1990), chicken (Yeung and Gidari, 1980), chick (Chang *et al.,* 1990), cow (Saneto *et al.,* 1980), monkey (Asaoka *et al.,* 1977), trout (Nimmo and Spalding, 1985), shark (Sugiyama *et al.,* 1981), little skate (Foureman and Bend, 1984), grass grub (Clark *et al.,* 1973), house fly (Clark *et al.,* 1973; Clark and Dauterman, 1982), American cockroach (Clark *et al.,* 1973), corn (Mozer *et al.,* 1983) and sheep (Clark *et al.,* 1973; Reddy *et al.,*1983; Ünsal and Öğüş, 1991; Abu-Hijleh, 1993, bovine (İşgör, 2004), *Schistosoma mansoni* (Walker, 1993), *Schistosoma japonicum* (Smith *et al.,* 1986, Smith *et al.,* 1988, Sanchez *et al.,* 2003).

1.7.1. Nomenculature and Classification of Glutathione-S-Transferases

By means of using various substrates, inhibitors, and antisera, it has been proposed that the cytosolic GSTs of rat, mouse, and man may be divided into six principal gene classes designated alpha, mu, pi, (Mannervik *et al.,* 1985), sigma, zeta and theta (Meyer *et al.,* 1991, Zhang *et al.,*1992).

On the basis of sequence similarity, plant GSTs can be divided into four classes: phi, zeta, tau and theta (Edwards, 2000). The phi and tau classes are unique to plants and are relatively well characterized, being encoded by large gene families in all plant species studied to date (Edwards *et al.,* 2000) In contrast, the theta and zeta GSTs are less well represented in plants and the presence of homologues in animals and fungi suggests common essential functions in all eukaryotes (Hayes and McLellan, 1999). Although the enzyme has been isolated from numerous animals and plant sources, the most thoroughly studied group of

isozymes are purified from rat liver cytosol. In spite of the presence of the membrane bound forms of GSTs known as kappa class GST (Pemble *et al*., 1996), most of the studies were done with the soluble forms.

After enriching the SDS-PAGE of rat hepatic cytosol for GST (referred to as a "Y" fraction or a "liganding-containing" fraction), Bass *et al*., in 1977 resoled three electrophoretic bands for GST that were designated Ya,Yb,Yc according to their decreasing anodal mobility. Later it was found with the other researchers (Hayes, 1983) that the Ya and Yc bands represent class alpha GST, whereas the Yb band represents class mu.

The first studies with the human liver GSTs resulted with the separation of cationic forms (Kamisaka *et al.,* 1975) which are now known to be related to the alpha family of the rat GSTs.

In later studies of human liver from various sources, 'near-neutral' and 'anionic' forms were found and shown to be homologues with the μ (Warholm *et al.*, 1981) and π families in rat respectively (Mannervik *et al.*, 1985a). The classification of cytosolic GSTs from rat and man, according to this nomenclature system is shown in Table 1.4.

Several nomenclatures have been proposed for rat GST subunits over the years. The most widely used one was proposed by Jackoby *et al.*, using Arabic numeral nomenclature. This system is of value because it is unambiguous and allows simple displaying of subunit combinations. But this system has disadvantage that it is not clear to show which gene family each subunit belongs. The most important advantage of this system is its usefulness to group GSTs by subfamily and immediate identification of subunits that will dimerize. A class-based subunit nomenclature has been proposed. In this system subunits are grouped by gene family and then numbered according to their order of discovery; this system for defining GST was originally devised for the human transferases (Mannervik, 1992), but it is generally applicable. In this nomenclature system, single capital letter abbreviations are used to signify the alpha (A), the mu (M), the

pi (P), the sigma (S), and the theta (T)classes, and Arabic numerals are employed for numbering each of the separate gene products; for example, the class alpha subunits are called A1, A2, A3, etc. The dimeric GST isoenzymes are represented by the single letter suffix (signifying class) followed by hyphenated Arabic numerals (signifying each of the two subunits). Hence the class alpha heterodimer formed betweenYa1 (A1) and Yc1 (A3), are GST Ya1Yc1, is designated GSTA1-3 (Hayes and Pulford, 1995) (Table 1.5).

Table 1.4. Classification of Cytosolic GSTs from Rat and Man According to the Old Nomenclature System (Meyer, 1991, Husey,1992).

	Species	
Class	**Rat**	**Human**
Alpha	1-1 [Ya] 1-2 [YaYc] 2-2 [Yc] 8-8 [Yk]	α, β, γ [B_2B_2] δ [B_1B_2] ε [B_1B_1]
Mu	3-3 [Yb_1] 3-4 [Yb_1Yb_2] 4-4 [Yb_2] 3-6 4-6 6-6 [Yn]	μ
Pi	7-7 [Yf]	π
Theta	5-5 12-12 (Yrs-Yrs) Yrs-Yrs´ Yrs´-Yrs´	θ (T1-1) θ (T2-2)

The more recent and commonly used nomenclature for the mammalian subunit GSTs uses a lower case letter preceding ‘GST’ to name the species, and an upper case letter denotes the subfamily. According to this system the human theta subunits are named “hGSTT1” and “ hGSTT2” whereas the rat GST5 or GST12 subunits were renamed according to their homologies with the human subunits as “rGSTT1” and”rGSTT2”, respectively. The mouse subunit Yrs is now named “mGSTT2” (Hussey *et al.,* 1992, Lin *et al.,* 1994, Jemth *et al.,* 1996). When the

enzyme, instead of the subunit, is named, they are named with the repeated number of their subunits (i.e. hGSTT1-1, mGSTT2-2, rGSTT1-1, etc) according to the homodimeric structures. Finally the gene coding or each subunit adopts the names of the respective subunit in italics; for example h*GSTT1* for hGSTT1, h*GSTT2* for hGSTT2 (Landi, 2000).

1.7.2. Functions and Structure of GSTs

1.7.2.1. Catalytic Activities of GSTs

GSTs catalyze the nucleophilic addition of the tripeptide glutathione to the substrates of exogenous or endogenous origins that have electrophilic functional groups. In addition to their ability to catalyze the formation of conjugates, GSTs can also serve as peroxidases and isomerases (Mannervik and Danielson, 1988).

GSH is synthesized within the cytosol and depleted in it by conjugation reactions and by the reaction of H_2O_2 and biologically generated radicals across the cell membrane. Oxidation of GSH results in the formation of glutathione disulphide (GSSG), but this is rapidly returned to the reduced state by glutathione reductase, thus maintaining the GSH:GSSG ratio at around 99:1. The third group of GSH can participate in two main types of reaction involving either a one- or a two-electron transfer. These reactions allow GSH to perform key roles within a normal cell, including conservation of the redox status of a cell and participation in certain detoxification reactions (Kearns and Hall, 1998).

Table 1.5. Classification of Cytosolic GSTs from Rat and Man According to the New Nomenclature System (Hayes and Pulford, 1995).

	Class			
Species	**Alpha**	**Mu**	**Pi**	**Theta**
Rat	rGSTA1-2 [Ya_1Ya_2]	rGSTM1-1 [Yb_1Yb_1]	rGSTP1-1 [YfYf]	rGSTT1-1 [GST 5-5]
	rGSTA1-3 [Ya_1Yc_1]	rGSTM1-2 [Yb_1Yb_2]		rGSTT2-2 [Yrs-Yrs] [12-12]
	rGSTA2-3 [Ya_2Yc_1]	rGSTM2-2 [Yb_2Yb_2]		rGSTT2-2´ [Yrs-Yrs´]
	rGSTA3-3 [Yc_1Yc_1]	rGSTM1-3 [Yb_1Yb_3]		rGSTT2´-2´ [Yrs´-Yrs´]
	rGSTA4-4 [YkYk]	rGSTM2-3 [Yb_2Yb_3]		
	rGSTA1-5 [Ya_1Yc_2]	rGSTM3-3 [Yb_3Yb_3]		
	rGSTA2-5 [Ya_2Yc_2]	rGSTM4-4 [Yb_4Yb_4]		
	rGSTA3-5 [Yc_1Yc_2]	rGSTM3-5* [Yb_3Yn_2]		
	rGSTA2-2 [Ya_2Ya_2]	rGSTM6*-6* [YoYo]		
Man	hGSTA1-1 [ε] [B_1B_1]	hGSTM1a-1a	hGSTP1-1 [π]	hGSTT1-1
	hGSTA1-2 [δ] [B_1B_2]	hGSTM1a-1b		hGSTT2-2
	hGSTA2-2 [α, β, λ] [B_2B_2]	hGSTM1b-1b		
	hGSTA3-3*	hGSTM1b-2		
	hGSTA4-4*	hGSTM2-2		
		hGSTM2-3		
		hGSTM3-3		
		hGSTM4-4		

All GST classes function to lower the pKa of thiol group of bound GSH from 9.0 to between 6.0 and 6.9 thus enhancing the rate of the nucleophilic attack of GSH towards the electrophilic co-substrates. This deprotonation causes a 200-300 fold rate acceleration at physiological pH; representing a crucial step in the enzymatic catalysis (Caccuri *et al*., 1999). Evidence suggests that glutathione exists as the thiolate (GS^-) anion at neutral pH when complexes with GST acting as a nucleophile to attack the electrophile centers of xenobiotic or endogenous substrates.

Therefore, catalysis by GSTs occurs through the combined ability of the enzyme to promote the formation of GS^- and to bind hydrophobic electrophilic compounds at a closely adjacent site (Jakoby, 1978, Chen *et al.,* 1988, Graminski *et al.,* 1989, Huskey *et al.,* 1991).

1.7.2.2. Structure of the GSTs

For all cytosolic GST classes representative crystal structures are available with the exception of the kappa class. Including those structures of the members of mammalian GSTs are from classes α [hGSTA1-A from human liver (Sinning *et al*., 1993); μ [rGSTM1-1 from rat liver (Ji, 1992); π [pGSTP1-1 from pig lung (Rouimi *et al*., 1996); hGOTP1-1 from human placenta (Reinemer, 1992.)]; δ [s GSTS1-1 from squid digestive gland (Ji, 1995) and θ [from *Lucilia cuprina* (Wilce, 1995), from *Arabidopsis thaliana* (Reinemer, 1996), human (Rossjohn *et al*., 1998), *Fasciola Hepatica* (Rossjohn, 1997) and a GST from *Schistosoma japanicum* (SjGST), which is structure similar to μ type GSTs (Lin, 1994). A comparison of some structures is provided in Figure 1.23.

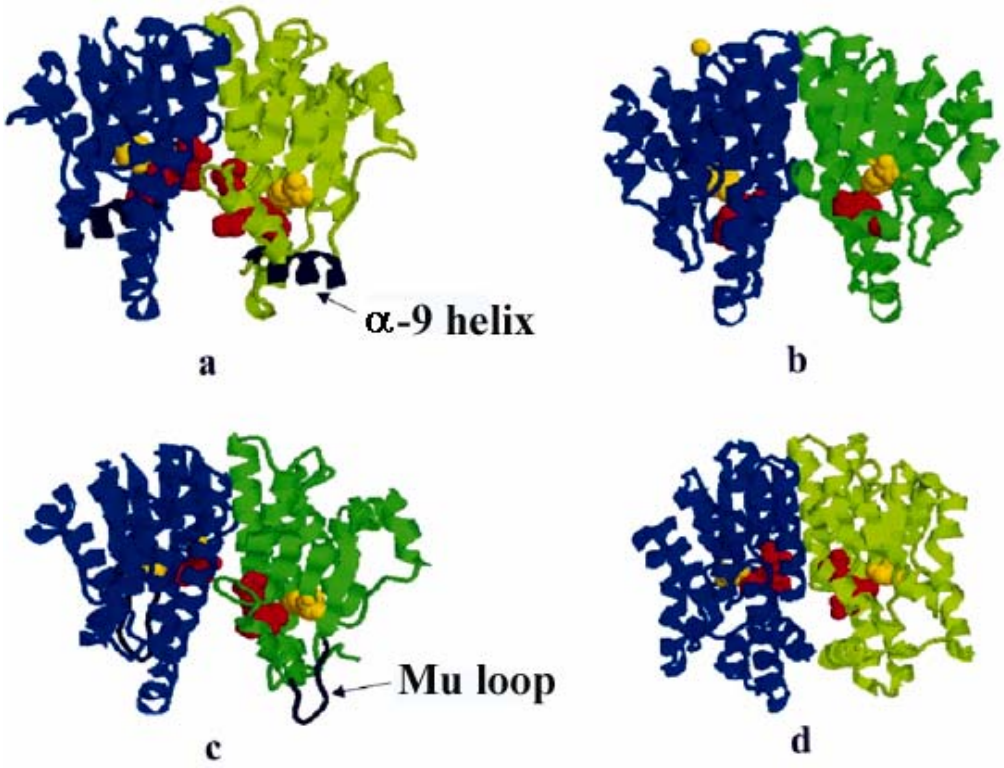

Figure 1.23. Mammalian GST structures (Sheehan, 2001)

Subunits are distinguished by colour (green and blue), and structures are represented to emphasize the relative arrangements around the active site of the right-hand subunit and the inter-subunit cleft. Catalytically essential tyrosine or serine residues are represented in space-filling mode and highlighted in yellow, while the ligand with which the enzyme was co-crystallized is shown in red, identifying the location of the active site. Class-specific features of the Alpha and Mu structures are shown in black. Protein database codes are given in parentheses: (a) human Alpha class (1GUH; (Sinning, 1993)); (b) human Pi class (1GSS; (Reinemer, 1992)); (c) rat Mu class (6GST; (Xiao, 1996)); (d) human Theta class (1LJR; (Rossjohn, 1998)).

Although there is low level of sequence identity across the classes, all the structures follow a similar folding, with each subunit consisting of two domains of different structure (Figure 1.23). Domain I, the N-terminal domain functions to provide the binding site for glutathione, called as G-site, and a Domain II contains essentially all of the H-site known as xenobiotic substrate binding domain. In addition, it has been also shown that the glutathione binding domain (G-site) is highly conserved (not identical) in all classes.

The N- terminal domain consists of 4β sheets with 3 flanking α-helices (Figure 1.24). This domain (approx. residues 1-80) adopts a topology similar to that of thioredoxin fold (Wilce, 1995). The fold consists of distinct N-terminal and C- terminal motifs which have β α β and β β α arrangement respectively and which are linked by a α-helix (α-2 in Figure 1.24).

β α β begins with an N terminal β – strand (β-1), followed by an α- helix (α-1) and then a second β strand (β-2) which is parallel to β-1. A loop region leads into a second α-helix (α-2), which connects with the C terminal motif. This motif consists of two sequential β-strands (β-3 and β-4), which are antiparallel and which are followed by a third α helix (α-3) at the c terminus of the fold. The four sheets are in the same plane, with two helices (α-1 and α-3) below this plane and α-2 above it, facing the solvent. The loop connecting α-2 and β-3 shows characteristic proline residue, which is in the less favored cis conformation and is highly conserved in all species.

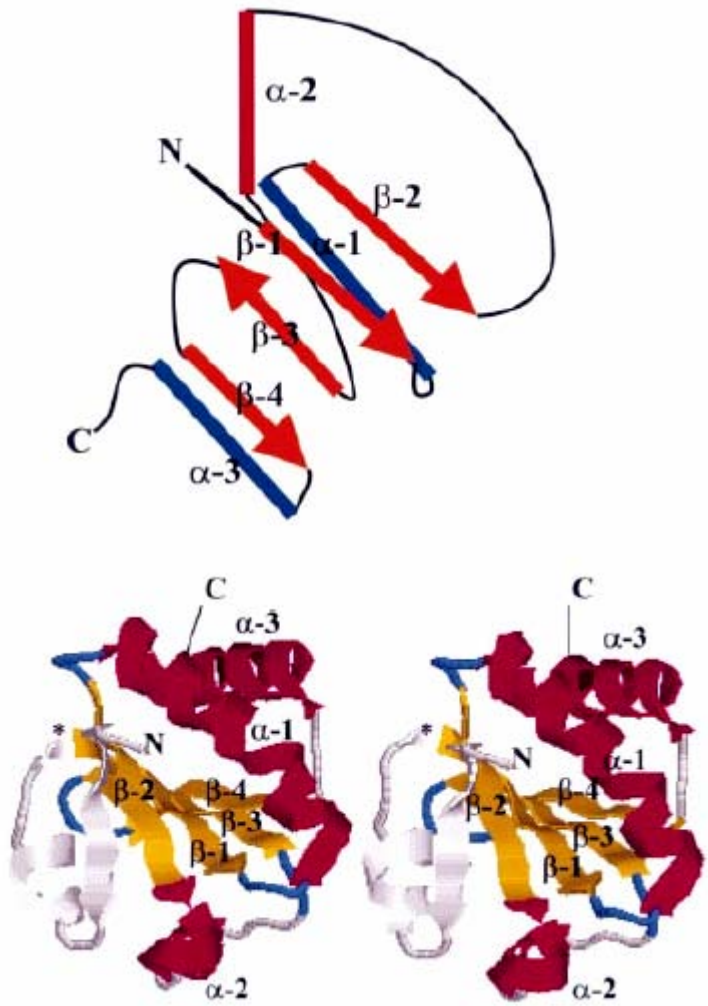

Figure 1.24. The thioredoxin fold (Sheehan, 2001)

A schematic diagram representing the thioredoxin fold is shown above a RasMol depiction of the thioredoxin dimer (Katti 1990). In the diagram, α-helices are shown as cylinders, while β-sheets are shown as orange arrows. The four β-sheets are essentially co-planar, with one helix (α- 2) shown in red above this plane and the other two α-helices (α-1 and α-3) shown in blue below the plane. The cis-Pro loop links α-2 to β-3. In GSTs, domain 2 is connected to the C-terminus by a short linker peptide. In thioredoxin itself, β-sheets are coloured yellow, while α-helices are magenta. The thioredoxin fold has an extra β-sheet and α-helix at the N-terminus (residues 1±21) ending at the point denoted by * where the fold proper begins. These additional N-terminal features are coloured grey.

GSTs are known as the cis-pro loop. Although it does not play direct role in catalysis, this loop appears to be important in maintaining the protein in a catalytically competent structure (Allocati *et al*., 1999). In GSTs, domain I is highly conserved and provides most of the GSH binding site. It is connected to domain by a short linker sequence (Figure 1.25).

Domain II (approx. residues 87-210) begins at the C terminus of the linker sequence and consists of five α helices in the case of pi and mu classes. (Ji, 1992 and Reinemer, 1991) and six α helices in the case of the α class (Sinning *et al*., 1993). The number of helices in domain II varies widely between classes. The C terminal domain is less similar between the three mammalian classes than the N-terminal domain (Figure 1.23 and 1.25) (Dirr, 1994 and Wilce, 1995). It contributes most of the residues that interact with the hydrophobic second substrate, as well as contributing a highly conserved aspartic acid residue (occurring in helix α -4) to the GSH binding site. Differences in the C terminal domain may be responsible for the differences in substrate specificity between the three classes (Wilce, 1995).

Although GSH binding site is very well defined for these cytosolic classes of GSTs, only a general description of the H-Site is available, primarily because for most GST enzymes there are no H-site defining product complex structures.

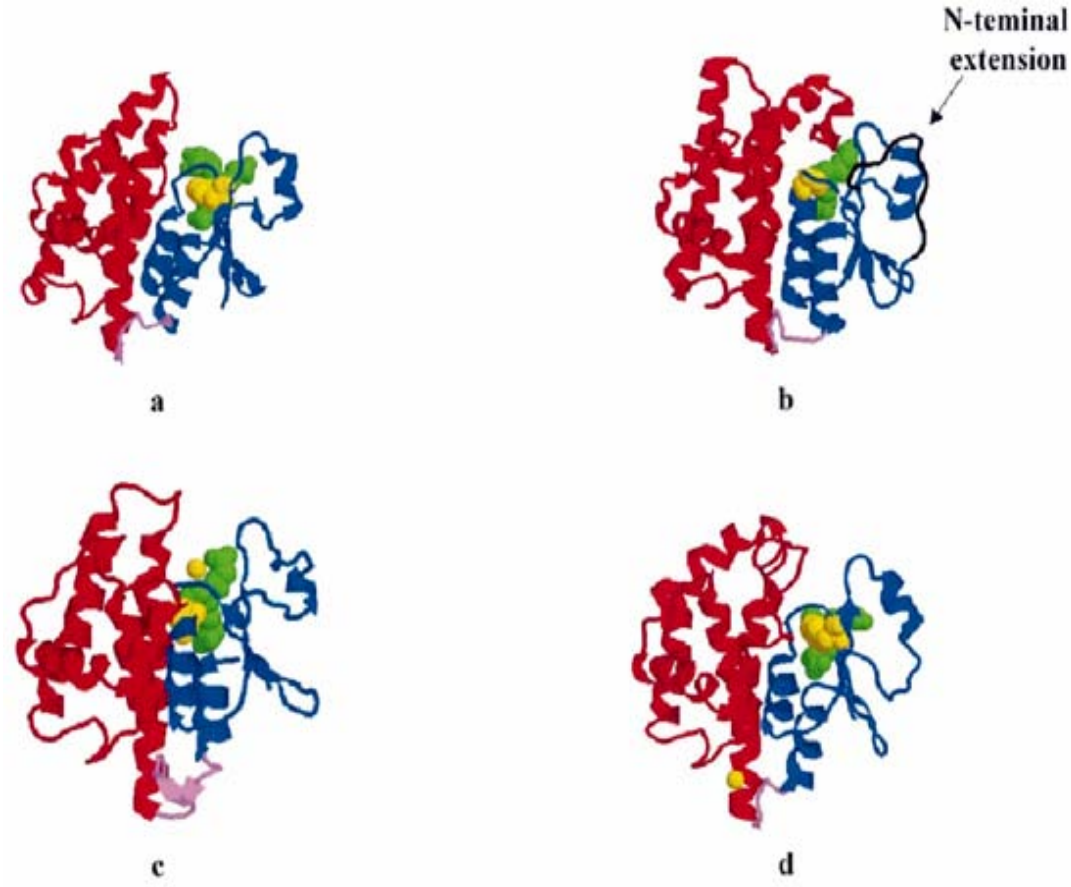

Figure 1.25. Domain structure of GST subunits (Sheehan, 2001).

Three-dimensional structures of individual GST subunits are shown. The N-terminal domain 1 is coloured blue, while the C-terminal domain 2 is red. Catalytically essential residues (tyrosine in a and d; cysteine in b and c) are coloured yellow and presented in space-filling mode, while ligands with which the protein was co-crystallized are shown in green. Linker strands connecting the two domains are shown in violet. Protein database codes and references are given in parentheses: (a) squid Sigma class (1GSQ; (Ji, 1995)); (b) human Omega class (1EEM; (Board, 2000)) [the C-terminal extension (residues 1±19) unique to this class is shown in black]; (c) bacterial (Proteus mirabilis) Beta class (1PM7; (Rossjohn *et al*., 1998)); (d) Fasciola hepatica Mu class (1FHE; (Rossjohn *et al*., 1997)).

It has been observed that GSH binds to the enzyme with three different modes; Class μ GSTs and SJ GST share a common GSH binding mode with the cysteinyl carbonyl hydrogen bonded to the indonyl nitrogen of Trp 7 (Ji, 1992; Lin, 1994). In class α, π, and σ of GSTs the cystenyl carbonyl makes hydrogen bond with a backbone amide group of Phe 8 (Sinning, 1993, Reinemer, 1991 and Ji, 1995). A third binding mode of GSH is presented by class theta GSTs, although an invariant tyrosine residue forms a hydrogen bond with the cysteinyl sulfur in class α, μ, π, σ and SJ GSTs, in class θ GSTs, however, instead of the invariant tyrosine residue nearby serine or another tyrosine residues located in the C-terminal domain of the enzyme interact with the sulphydryl group of GSH. These results suggested the separation of the soluble GSTs into two major subfamilies characterized by either serine residue (ser 9) (Theta and insect Delta classes; the *L.cuprina* GST was presumably termed a theta or theta like GST and has recently been reclassified as a member of the insect Delta classes (Board, 1997) or a "Tyr" residue (Try 8 in α, Tyr 6 in μ, Tyr 7 in π and Sigma classes) as the key residue in GSH activation. A conserved G-site aspartate (Asp101 in class Alpha, Asp105 in class Mu, Asp98 in class Pi, Asp96 in class Sigma) is also involved in catalysis by aiding proton release from certain transition-state conjugates, occurs for example during conjugation between CDNB and GSH (Kolm *et al.*, 1992, Widersten *et al.*, 1992).

In their biologically active form, cytosolic GSTs are either homodimers or heterodimers in which each subunit functions independently. The two subunits contact each other primarily by ball-and-socket hydrophobic interaction established by wedging the side chain of Phe residue (Ball) (Phe 52 α; Phe 56 μ; Phe 47 π) from domain I of one monomer, into a hydrophobic socket of domain II of its partner monomer of the class α, μ, and π enzymes.

Three membrane bound glutathione transferases are known, one of which appears to be involved in xenobiotic mechanism. Microsomal GSH transferase I is an integral membrane protein that has been characterized from both rats and humans where it is found in large amounts in liver and is distributed in both

microsomal and outer mitochondrial membrane. This protein has no relationship with any of the known cytosolic enzymes with respect to sequence. However, it shows some similarity to two other membrane bound GSH transferases, leukotrienes C_4 synthase and microsomal GSH transferase II, in which the three proteins are about the same size, share a small amount of sequence identity and are all membrane bound. There is no so much information about the xenobiotic mechanisms of microsomal GSTs.

1.7.3. GSTs Catalyzed Reactions and Substrates

1.7.3.1. Glutathione Conjugation and Detoxification

All GSTs have the ability to conjugate GSH with compounds containing an electrophilic center. The electrophilic functional group for conjugation reactions can be provided by a carbon, nitrogen, or a sulfur atom. Such groups are present in arene oxides, aliphatic and aromatic halides, α,β- unsaturated carbonyls, organic nitrate esters, organic thiocyanates, olefins, organic peroxides, quinines and sulfate esters (Mannervik, 1985, Mannervik and Danielson, 1988). The range of compounds that contain electrophilic center is extremely large and includes the parent chemical or metabolite of the carcinogens benzo[a]pyrene, 5-methylcrysene, aflatoxin B1, 7,12-dimethybenz[a]anthracene, and 4-nitroquinoline-N-oxide (Table 1.6).

Table 1.6. Examples of GSTs Substrates from Different Compound Categories (Hayes and Pulford, 1995).

Compound Type	**Substrates**
Metabolites of Carcinogens	Aflatoxin B_1-8,9-epoxide Benzo[*a*]pyrene-7,8-diol-9,10-oxide 5-hydroxymethylchrysene sulfate 7-hydroxymethylbenz[*a*]anthracene sulfate 4-nitroquinoline *N*-oxide
Pesticides	Alachlor Atrazine Dichlorodiphenyltrichloroethane (DDT) Lindane Methyl parathion
Oxidative-damage products	Acrolein Base propenols Cholesterol α-oxide Fatty acid hydroperoxides 4-hydroxynonenal
Anticancer drugs	1,3-*bis*(2-chloroethyl)-1-nitrosourea (BCNU) Chlorambucil Cyclophosphamide Melphalan Thiotepa Fosfomycin

1.7.3.2. Model Substrates for the Characterization of GST Isoenzymes

The GST isoenzymes display marked differences in their abilities to conjugate GSH with various electrophiles. 1-chloro-2,4-dinitrobenzene (CDNB) is known as the universal substrate for GSTs since it is used for the demonstration of multiple forms of GSTs in various biological species. When conjugated with GSH it gives *S*-(2,4-dinitrophenyl) glutathione, a compound possessing an absorbance spectrum sufficiently different from that of CDNB to allow a simple spectrophotometric assay at 340 nm (Habig *et al.*, 1974). Reactions of the model substrates, that have been proved to be useful in classifying the GST isoenzymes, are shown in Figure 1.26.

1.7.4. Chromosomal location and Evolution of GSTs in mammals

1.7.4.1. Chromosomal Location

Human GSTT1 and GSTT2 genes were colonized by cell-cell hybridization, in the same chromosomal region on human chromosome 22 and, by in situ hybridization, to the sub-band 22q11.2 (Tan, 1995). The mGSTT1 gene was found to be clustered with mGSTT2 on chromosome 10 by using in situ hybridization method (Whittington, 1999). However, depending on the express sequence tags database, in mouse, it is suggested that, different from humans, there may be two additional members of the theta class that share 70% and 88% protein sequence identity with mGSTT1, and less than 55% sequence identity with mGSTT2 genes (Whittington, 1999).

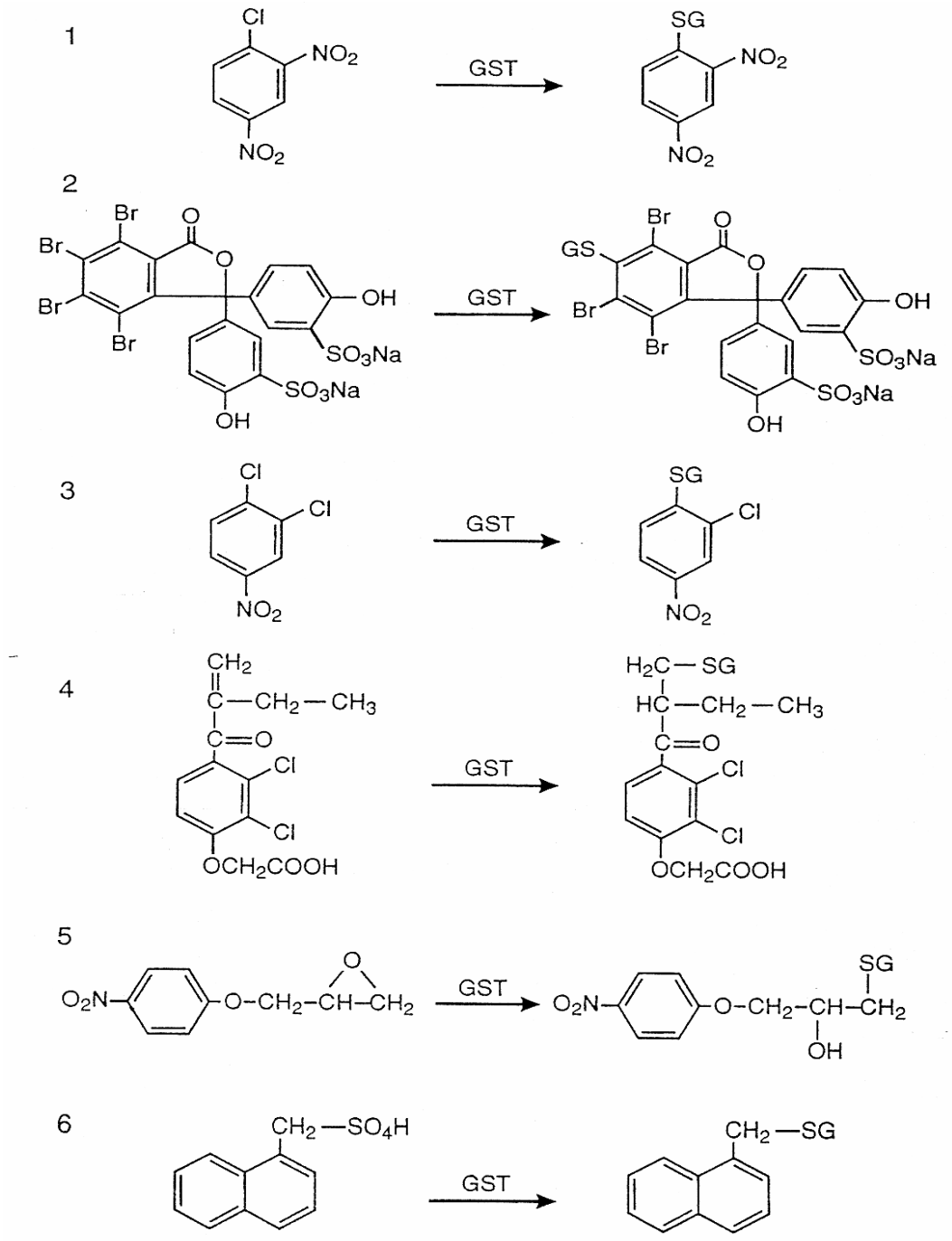

Figure 1.26. Model substrates used for characterization of GSTs: (1) CDNB; (2) bromosulfophthalein; (3) DCNB; (4) ethacrynic acid; (5) EPNP; (6) 1-menaphthyl sulfate; (7) 4-NBC; (8) 4-nitrophenylacetate; (9) 4-NPB; (10) trans-4-phenyl-3-buten-2-one; (11) styrene-7,8-oxide; (12) cumen hydroperoxide (Hayes and Pulford, 1995).

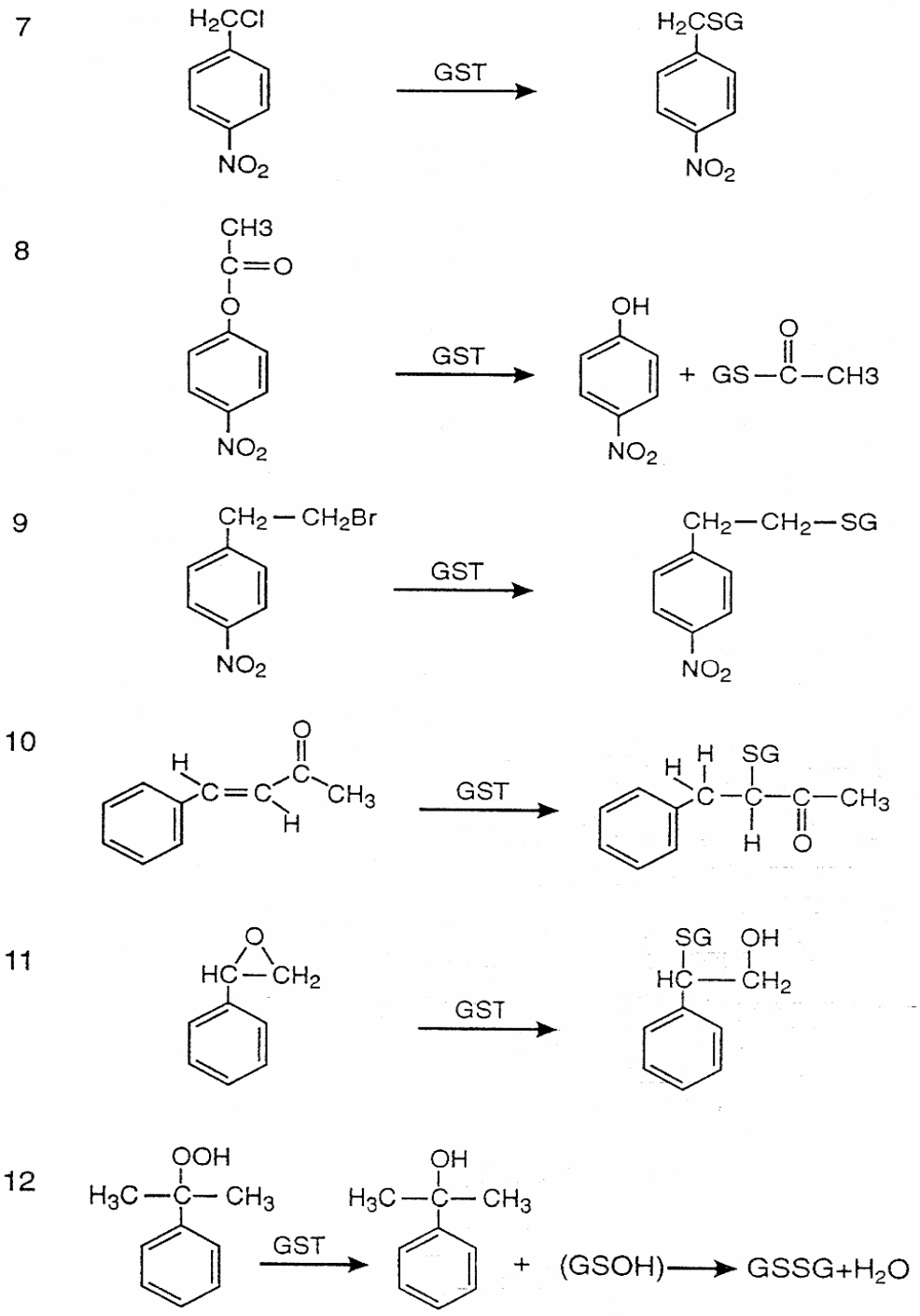

Figure 1.26 (continued)

All members of the GST superfamily catalyze the nucleophilic addition of GSH to bind a variety of electrophilic compounds, thus favoring their excretion (Armstrong, 1997). Despite their low sequence homology, all of GST isoenzymes have very similar three dimensional structures and a very similar G-site topology as it is explained above (Armstrong, 1997, Rossjohn, 1997, Wilce, 1995). For example, the theta and sigma class enzymes have relatively flat and more hydrophilic interphase, but α, μ and π classes have characteristic ball and socket interaction. However, on the other hand, sigma class enzyme uses the same catalytic tyrosine residues as α, μ and π enzymes.

Many of the researchers have used sequence comparisons to generate phylogenetic tree to identify likely patterns of divergence. Alignment of cytosolic GST, amino acid sequences show that members of the theta class seem to be the closest to the GSTs found in many less advanced species, suggesting that this class might represent the ancestral class (Pemble, 1992). On the basis of sequence identity of Kappa class N-terminal with that of class theta is consistent with the proposed evolutionary path that theta GST should have arisen from the ancestral mitochondrial GST Kappa (Pemble, 1996). Alternatively the theta class may be only older than Alpha, Pi and Mu GSTs and have all diverged from a common ancestor (Board, 1997). Ideally it should be possible to compare all full-length sequences known to code for GSTs, but in practice a subset of sequences is usually used to avoid misleading results (Sheehan *et al.*, 2001).

The highly conserved 3'- noncoding sequences of the mu and theta genes also suggest that the mu gene diverged from this precursor before the pi or alpha gene. It is also concluded that the progenitor of the theta class may be kappa class gene which encodes the mitochondrial enzyme (Pemble *et al.*, 1996).

The molecular architecture, catalytic outcome and kinetic mechanism for GSH binding should be preserved during the evolutionary development, if those enzymes diverged from a common ancestral protein (Board, 1997). The results obtained from crystallographic studies was supported this suggestion that with the

crystal structure study it is concluded that the mechanism of losing one molecule of water when GSH binds to the active site and a second water molecule is released when the GSH conjugate is bound, is preserved in α, μ and π enzymes (Caccuri and Giovanni, 1999).

The thermodynamic and kinetic efficiency of substrate binding to GST theta, resulted in a low affinity for GSH, a value at least four times higher than that found in the more recent evolved GSTs. It appears with this result that alpha, mu, and pi GSTs are under an evolutionary pressure in the direction of lower K_d values (Caccuri *et al.*, 2001).

Other important factors must be considered is the dynamics of this enzyme family. The mobility profiles derived from the crystallographic temperature factors along the polypeptide chain of α, μ, π and θ GSTs showed that α, μ and π GSTs have a similar and well defined flexibility pattern with a high mobility, but the hGSTT2-2 enzyme showed a completely different flexibility concluding that GSTS have utilized flexibility in terms of an evolutionary progression (Caccuri *et al.*, 2001).

Although most of the data are consistent with class Kappa's being the progenitor of class theta and thus of the soluble GSTs, this point should be resolved when the crystal structures and enzyme mechanisms of several bacterial GSTs and of class Kappa GSTs are characterized (Pemble *et al.*, 1996).

1.8. Protein Engineering

1.8.1. Design

Nature has evolved over billions of years to provide an enormous number of proteins, which fold into a variety of structures and carry out a diversity of functions. Studying and manipulating natural proteins has lead scientists to understand their folding pathways, thermodynamic stability, and catalytic properties. Such understanding is enhanced and ultimately tested by the ability to

design systems to achieve desired structures and functions, with goal of eventually producing novel macromolecules that will be “made to order'" for solving important chemical and biochemical prob1ems and having applications ranging from industrial catalysis to biomedical engineering. Two very different approaches have been pursued in novel protein design: (i) engineering natural proteins for modification and improvement of their functions, (ii) designing functional proteins entirely *de novo* (Lesley, 2001).

1.8.2. Engineering of Natural Proteins

Many natural proteins comprise structural scaffolds that are quite robust and tolerant of a wide variety of sequence modifications (Lim, 1989). Modern genetic engineering procedures have made it possible to produce natural proteins in large quantities and to modify their primary structures, with concomitant control of physicochemical and biological characteristics. As a result, it is possible to tinker with natural structures and thereby engineer proteins with modified specificity and activity.

1.8.2.1. Alteration of Natural Proteins Properties

Natural proteins have been engineered to exhibit new functions (such as catalytic activities). A very powerful and widely applicable approach is the design of catalytic antibodies. Lerner and coworkers explored the antibody's tolerance of enormous variation of hypervariable loops width corresponding binding specificity (Lerner *et al.*, 1991). By using antigens that resemble the transition state of a reaction, antibodies can be raised to catalyze the reaction by specific binding and stabilizing the rate-determined transition state on the reaction pathway. Hundreds of catalytic antibodies have been deve1oped for catalysis of a variety of chemical reactions, some for which no natural enzyme is known. Antibodies have been produced to catalyze hydrolysis of phosphate triesters by use of an amine oxide hapten to mimic the electrostatic features of the transition state (Barbas, 1993).

Enzymatic catalysts are of significant industrial interest because they are able to perform complex chemistry efficiently and because they are biodegradable. Their commercial use, however, has been limited because they are often too fragile under conditions of commercial manufacturing processes. Recently, a new technology is developed by scientists at Akus Biology (Cambridge, MA) of crystallizing and chemically cross-linking (with gluteraldehyde, etc.) enzymes to produce stable heterologous catalysis from crude protein mixtures. The cross-linked enzyme crystals (CLECs) retain catalytic activity while gaining thermal stability, conformational stability and reduced proteolytic degradation. It is reported that the resulting products can withstand extremes of pH, temperature (above 50^{o}C), and use in organic solvents (Margolin, 1996). The stability of CLECs may be a result of the crystalline nature of the material, combined with the covalent cross-linking of the enzyme mo1ecu1es. CLECs are being explored for applications in aqueous solutions (Persichetti *et al.*, 1995) and in organic solvents (Schmitke *et al.*, 1996). In recent years, there has been much interest in the use of enzymes as catalysts in organic syntheses and polymerization. However, the synthetic potential of enzymes has been limited by the low activity of enzymes in organic solvents, in large part due to conformational changes that occur upon dehydration with lyophilization (Klibanov, 1997). CLECs, on the other hand, are solid crystalline particles that are insoluble in aqueous and organic solvents and show superior catalytic activity as compared to the "amorphous" enzymes in anhydrous organic medium (Haring and Schreier, 1999).

1.8.2.2. Properties of Recombinant Proteins

Besides modifications of natural proteins through changes of small amount of residues as mentioned above, another approach to give novel function is by rearrangement of natural proteins to combine properties from different proteins and, ultimately, to execute multiple functions in a single polypeptide.

Proteins that exhibit two biological functions on a single polypeptide chain exist in nature, with different functions carried out by different domains. Such combinations not only promote optional performance of the protein but also allow efficient production of a variety of polypeptide chains from limited genetic constructs (Winter, 1991).

With the advance of molecular biology, fusion proteins can be readily produced by ligation of genes encoding different proteins or domains. The resulting fusion proteins, in many cases, exhibit the individual biological activities of each protein domain. Fusion proteins have been used to facilitate recombinant protein expression in heterologous hosts. Reporter enzymes-proteins with good expression levels and easy assays-have been fused with target proteins for increased stability, ease of detection and protein secretion (Carter *et al*., 1985). Fusion genes encoding domains that recognize specific ligands are widely used in affinity chromatography to assist purification of recombinant proteins (Sassenfeld, 1990, Nygren *et al.*, 1994).

Monoclonal antibodies have been genetically engineered and endowed with new properties (Quinn *et al.*, 1999, Blake, 2001). Therapeutic antibodies are made by fusing gene segments encoding antigen-binding domains (Fv or Fab fragments) to genes encoding toxins (Chaudhary, 1989) and enzymes (Blake, 2001). The engineered antibodies can target toxins or enzymes to specific types of cells. Another example is immunoadhesins in which a ligand specific for a cell-surface receptor is attached to an Fc fragment. The proton binds to the surface of cells infected with HIV and kills the cells by antibody-dependent cell-mediated cytolysis (Robertson *et al.*, 1987).

Genes encoding subunits form a complex enzyme have been fused together to produce fusion proteins to elucidate the structure-property relationships of enzyme complexes (Wild, 1990). Genes encoding enzymes that are involved in sequential reactions have also been joined. The product of the reaction catalyzed

by the first enzyme serves as the substrate of the second enzyme domain. The fusion protein is used as a conceptual "chain reaction channel" to achieve higher reaction efficiency (Lilius *et al*., 1991).

Genetically engineered affinity domains are fused to proteins of interest to facilitate enzyme immobilization (Corbisier *et al.*, 1999, Quinn *et al.*, 2001, Choi *et al*., 2003). Such fusion proteins could be immobilized by taking advantage of the specific binding of the affinity peptide to an affinity adsorbent, while the partner domain exhibits biological activity on the surfaces (Bontidean *et al*., 2000). Of those fusion proteins the purification and immobilization can be done in a single step through the specific recognition processes drawn from nature, e.g., antibody-antigen, enzyme-substrate or receptor-ligand interactions. This fusion protein approach allows immobilization of enzyme without denaturation and with retention of high catalytic activity.

1.8.3. Recombinant Protein Expression

Expression of a gene product for the purpose of protein purification remains a very empirical task. Typically, expression and purification of proteins are accomplished using an *E. coli* or other prokaryotic vector-host expression system. The choice of bacterial systems is often due to the ease of propagation of the host, low cost, and the availability of sophisticated cloning vectors (Lu *et al*., 1997, Dieckman, 2002).

A cloning vector is an autonomously replicated DNA into which other DNAs can be inserted. Any DNA inserted into the cloning vector will then replicate passively with the vector, so that many copies of the original piece of DNA can be obtained. Cloning vectors can be made from essentially any DNA that can replicate autonomously in cells (Synder and Champness, 1997).

1.8.4. Recombinant Proteins with 6xHis Tag and Purification on Ni-NTA Resin

GSTs are conventionally purified with GSH affinity chromatography or other GSH-derivative affinity systems. However, there are several drawbacks with these purification methods. First, most of the GST mutants, which are the subjects of a wide range of investigations involving the functional roles of residues of GSTs, cannot be readily purified by these method because their GSH binding affinity may have been affected by mutations. Second, because of the necessity of the correct GST G-site structure for GSH binding, GSH affinity purification cannot be readily performed under denaturing conditions. For the recovery of recombinant protein from inclusion bodies, denaturing purification followed by solid-state refolding may be helpful. Finally, because of the enzymatic reaction, it is not proper to use GSH-linked chromatography gel as an affinity immobilization matrix for GST in biosensor or bioassay applications (Chen, 2000).

Immobilized metal-ion affinity chromatography (IMAC) is a well known technique for protein purification. The method is based on the ability of certain metal ions, such as Ni^{2+}, Cu^{2+} and Zn^{2+} to bind strongly and reversibly to peptides and proteins containing histidines or cysteine residues. Various chelators such as nitrilotriacetic acid (NTA) or iminoacetic acid (IAA) are commonly used to bind metals on a solid support (usually sepharose) in metal-ion affinity chromatography (Andreescue *et al*., 2001).

The 6xHis/Ni-NTA system is a fast and versatile tool for the affinity purification of recombinant proteins. It is based on the high-affinity binding of six consecutive histidine residues (the 6xHis tag) to immobilized nickel ions, giving a highly selective interaction that allows purification of tagged proteins or protein complexes from <1% to >95% homogeneity in just one step. The tight association between the tag and the Ni-NTA resin allows contaminants to be easily washed away under stringent conditions, yet the bound proteins can be gently eluted by competition with imidazole, or a slight reduction in pH (Crowe *et al*., 1996).

The six histidine residues that comprise the 6xHis tag can be attached at either end of the recombinant protein, are uncharged at physiological pH, and are very poorly immunogenic in all species (Crowe *et al*., 1996).

Clemmitt and Chase (2000) investigated a facilitated processing of an intracellular, polyhistidine-tagged protein, GST-$(His)_6$, directed from unclarified *E. coli* homogenates using expanded beads of STREAMLINE chelating. They used *E. coli* DH5α, containing modified version of pGEX-5X-1 encoding the IPTG-inducible expression of GST-$(His)_6$.

In 1999, Chen *et al* prepared a C-terminally polyhistidine-tagged protein of *S. japonicum* GST, named as SjGST/His. They constructed a plasmid carrying the SjGST/His gene by cloning the SjGST/His gene fragment of pGEX-5X-2 (Pharmacia Biotech) into the multiple cloning sites of pET-30b (Novagen), which are located before the gene of the six-His tag. They used *E. coli* BL21(DE3) as strain, purchased from Novagen.

1.8.5. pET System (Glutathione-S-transferase Gene Fusion System)

The parasite *Schistosoma japonicum* GSTs, the major detoxification enzymes in *S. japonicum*, have promising vaccine potential against Schistomiasis, and their inhibitors are novel antischistosomal drugs (Chen *et al*., 1999).

Glutathione-S-transferase gene fusion system is an integrated system for the expression, purification and detection of fusion proteins produced in *E. coli*. The pET plasmids provide a multiple cloning site for fusing a gene of interest to the C-terminus His tag of GST from *S. japonicum* (Frangioni *et al*., 1993) (Figure 1.27). This 26.5 kDa recombinant protein contains four cysteine residues, with only the Cys169 residue buried inside the molecule and the other three, Cys85, Cys138, and Cys178, located on the surface of the protein other Cys85, Cys138, Cys178 and Gly212, Gly213, Gly 214, and His216 are located on the surface of the protein. The structure of the recombinant protein produced from *E. coli*

indicates that neither intra- nor inter-disulfide linkage exists in the active dimeric enzyme (Chen *et al*., 1999).

Figure 1.27. The 3D structure of Schistosomal GST (Frangioni *et al*., 1993).

Sensors based on fusion proteins (GST-SmtA and MerR) (Bontidean *et al*., 1998; Corbisier *et al*., 1999; Bontidean *et al*., 2000; Bontidean *et al*., 2004) and synthetic phytochelatins (Bontidean *et al*., 2003) with distinct binding sites for heavy metal ions have been developed and characterized. A capacitance signal transducer has been used to measure the conformational change following binding. The proteins have been over expressed in *E. coli*, purified, and immobilized in different pathways to a self-assembled thiol layer on a gold electrode placed as the working electrode in a potentiostatic arrangement in a flow analysis system.

1.8.5.1. pET 42 a-c Vectors (Novagen)

The pET system is a system, developed for the cloning and expression of the recombinant proteins in *E. coli* by Novagen (Madison, WI, USA).

pET 42 a-c vectors contain a *lac* operator sequence just down stream of T7 promoter and pBR322 origin. They also carry the natural promoter and coding sequence for *lac* repressor (*lac*I). When this type of vector is used in DE3 lysogens to express target genes, the *lac* repressor acts both at the *lac*UV5 promoter in the host (*E.coli* BL21(DE3) strain) chromosome to repress transcription of the T7 RNA polymerase gene by the host polymerase and the T7*lac* promoter in the vector to block transcription of the target gene by any T7 RNA polymerase that is made (Figure 1.28). Expression is induced by the addition of isopropyl-β-D-thiogalactopyranoside (IPTG) to the bacterial culture.

The pET-42 vectors are designed for cloning and high-level expression of peptide sequence fused with the 220 aa GST-Tag, S-tag proteins and two His-tag and they contain Psh A I site within sequences encoding Factor Xa and thrombin cleavage sites. All vector-encoded protein sequences can be removed by Factor Xa or thrombin digestion (Figure 1.29).

The selective marker kan^R (kanamycin resistance) is available with the vectors. The *kan* gene is in the opposite orientation from the T7 promoter, so induction of the T7 promoter should not result in an increase in the*kan* gene product.

The pET-42 vectors contain an f1 origin of replication that allows the production single stranded plasmid DNA for mutagenesis and sequencing applications.

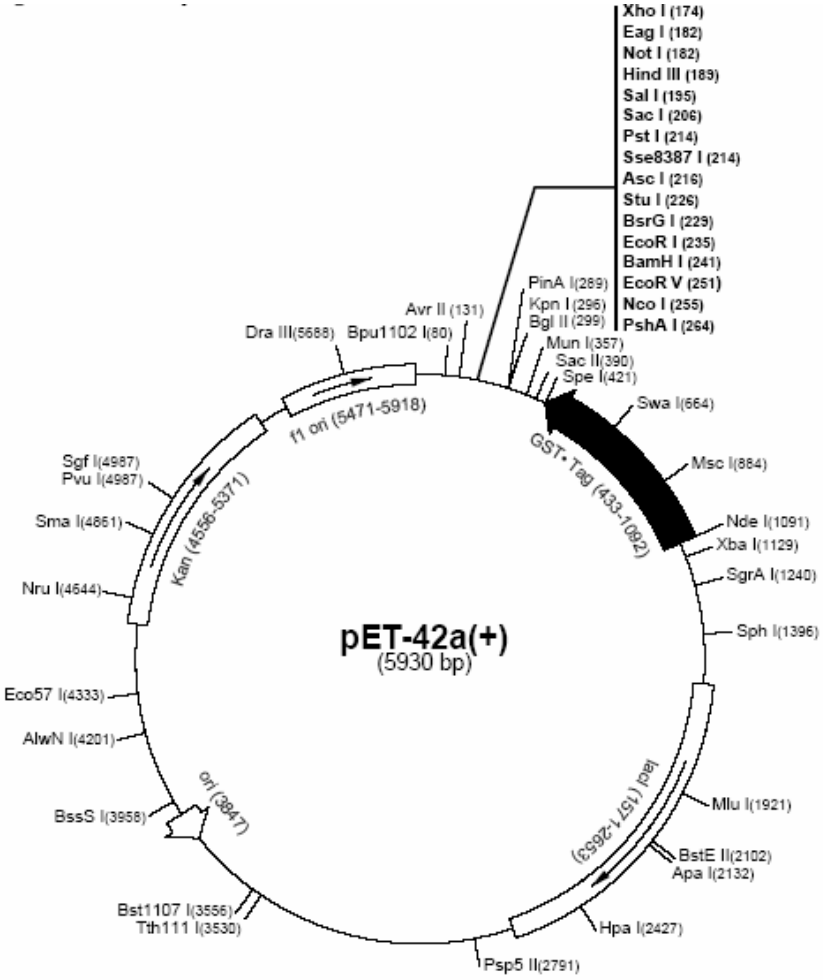

Figure 1.28. pET-42a vector map (Novagen, WI, USA).

Figure 1.29. pET-42a(+) cloning/expression regions (Novagen, WI, USA).

Amino acid sequence of GST-(His)6 recombinant protein is given in figure 1.30. The residues required for heavy metal binding are marked with (*).

```
>1M9B:A GLUTATHIONE S-TRANSFERASE 26,5 KDa
MSPILGYWKIKGLVQPTRLLLEYLEEKYEEHLYERDEGDKWRNKKFEL
GLEFPNLPYYIDGDVKLTQSMAIIRYIADKHNMLGGCPKERAEISMLE
                                                *
GAVLDIRYGVSRIAYSKDFETLKVDFLSKLPEMLKMFEDRLCHKTYLN
                                                  *
GDHVTHPDFMLYDALDVVLYMDPMCLDAFPKLVCFKKRIEAIPQIDKY
                                      *           *
LKSSKYIAWPLQGWQATFGGGDHPPK (-HHHHHH)
                             * * *  *       * * * * * *
```

Figure 1.30. FASTA format of recombinant glutathione S-Transferase-$(His)_6$

1.9. Scope of the Work

The past few years have seen a dramatic change in biosensor technology. This change can be attributed to the convergence of three different strands of research. Researchers have focused their work on producing sensors or related technologies that meet the needs of industrial and governmental analysis. The rapid advancement in the field of molecular biology has helped a new generation of biosensors. The biorecognition elements can be optimized according to desired conditions on the molecular level, to be more rugged, efficient, thermally stable, cheaper or more rapid to produce (O'Connell and Guilbault, 2001).

Protein-based biosensors are used for heavy metal detection, such as GST-SmtA, Mer R (Bontidean *et al*., 2000), EC20 (Bontidean *et al*., 2000), Mer P (Mortari, 2004). These proteins are genetically modified for Hg^{2+} detection.

In this study, the aim of the work is to develop a protein-based biosensor for detection of heavy metals (Cu^{+2}, Zn^{+2}, Hg^{+2} and Cd^{+2}) at very low concentrations. A C-terminally polyhistidine-tagged protein of *S. japonicum* GST was expressed in the *E.coli* BL21(DE3) host, purified, characterized and used as biorecognition element in developed heavy metal biosensorfor the first time in the literature. Expressed recombinant protein GST-$(His)_6$ has not been used before at heavy metal detection.

In this respect, by using the pET-42a plasmid, C-terminally polyhistidine-tagged *S. japonicum* GST gene was transferred to host. The expression was induced by the addition of IPTG (Isopropyl β-D- thiogalactoside). Cells were harvested by centrifugation and disrupted by sonication. GST-$(His)_6$ proteins were removed from the S protein and the second His-tag by thrombin digestion. Cleaved GST-$(His)_6$ proteins were purified by using Glutathione Sepharose 4B affinity column and Ni-NTA (Ni-Nitrilotriacetic acid) spin columns.

GST-$(His)_6$ activities were assayed using the GST substrate 1-chloro-2,4-dinitrobenzene (CDNB). Protein expression was tested by SDS-PAGE and Western blot analysis, using the goat/anti GST polyclonal antibody and monoclonal anti-His antibody.

Biosensor was prepared by immobilizing the GST-$(His)_6$ with its N-terminal amine group by 1-(3-dimethylaminopropyl)-3-ethyl-carbodiimide hydrochloride (EDC) coupling on the gold surface. After immobilization of the recombinant protein, the electrode was treated with 1-dodecanthiol to block any uncovered spots of the sensor surface. Cyclic voltammetric measurements were performed to check the quality of the surface.

The capacitive measurements were done by developed biosensor, inserted as the working electrode in the constructed four-electrode flow cell. The conformational change resulting from the binding of the metal ion to the recombinant protein which caused in the capacitance change proportional to the concentration of the metal ions was determined. The buffer system and the working pH of the biosensor were optimized.

Reproducibility, recovery, stability and storage conditions, and the life time of the biosensor were optimized and studied.

CHAPTER II

MATERIALS AND METHODS

2.1 Materials

BL21(DE3) *E. Coli* Competent cells, BL21(DE3) *E. Coli* Glycerol stock, pET-42a plasmid, kanamycin sulfate, Thrombin cleavage capture kit was purchased from Novagen Company. Ni-NTA Spin kit, Ni-NTA AP conjugate, RGS-His Ab (BSA free) and 6xHis Protein Ladder were purchased from Qiagen Company. Bulk GST purification module and Anti-GST Ab were purchased from Amersham Company. Isopropyl β-D- thiogalactoside (IPTG), Luria Broth, LB agar, 1-chloro-2,4-dinitrobenzene (CDNB), reduced glutathione (GSH), bovine serum albumin (BSA), ethylenediaminetetraacetic acid (EDTA), sodium dodecyl sulphate (SDS), SDS-PAGE molecular weight markers, ammonium persulphate (APS), ammonium sulfate (AS), bromophenol blue, coomassie brilliant blue R-250, coomassie brilliant blue G, sucrose, N,N'-methylene-bisacrylamide (Bis), hydroxymethyl aminomethane (Tris), N,N,N',N'-tetramethylenediamine (TEMED), acrylamide, silver nitrate, glycine, glycerol, sodium carbonate, sodium thiosulfate, formaldehyde, microcentrifuge filtration units and cellulose membrane dialysis tubing, high and low range molecular weight standards were purchased from Sigma Chemical Company, St. Louis, MO, U.S.A.

Gold rods, 99.99% (Catalog No. 26,583-7, 3 mm in diameter), Thioctic acid, Bovine serum albumin (BSA), Tricine, Acetonitrile, Molecular Sieves, 1-dodecanthiol, KCl, $HgCl_2$ and $ZnCl_2$ were purchased from Sigma-Aldrich. 1-(3-dimethylaminopropyl)-3-ethyl-carbodiimide hydrochloride (EDC) was purchased from Fluka AG. Tris, Di-sodium tetraborate, Boric acid, $CuCl_2$, $Cd(NO_3)_2.4H_2O$ were purchased from Merck. Absolute ethanol (99.7) was purchased from Etax. EDTA was purchased from BDH. $K_3[Fe(CN)_6]$ was purchased from Reidel-de Haen. 0.22 µm filters, Microcon centrifugal filter devices (3000 MW CO) were purchased from Millipore. AP-D suspension, OP-Chem polishing cloths were purchased from Struers. Chromium trioxide was purchased from ICN.

All chemicals were of analytical grade and were obtained from commercial sources at the highest grade of purity available.

2.2 Methods

2.2.1. Preparation of Competent Cells

An *E. coli* host strain from the glycerol stock was streaked onto a LB agar plate and was growth overnight at 37^{o}C. A single colony of BL21 (DE3) cells was isolated and inoculated into 5ml Luria Broth medium. Medium was incubated overnight at 37^{o}C with shaking at 250 rpm.

The overnight cell culture was inoculated into 50 ml Luria Broth medium. Culture was incubated at 37^{o}C with shaking at 250 rpm until the OD at 600 nm reached to 0.4. After incubation, cell culture was cooled with ice bath. Cells were harvested with centrifugation at 4000 rpm for 5 minutes at 4^{o}C. Supernatant was discarded and pellet was resuspended in 1:1 (v/v) 0.1 M ice-cold $CaCl_2$. Suspension was centrifuged at 4000 rpm for 5 minutes at 4^{o}C. Pellet was resuspended in 0.5 ml 0.1 M ice-cold $CaCl_2$. Suspension was kept on ice for 1 hour and stored at 4^{o}C until used. Cells were used for transformation within 24 hours.

2.2.2. Transformation of Competent Cells with pET-42a DNA

The five sets of 1.5 ml snap-cap polypropylene tubes were placed on ice to pre-chill. 200µl aliquots of competent cells were pipetted into the pre-chilled tubes. Different concentrations of plasmid DNA were prepared with Tris/EDTA (TE) buffer. 1µl diluted plasmid DNA (1.2 ng, 2.4 ng, 4.8 ng, 10 ng and 48 ng of plasmid DNA) was added to the tubes. The tubes were stored on ice for 10 minutes. After the storage on ice, suspensions were transformed to 42^{o}C water bath and incubated for 90 seconds without shaking. After 90 seconds heat-shock, the tubes were transferred on ice and stored for 2 minutes. After chilling the tubes for 2 minutes, 400µl of room temperature SOC medium was added to each tube. Cultures were incubated at 37^{o}C for 1 hr with shaking (outgrowth). After outgrowth the culture for 1 hr, 50µl transformed competent cells were spreaded onto a LB agar plates containing 30 µg/ml kanamycin sulfate and the plates were leaved on the bench for several min to allow excess liquid to be absorbed, and then inverted and incubated at 37^{o}C for 16 hours.

Selection of transformants was accomplished by plating LB agar containing kanamycin sulfate for the plasmid encoded kanamycin resistance.

2.2.3. Plasmid Isolation

A transformed colony from the LB agar plate 30 µg/ml containing kanamycin sulfate was inoculated into 50 ml Luria Broth medium containing 30 µg/ml kanamycin sulfate. The culture was incubated overnight at 37^{o}C with vigorous shaking. After overnight incubation, 1.5 ml of the culture was poured into a 1.5 ml of microfuge tubes. The tubes were centrifuged at 12,000 xg for 1 min at 4^{o}C in a microfuge. Step 3 and 4 were done one more time with using the same tubes. The medium was removed by aspiration. The bacterial pellet was leaved as dry as possible. Pellet was resuspended in 100µl ice-cold solution I (50 mM glucose, 25 mM Tris-HCl (pH 8.0), 10 mM EDTA (pH 8.0)) by vigorous, vortexing. 200µl of freshly prepared solution II (0.2 N NaOH, 1%SDS) was added into tube. The tube was tightly closed and the contents were mixed by inverting the

tube rapidly 5 times. 150µl of ice-cold solution III (60 ml 5 M potassium acetate, 11.5 ml concentrated glacial acetic acid, 28.5 ml distilled water) was added into the tube. The tube was closed and vortexed gently in an inverted position for 10 sec to disperse solution III though the viscous bacterial lysate. Then, the tube was stored on ice for 5 min. After storage on ice, the tube was centrifuged at 12,000 xg for 5 min at 4^{o}C in a microfuge. The supernatant was transferred to a fresh tube. Into this tube, an equal value of phenol chloroform (1:1) was added and mixed by vortexing. After centrifuging at 12,000g for 2 min at 4^{o}C, supernatant was transferred to a fresh tube. Double-stranded DNA was precipitated with 2 volumes of absolute ethanol at room temperature. The tube was mixed by gentle vortexing and allowed the mix to stand for 2 min at room temperature. Then, the tube was centrifuged at 12,000 xg for 5 min at 4^{o}C and supernatant was removed by gentle aspiration.

The tube was standed in an inverted position on a paper towel to allow all of the fluid to drain away. The pellet of double-stranded DNA was rinsed with 1 ml of 70% ethanol at 4^{o}C. Supernatant was removed and the pellet of nucleic acid was allowed to dry in the air for 10 min. The nucleic acids were redissolved in 50µl of TE buffer (pH 8.0) and vortexed briefly. Double-stranded DNA was loaded onto % agarose gel to analyze.

2.2.4. Induction

2.2.4.1. For Small Amount of Bacterial Culture

A transformed colony from the LB agar plate containing 30 µg/ml kanamycin sulfate was inoculated into 2 ml Luria Broth medium containing kanamycin sulfate. For controlled the induction, two cultures were prepared. Cultures were incubated with shaking at 37^{o}C until the OD_{600} reached 0.6. After OD_{600} reached 0.6, the cultures were stored at 4^{o}C overnight. The following morning, the cells were collected by centrifugation at 5000 xg for 5 min at 4^{o}C. Supernatants were discarded and pellets were resuspended with 2 ml fresh medium. The suspensions were inoculated to 50 ml medium containing 30 µg/ml

kanamycin sulfate in 250 ml glass bottles. Cultures were incubated with shaking at 37^{o}C until the OD_{600} reached 0.6. After OD_{600} reached 0.6, Isopropyl β-D-thiogalactoside (IPTG) were added one of the glass bottles from a 100 mM stock to a final concentration of 1 mM and continued the incubation for 3 hours. After incubation for 3 hr, the bottles were placed on ice for 5 min. Then, cells were harvested by centrifugation at 5000 xg for 5 min at 4^{o}C. The cells were resuspended in 0.25 culture volume of cold 20 mM Tris-HCl (pH 8.0) and centrifuged as above. The supernatants were removed and induced and uninduced cells were stored as a frozen pellet at 70^{o}C until sonication.

2.2.4.2. For Large Amount of Bacterial Culture

A transformed colony from the LB agar plate containing kanamycin sulfate was inoculated into 2 ml, two culture tubes of Luria Broth medium containing kanamycin sulfate. For controlled the induction, one control and two sample culture bottles were prepared. Cultures were incubated with shaking at 37^{o}C until the OD_{600} reached 0.6. After OD_{600} reached 0.6, the cultures were stored at 4^{o}C overnight. The following morning, the cells were collected by centrifugation at 5000 xg for 5 min at 4^{o}C. Supernatants were discarded and pellets were resuspended with 2 ml fresh medium. The suspensions were inoculated to 600 ml medium containing 30 µg/ml kanamycin sulfate in 1000 ml two glass bottles. The total culture volume was 1200 ml. Cultures were incubated with shaking at 37^{o}C until the OD_{600} reached 0.6. After OD_{600} reached 0.6, IPTG were added two sample glass bottles from a 100 mM stock to a final concentration of 1 mM and continued the incubation for 3 hours. After incubation for 3 hr, the bottles were placed on ice for 5 min. Then, cells were harvested by centrifugation at 5000 xg for 5 min at 4^{o}C. The cells were resuspended in 0.25 culture volume of cold 20 mM Tris-HCl (pH 8.0) and centrifuged as above. The supernatants were removed and induced and uninduced cells were stored as a frozen pellet at 70^{o}C until sonication.

2.2.5. Sonication

Induced and uninduced cell pellets were weighted and sonication buffer (PBS buffer: 140 M NaCl, 2.7 mM KCl, 10 mM Na_2HPO_4, 1.8 mM K_2HPO_4, pH 7.4) were added into tubes (2 ml/gr wet weight). Cells were lysed by sonication for 5 min with 10 second pulse at amplitude 40 for 5 ml sonication amount and for 5 min with 10 second pulse at amplitude 60 for 15 ml sonication amount in ice bath. After sonication, sonicates were centrifuged at 12,000 xg for 5 min. Supernatants were discarded and pellets were saved. Enzyme activity and protein determinations were done from the pellets.

2.2.6. Protein Determinations

The protein concentration in the prepared bacterial sonicates, were determined by the method of Lowry *et al.* (1951) with crystalline bovine serum albumin (BSA) as a standard. Aliquots of 0.1 to 0.5 ml of 1:10 diluted bacterial sonicates were taken into test tubes and were completed to a final volume of 0.25 ml with distilled water. Then, alkaline copper reagent was prepared by mixing 2% copper sulfate, 2% sodium potassium tartarate and 0.1 N NaOH containing 2% sodium carbonate in a ratio of 1:1:100, respectively. Afterwards, 1.25 ml of the alkaline copper reagent was added to each tube, mixed by vortex and allowed to stand undisturbed for 10 minutes at room temperature. Finally, 0.125 ml of 1 N Folin Phenol reagent was added to each test tube, mixed immediately within 8 seconds by vortex and incubated 10 minutes. The intensity of color developed in each tube was measured at 660 nm.

The protein concentration in the bacterial sonicates were calculated from a standard calibration curve that was constructed from the corresponding $O.D_{660nm}$ values of BSA standards (0 to 150 μg). The protein concentration in the prepared bacterial sonicates were found to be in the range of 1.0 to 5.0 mg/ml.

2.2.7. GST Activity Assay with CDNB

Recombinant GST proteins produced using a pET-42a plasmid in BL21(DE3) *E. Coli* host was assayed using the GST substrate 1-chloro-2,4-dinitrobenzene (CDNB). GST from many sources, including the schistosomal form used in the pET system, has a high affinity for CDNB (Habig, 1974). The enzyme catalyzes the conjugation of CDNB with glutathione and results in a CDNB-glutathione product with a strong molar absorptivity at 340 nm ($\varepsilon = 9.6\ mM^{-1}cm^{-1}$).

In this assay, a sample containing recombinant GST protein was incubated in a reaction buffer containing CDNB and glutathione. The reaction mixture is shown in Table 2.1. The change in absorbance at 340 nm was monitored for 5 minutes and the relative amount of recombinant GST protein in the sample was calculated by using the formula:

$$\text{Unit of enzyme activity (nmole/min)}: \frac{dA/Min}{\varepsilon_{CDNB}\ (9.6\ mM^{-1}cm^{-1})} \times \frac{\text{Total cuvette volume}}{\mu l \text{ sample added}}$$

Table 2.1. The Constituents of the Incubation Mixture for Recombinant GST Enzyme Assay with CDNB as Substrate.

Constituents of The Reaction Mixture	**Added volume (µl)**
Distilled Water	880
10x Reaction buffer [a]	100
100 mM CDNB	10
100 mM GSH	10
Enzyme Source - Bacterial sonicate (1.0–2.0 mg/ml), or purified recombinant protein fraction	0,5

[a] 10x PBS buffer, pH 6.9: 430 mM Na_2HPO_4, 147mM KH_2PO_4, 1.37mM NaCl, 27mM KCl

2.2.8. Thrombin Cleavage Standardization

Thrombin cleavage was done for cleaved and removed the His tag-S-protein from GST-$(His)_6$ with Novagen Thrombin Cleavage Capture kit.

Biotinylated thrombin (50 Unit) was diluted in thrombin dilution/storage buffer (50mM Sodium citrate, pH 6.5, 200mM NaCl, 0.1% PEG-8000, 50% Glycerol) with serial dilutions to make 0.04, 0.02, 0.01 and 0.005 U enzyme/µl. Reaction mixture was prepared in five 0.5 PCR tubes as shown in Table 2.2. Reactions were incubated at 22^{o}C. For SDS-PAGE electrophoresis to show the complete cleavage, 20µl aliquots were taken into 10µl 4xSDS sample buffer after 4, 8 and 16 hrs. The extent of cleavage of the samples was determined by SDS-PAGE analysis. Protein bands on the gels were stained by rapid silver staining method.

Table 2.2. The Constituents of the Incubation Mixture for Cleavage of Recombinant GST from S-protein.

Constituents of The Reaction Mixture	**Added volume**
10x Thrombin Cleavage Capture buffer [a]	5µl
Target protein	10µg
Diluted thrombin [b]	1µl
Distilled water	xµl
Total Volume	**50µl**

[a] 200 mM Tris-HCl, pH 8.4, 1.5 M NaCl, 25 mM $CaCl_2$

[b] 5th tube was control tube; 2 µl Dilution storage buffer was added instead of thrombin

2.3. Glutathione Sepharose 4B Affinity Column Purification

Glutathione Sepharose 4B affinity purification of the GST-$(His)_6$ proteins was done by two different purification methods. Little amount of the recombinant protein was purified by batch purification method. Large amount of the recombinant protein was purified by column purification.

2.3.1. Batch Purification of GST-$(His)_6$ Using Bulk Glutathione Sepharose 4B

Batch purification of GST-(His_6) proteins was done with Amersham Biosciences Bulk GST Purification Module.

2.3.1.1. Preparation of Glutathione Sepharose 4B

Glutathione Sepharose 4B as supplied is approximately a 75% slurry. The following procedure resulted in a 50% slurry. 1.33 ml of the original Glutathione Sepharose 4B slurry per ml of bed volume required was dispensed into a sterile falcon tube (Table 2.3). The matrix was sediment by centrifugation at 500 xg for 5 minutes. The supernatant was carefully decanted. Resin was washed by adding 10 ml of cold (4°C) 1X phosphate buffer saline (PBS) (0.14 M NaCl, 2.7 mM KCl, 10.1 mM Na_2HPO_4, 1.8 mM KH_2PO_4, pH 7.3) per 1.33 ml of the original slurry of Glutathione Sepharose 4B to remove the 20% ethanol storage solution. The matrix was sediment by centrifugation at 500 xg for 5 minutes. The supernatant was carefully decanted. For each 1.33 ml of the original slurry of Glutathione Sepharose 4B dispensed, 1 ml of 1X PBS was added. This resulted in a 50% slurry.

2.3.1.2. Batch Binding

After Glutathione Sepharose 4B preparation, 2 ml of the 50% slurry of the matrix, equilibrated with 1X PBS was added to 4 ml of cleaved protein solution. The suspension was incubated with gentle agitation at room temperature for 30

minutes. After incubation, the suspension was centrifuged at 500 xg for 5 minutes at 4^{o}C to sediment the gel. Supernatant was discarded and washed with 10 bed volumes of 1XPBS. The suspension was centrifuged at 500 xg for 5 minutes at 4^{o}C. Washing step was repeated twice more for a total of three washes. Bound fusion protein was eluted directly at this stage using Glutathione Elution Buffer.

Table 2.3. Reagent Volume Requirements for Different Protein Yields.

Component	**5 mg**	**1 mg**
Culture Volume	1.25 liters	0.25 ml
Volume Sonicate	15 ml	5 ml
Glutathione Sepharose Bed Volume*	625 µl	125 µl
1X PBS**	6,25 ml	1,25 ml
Glutathione Elution Buffer	625 µl	125 µl

*To obtain the desired bed volume, twice the volume of 50% prepared Glutathione Sepharose slurry was used. (1 ml of 50% Glutathione Sepharose slurry gave a bed volume of 0.5 ml).
**This volume was "per wash." Three washes were required.

2.3.1.3. Elution of Recombinant Protein

Elution buffer was prepared by adding 10 mM reduced glutahione into a 50 ml 50 mM Tris-HCl, pH 8.0 buffer. 1-10 ml aliquats were prepared from this solution and stored at -20^{o}C until needed. The bound recombinant proteins were eluted by the addition of 1 ml of Glutathione Elution Buffer per ml bed volume of the sedimented gel. Suspension was incubate at room temperature (22-25°C) for 10 minutes to elute the recombinant protein. The suspension was centrifuged at 500 xg for 5 minutes at 4^{o}C. Supernatant was collected. The elution and collection steps were repeated 3 times more. The four eluates were pooled. The yield of recombinant protein was estimated by measuring the absorbance at 280 nm.

2.3.2. Column Purification of Fusion Proteins Using Glutathione Sepharose 4B

2.3.2.1. Column Preparation

The sufficient 75% slurry for use were transfered to the disposable column**.** The column was tap to dislodge any trapped air bubbles in the matrix bed and allowed to settle. the bottom cap of the column was removed and saved for later use. The column was allowed to drain.The Glutathione Sepharose 4B was washed by adding 10 ml of cold (4°C) 1X PBS per 1.33 ml of the original slurry of Glutathione Sepharose 4B dispensed to remove the 20% ethanol storage solution. Residual ethanol interferes with subsequent procedures.

Glutathione Sepharose 4B equilibrated with 1X PBS is stored at 4°C for up to 1 month.

2.3.2.2. Column Binding

The cleaved protein solution was applied to the column of drained and washed Glutathione Sepharose Disposable Column.The end cap was remove and allowed the cleaved protein solution to flow through the column.The matrix was wash by the addition of 10 bed volumes of 1X PBS. The column was allow to drain. Wasing step was repeated twice more for a total of three washes. The flow-through was collected for the further protein concentration, SDS-PAGE and western blotting analysis.

2.3.2.3. Column Elution

Once the column with bound protein had been washed and drained, the bottom cap was replaced. The recombinant protein was eluted by the addition of 1 ml of Glutathione Elution Buffer per ml bed volume. The column was incubate at 4°C for 15 minutes to elute the recombinant protein. The bottom cap was removed and the eluate was collected. This contained the recombinant protein. The elution and collection steps were repeated 3 times more. The four eluates were pooled.

The yield of recombinant protein was estimated by measuring the absorbance at 280 nm.

The pooled recombinant protein fractions from the Glutathione Sepharose 4B were dialysed with 50 mM NaH_2PO_4, 300 mM NaCl, 10 mM imidazole, pH 8.0, containing 5 mM β-mercaptoethanol, dialysis buffer before the application onto the Ni-NTA columns.

2.4. Ni-NTA Column Purification of GST-$(His)_6$

Ni-NTA column purification of GST-$(His)_6$ proteins was done with Novagen Ni-NTA spin kit.

2.4.1. Recombinant Protein Purification Under Native Conditions

The Ni-NTA spin columns were equilibrated with 600µl Lysis Buffer (50 mM NaH_2PO_4, 300 mM NaCl, 10 mM imidazole, pH 8.0, containing 5 mM β-mercaptoethanol). The columns were centrifuged for 2 min at 700 xg at 7^oC. 600 µl of the affinity eluate containing the 6xHis-tagged GST protein was loaded up to the pre-equilibrated Ni-NTA spin column. Columns were centrifuged for 2 min at 700 xg at 7^oC, and the flow-throughes were collected for the further protein concentration, SDS-PAGE and western blotting analysis to check binding efficiency. By adding 10 mM imidazole, the binding of non-tagged contaminating proteins was inhibited, leading to greater purity in fewer steps.

Ni-NTA spin columns were wash twice with 600µl Wash Buffer (50 mM NaH_2PO_4, 300 mM NaCl, 20 mM imidazole, pH 8.0, containing 5 mM β-mercaptoethanol). Centrifuge for 2 min at 700 x g at 7^oC. The number of wash steps required to obtain highly pure protein was determined primarily by the expression level of the 6xHis-tagged protein. When the expression level was high, two washes were usually sufficient for removal of contaminants. For very low expression levels or highly concentrated lysates, three wash steps were required to achieve high purity.

The flow-throughes (wash fractions) were saved for analysis by protein concentration, SDS-PAGE and western blotting analysis to check the stringency of the wash conditions.

The recombinant proteins were eluted 3 times with 200µl Elution Buffer (50 mM NaH_2PO_4, 300 mM NaCl, 250 mM imidazole, pH 8.0, containing 5 mM β-mercaptoethanol). The columns were centrifuged for 2 min at 700 xg at 7^oC, and the eluates were collected. Most of the 6xHis-tagged protein (>70%) was eluted in the first 200 µl eluate. The remainder will elute in the second and third 200µl.

The pooled recombinant protein fractions from the Ni-NTA columns were dialysed with PBS buffer: 140 M NaCl, 2.7 mM KCl, 10 mM Na_2HPO_4, 1.8 mM K_2HPO_4, pH 7.4, containing 5 mM β-mercaptoethanol before dividing into 0.4 ml aliquats. The aliquats were stored at -80^oC.

2.5. SDS-Polyacylamide Gel Electrophoresis

Polyacrylamide slab gel electrophoresis, in the presence of the anionic detergent sodium dodecyl sulfate (SDS), was performed on 5% stacking gel and 12% separating gel in a discontinuous buffer system as described by Laemmli (1970). The eight proteins given below were used as molecular weight standards.

- Albumin, bovine serum	(M_r 66000)
- Ovalbumin, chicken egg	(M_r 45000)
- Glyceraldehyde-3-phosphate dehdydrogenase, rabbit muscle	(M_r 36000)
- Carbonic anhydrase, bovine erythrocytes	(M_r 29000)
- Trypsinogen, bovine pancreas	(M_r 24000)
- Trypsin Inhibitor, soybean	(M_r 20000)
- α-Lactalbumin, bovine milk	(M_r 14200)

2.5.1. Preparation of Reagents

(A) Stock Separating Gel Buffer (1.5 M Tris-HCl, pH 8.8)

36.3 g Tris base were dissolved in about 100 ml distilled water and pH 8.8 was adjusted with 1 M HCl. Finally completed to 200 ml.

(B) Stock Stacking Gel Buffer (0.5 M Tris-HCl, pH 6.8)
12.1 g Tris base were dissolved in about 100 ml distilled water and pH 6.8 was adjusted with 1 M HCl. Finally the volume was completed to 200 ml.

(C) Stock Gel Solution (Acrylamide-BIS, 30% A, 2.67% C)

60.0 g acrylamide were dissolved in about 150 ml distilled water and then 1.6 g BIS (Bis-acrylamide) were added and solution was completed to 200 ml with distilled water. Finally, the solution was filtered through course filter paper.
Note: % A represents acrylamide monomer percent concentration and % C indicates the cross-linking monomer concentration, which were calculated as below:

% A = [(gm acrylamide/total volume)] X 100

% C = [gm BIS/(gm acrylamide + gm BIS)] X 100

(D) 10 % SDS Solution

10 g SDS were dissolved in water with gentle stirring and completed to a final volume of 100 ml.

(E) Catalyst (10% Ammonium Persulfate “APS”)

Prepared freshly by dissolving 100 mg ammonium persulfate (APS) in a final volume of 1 ml distilled water.

(F) 5 X Electrode (Running) Buffer (25 mM Tris, 192 mM Glycine, pH 8.3)

Stock running buffer solution was prepared by dissolving and completing 15 g Tris base, 72 g glycine to 1 liter distilled water. The pH of the buffer was not

adjusted with acid or with base. This buffer was diluted 1:5 and 1 g solid SDS was added to 1 liter of buffer before use.

(G) 4 X Sample Dilution Buffer (SDS Reducing Buffer)

0.25 M Tris-HCl buffer, pH 6.8 containing 8% SDS, 40% glycerol, 20 % 2-mercaptoethanol, 0.004% bromophenol blue. It was prepared by mixing the following volumes of given solutions:

2.5 ml	1 M Tris-HCl, pH 6.8
4.0 ml	Glycerol
2.0 ml	2-mercaptoethanol
0.4 ml	Tracking Dye
0.8 gm	10 % SDS
Distilled water to 10.0 ml	

2.5.2. Electrophoresis Procedure

Vertical slab gel electrophoresis was carried out using the EC120 Mini Vertical Gel System (E-C Apparatus Corp., NY, U.S.A.) that can be used to run two gels simultaneously. The assembly of the glass plate cassettes (8.3 X 7.4 cm) and the process of gel casting were done according to instruction manual provided with the apparatus. Once the cassettes were properly assembled and mounted, the preparation of the separating and stacking gels was started.

The 12% separating gel and 5% stacking gel polymerizing solutions were prepared just before use by mixing the given volumes of stock solutions in the written order as given in Table 2.4. The separating gel solution was first prepared with the TEMED added just before casting the gel into the glass assembly from the edge of one of the spacers until the desired height of the solution (about 5 cm) was obtained. Then, the liquid gel was overlaid with distilled water (about 0.5 ml), without disturbing the gel surface, to obtain an even interface between the separating gel and the stacking gel. The gel was then allowed to polymerize at room temperature for a minimum of 30 minutes. After polymerization, the layer of

water was removed completely using filter paper without hurting the gel surface. The stacking gel was then poured on the top of the resolving gel and the comb was inserted into the layer of the stacking gel without trapping air bubbles under the teeth of the comb. The gel was then allowed to polymerize for a minimum of 30 minutes. After the gel was polymerized, the comb was removed carefully and the wells were washed with distilled water and filled with electrode buffer. At this point, the gel cassettes were removed from the casting stand, mounted and clamped onto the running frame with the notched glass plate of each cassette facing inside. When running only one gel, the blank plastic plate, provided with the system, was mounted in the place of the second cassette in the casting stand and in the running frame.

Aliquots from the protein samples to be analyzed and from the standards mixture were diluted 3:1 with the 4X sample buffer (3 parts sample and 1 part sample buffer), to have the samples in 62.5 mM Tris-HCl buffer, pH 6.8, 2% SDS, 5% 2-mercaptoethanol, 10% glycerol and 0.001% bromophenol blue. Then the samples and standards were placed in a boiling water bath for 2 minutes. Afterwards, protein samples and molecular weight standards (20µl) were loaded into different wells using sample application tips.

Table 2.4. Formulations for SDS-PAGE Separating and Stacking Gels

	Separating Gel	**Stacking Gel**
Monomer Concentration	**12 %**	**5 %**
Acrylamide/bisacrylamide	6.0 ml	0,813 ml
Distilled water	5.0 ml	2,858 ml
1.5 M Tris-HCl, pH 8.8	3,8 ml	----
0.5 M Tris-HCl, pH 6.8	----	1,25 ml
10% (w/v) SDS	150 µl	50 µl
10 % APS	93 µl	25µl
TEMED	7,5 µl	5 µl
Total monomer	15 ml	5 ml

After loading the samples, the running buffer (135 ml) was added to the compartment formed by the running frame and the cassettes (the upper buffer compartment) and the system was checked for leakage. The running buffer (250 ml) was then also added to the outer tank (the lower buffer compartment). Thereafter, the running frame was inserted into the outer tank, the safety cover was replaced and the leads were plugged into the EC 250-90 electrophoresis power supply. The power supply was adjusted to give a constant current of 15 mA when the samples were in the stacking gel and 30 mA when the samples passed to the separating gel. Under these conditions the voltage was about 50 V at the beginning and elevated up to 100 V at the end of the run that took a total of about 2 hours.

The power supply was switched off, when the dye front is just 0.5 cm from the lower end of the glass plates, the running frame was taken out and the buffer was removed from the upper buffer compartment. Afterwards, the clamps were detached and the cassettes were removed from the running frame. To gain access to the gels in the cassette, the glass plates were pried apart using a spatula taking care not to chip the edges of the glass plates. The left-top corner of each gel was cut to indicate the order of wells. The gels, usually adhered to one of the glass plates, were taken carefully using gloves and placed in the previously prepared appropriate solutions to stain the samples which have been resolved on the gels, or to prepare the gels for subsequent blotting.

2.6. Silver Staining of the SDS-PAGE Gel

The silver staining of the SDS-PAGE gels was carried out according to the rapid silver staining method of the Donelson Lab (2000) as explained in Table 2.5.

The relative mobility (R_f) of each protein was determined by dividing its migration distance from the top of the separating gel to the center of the protein band by the migration distance of the bromophenol blue tracking dye from the top of the separating gel.

$$R_f = \frac{\text{Distance of protein migration}}{\text{Distance of tracking dye migration}}$$

The R_f values were plotted against the known molecular weights (logarithmic scale ordinate) and standard line was drawn and its slope was used in the calculation of the molecular weight of proteins.

2.7. Electroblotting of the Gels from SDS-PAGE

Electroblotting was carried out using EC140 Mini Blot Module of the EC120 Mini Vertical Gel System (E-C Apparatus Corp., NY, U.S.A.), and Polyvinylidene difluoride (PVDF) was used as a blotting membrane. The gels obtained from the SDS-PAGE were electroblotted directly. Biotinylated low range molecular weight markers given below were used as molecular weight standards

- Phoshorylase b[4]	(M_r 97400)
- Albumin, bovine serum	(M_r 66200)
- Ovalbumin, chicken egg	(M_r 45000)
- Carbonic anhydrase, bovine erythrocytes	(M_r 31000)
- Trypsin Inhibitor, soybean	(M_r 21500)
- Lysozyme	(M_r 14400)

Prior to electroblotting, the gels taken from SDS-PAGE were placed for 30 min, with shaking, in the Towbin transfer buffer (25 mM Tris, 192 mM glycine and 20 % methanol) (Towbin *et al.*, 1979).

While the gels were incubated in the transfer buffer, the other system components and the transfer membrane were prepared. All of the electroblotting procedure was carried out wearing gloves. The PVDF transfer membrane, with the dimensions of the gel to be transferred, was soaked in 100 % methanol for 30 seconds with shaking, to overcome the hydrophobicity of the membrane. Then, the

wet membrane is washed several times with distilled water and then with transfer buffer until it was equilibrated (it should submerged into the solution not floating over it), the point at which the membrane is ready to bind the proteins. The membrane should not be allowed to dry; otherwise proteins will not bind to it. The membrane does dry during the procedure; the wetting procedure should be repeated again. Afterwards, two pieces of filter paper, the Scotch Brite sponge pads, and the transfer membrane were soaked in the transfer buffer for 15 min with continuous shaking. The blotting stack was assembled on the top of stainless steel grid cathode located in the trough of the frame stand of the Mini Blot Module, to which a small amount of transfer buffer was added. The configuration of the assembly was as follows:

Top	Cover with Palladium Wire Anode
	Sponge Pad
	Sponge Pad
	Filter Paper
	PVDF Transfer Membrane
	Gel
	Filter Paper
	Sponge Pad
Bottom	Frame stand with Stainless steel Grid Cathode

After the above assembly was prepared, the cover of the electroblotting module was pressed onto the blotting stack and fixed with the clamps after turning assembled blotting module upright and then filled with the transfer buffer (about 100 ml). Thereafter, the fully assembled module was inserted into the outer tank and the safety cover with leads was replaced. The red lead was connected to the anode (+) and the black lead to the cathode (-), were the proteins will be transferred as anions to the direction of anode. The transfer process was performed at room temperature for 50 minutes using a constant voltage of 15–20 V. when the blotting was finished, the PVDF membrane was immediately removed and placed

in the proper solutions, previously prepared, either for total protein staining or immunostaining.

Table 2.5. Procedure for Rapid Silver Staining of Proteins in Polyacrylamide Gels.

Steps	Solution[a]	Time of Treatment[b]
1) Fix	40 % Methanol; 0.5 ml 37 % HCOH /liter Water	10 min
2) Wash	With sterile dH_2O	2 X 5 min
3) Pretreatment	$Na_2S_2O_3.5H_2O$ (0.2 g/liter)	1 min[c]
4) Rinse	With sterile dH_2O	2 X 20 sec[c]
5) Impregnate	$AgNO_3$ (0.1%)	10 min
6) Rinse	With sterile dH_2O	Several sec[c]
7) Wash	With developer Solution	Several sec[c]
8) Develop	Developer Solution: Na_2CO_3 (3% wt/vol); 0.5 ml 37 % HCOH /liter; $Na_2S_2O_3.5H_2O$ (0,0004% wt/vol)	Until bands appear
9) Stop	2,3 M Citric acid / 50 ml of developer	10 min
10) Wash	With sterile dH_2O	10 min
11) Storage	40 % Methanol 0.5 ml 37 % HCOH /liter	Store at 4^oC

[a] Solutions freshly prepared in a quantity that is 10-fold larger than the volume of the gel.
[b] Steps 1-10 were carried out on a shaker at room temperature (20-25³C).
[c] The times indicated here should be observed exactly in order to ensure a reproducible image development.

2.7.1. Immunostaining of the PVDF Membranes

Immunostaining was carried out according to the instruction manual provided with the Amplified Alkaline Phosphatase (AP) Western Blotting Kit (Bio-Rad) that was used in the immunostaining of the electroblotted PVDF membranes. All of the incubations were performed in a minimum of 6 ml of solutions in each step with continuous shaking at room temperature.

The electroblotted PVDF membrane was incubated in the blocking solution (5 % non-fat dry milk in TTBS buffer) for 1 to 2 hours. Afterwards, the membrane was incubated with the antibodies diluted in the blocking solution for 1 to 2 hours in the monoclonal anti-GST antibody (1/2000 diluted) and the monoclonal RGS-His antibody (1/2000 diluted). The membrane was then washed five times, each for 5 min with TTBS and incubated with the secondary antibody (biotinylated goat anti-rabbit) with the 1/3000 dilution in TTBS for 1 to 2 hours. During the secondary antibody incubation period, the streptavidin-biotinylated AP complex was prepared by the addition of streptavidin to biotinylated AP (both 1/3000 diluted in TTBS) and allowed to stand at least 1 hour and not more than 3 hours at room temperature.

After the incubation with secondary antibody, the membrane was washed again with TTBS (five times, each 5 min) and then incubated for 1-2 hours in the previously prepared streptavidin-biotinylated AP complex. Afterwards, the membrane was washed three times, 5 min each, again with TTBS and the AP color developing solution (BCIP/NBT) was added. The specific protein bands started to appear after 10 - 30 min. Finally, the membranes were carefully dried and the images were obtained using a scanner connected to the computer.

2.8. Working Electrode Preparation

2.8.1. Gold Bar Pre-treatment

Gold electrodes (99.99%, 3 mm in diameter) were polished for 5 minutes using 1 g of 0.1 µm alumina suspension geometrically diluted up to 100 ml Millipore water on Brown cloth by using hand-made polishing equipment (Figure 2.1). The electrodes were then thoroughly washed using deionized water to remove alumina particles.

After first polishing, electrodes were polished until a mirror surface was obtained using 0.1 µm alumina suspension, containing 1% CrO_2, geometrically diluted up to 100 ml Millipore water on Black cloth. The electrodes were then thoroughly washed using deionized water to remove alumina particles.

The surfaces of the electrodes were checked by using a Zeiss optical microscope to assure polishing and alumina particle removal.

After mechanical polishing, electrodes were plasma cleaned by using Harrick Oxygen Plasma Cleaner for 10 min.

2.8.2. Thioctic Acid Deposition

After cleaning, the electrodes are rinsed using pure ethanol (99.7%) and immersed in 2% thioctic acid in pure ethanol, then left to react 12 hours.

2.8.3. Protein Coupling

After self-assembled thioctic acid layer formation, the electrodes were washed with pure ethanol and blowed dry with N_2-gas. They were immersed into 0.01% EDC (W/V) in dried acetonitrile.

Figure 2.1. Home-made polishing equipment (Chemicentrum, Lund).

The proteins were concentrated by ultrafiltration. Protein solution was put into the microcon filters (MW 3000 CO) and 0.5 ml of 0.1 M Tris-tricine buffer pH 8.6 was added and centrifuged at 12000 rpm, for 75 min at 10^{o}C.

The recover the proteins, the filter was turned up side down and centrifuged for 10 min at 6000 rpm. After centrifugation, proteins were diluted up to 0.04 mg/ml by using 0.1 M Tris-tricine buffer, pH 8.6.

After EDC activation, electrodes were washed with 0.1 M Tris-tricine buffer, pH 8.6, and immersed in the protein solution and left to react 20 hours.

2.8.4. Dodecanthiol Treatment

Prior to use, the protein-coupled electrodes were washed with 0.1 M Tris-tricine buffer, pH 8.6. Then, the electrodes were immersed into 10 mM 1-dodecanthiol in pure ethanol for 20 minutes, and washed with 0.01 M Tris-tricine buffer, pH 8.6.

2.9. Capacitance Measurements

The biosensor was inserted as the working electrode in a specially constructed four-electrode flow cell with a dead volume of 10 µl as shown in Figure 2.2. The electrodes were connected to a fast potentiostat. A platinum foil and platinum wire served as auxillary reference electrodes, respectively. An extra reference electrode (Ag/AgCl) was placed in the outlet stream. The buffer solutions were pumped by Minipulse 3 peristaltic pump with a flow rate of 0.25 ml/min.

The heavy metal standards [$Cd(NO_3)_2.4H_2O$, $CuCl_2.2H_2O$, $ZnCl_2$, $HgCl_2$] were injected into the flow via a 250 µl sample loop in a range of 10 mM-1 fM. The carrier buffer (10 mM Tris-tricine, pH 8.6) was filtered through a 0.22 µm Millipore filter and degassed before.

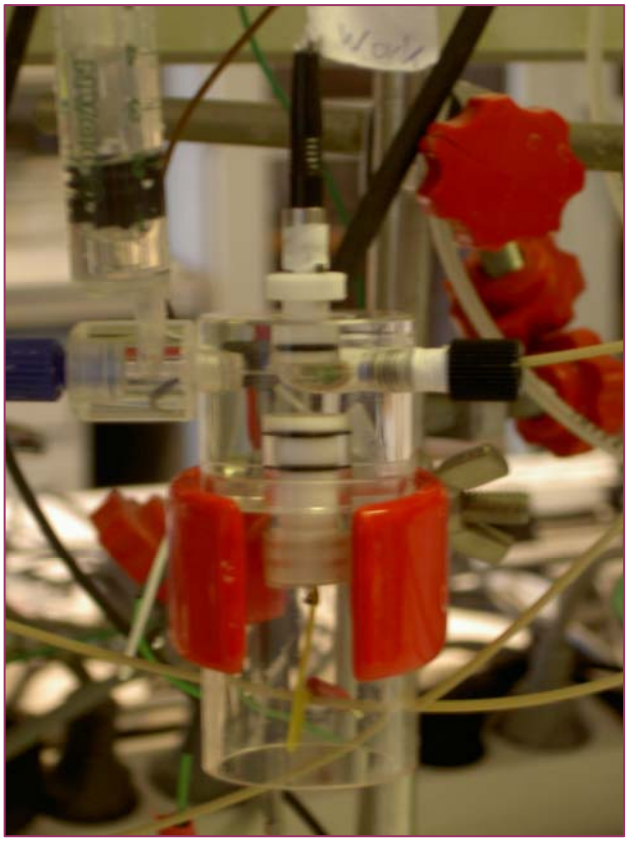

Figure 2.2. Constructed four-electrode flow cell

The working electrode had a resting potential of 0 mV vs. the Ag/AgCl reference electrode. Measurements were made by applying potential pulse 50 mV and recording the current transients following the potential step according to equation,

$$i(t) = \frac{u}{R_S} \exp(-\frac{t}{R_S C_{tot}})$$

where, ***i(t)*** is the current at time *t*, ***u*** is the applied pulse potential, $\boldsymbol{R_s}$ is the resistance of recognition layer, $\boldsymbol{C_{tot}}$ the total capacitance at the electrode/solution interface.

The current values were collected with a frequency of 50 kHz, and the first 10 values were used for the evaluation of the capacitance. An equal current transient but with opposite sign was obtained when the potential was stepped back to the resting value. The platinum reference electrode controls the working electrode potential, but it does not have a well-defined potential. However, such an electrode is necessary to obtain a sharp response in a small dead volume cell. Therefore, the platinum and Ag/AgCl reference electrodes were compared potentiometrically just before a step was applied. The computer adjusted the working electrode potential so that the potentiostat behaved as if it had Ag/AgCl reference controlling the working electrode.

2.10. Cyclic Voltammetry Measurements

Cyclic voltammograms were recorded in 5 mM $K_3[Fe(CN)_6]$, 0.1 M KCl in a batch cell, with the unmodified and modified electrode as the working electrode, an Ag/AgCl as reference electrode, and a platinum flag as the auxillary electrode with scan rate of 100 mV/s. The electrodes were connected to an Autolab Potentiostat-Galvanostat (Utrecht, Netherlands), connected to a computer.

CHAPTER III

RESULTS

3.1. Transformation of Competent Cells with pET42a DNA

After preparing competent BL21(DE3) *E. Coli* cells by $CaCl_2$ treatment and introduction of pET-42a plasmid carrying C-terminally polyhistidine-tagged *S. japonicum* GST, transformed bacterial cells were incubated at 37^{o}C in kanamycin sulfate containing plates and selection of transformants was accomplished by the plasmid encoded kanamycin resistance (Figure 3.1). It was performed by pET expression system manual method.

One colony was taken from the culture and the further procedures were accomplished.

3.2. Plasmid Isolation

Plasmid isolation from transformed cells was done for confirming the transfer of plasmid DNA into the competent cells according to Gr (-) bacteria plasmid isolation method of Maniatis (1989). As seen in Figure 3.2**,** the two bands

indicated by arrows in Lane 5 containing DNA isolated from transformed cells, correspond to the pET42a plasmid bands in Lane 2.

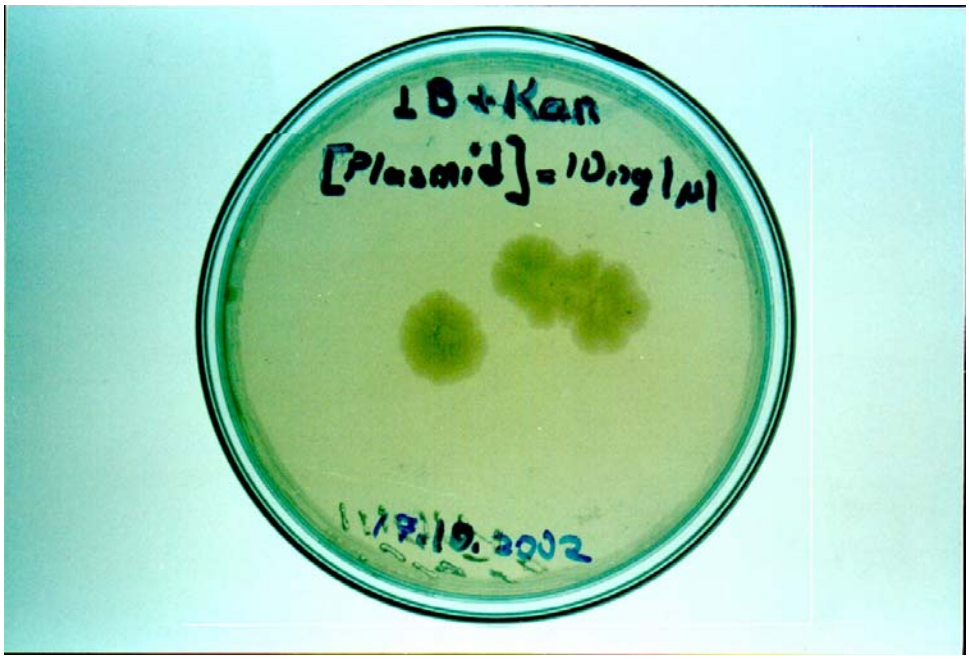

Figure 3.1. Transformed colonies on a LB agar plate containing kanamycin sulfate

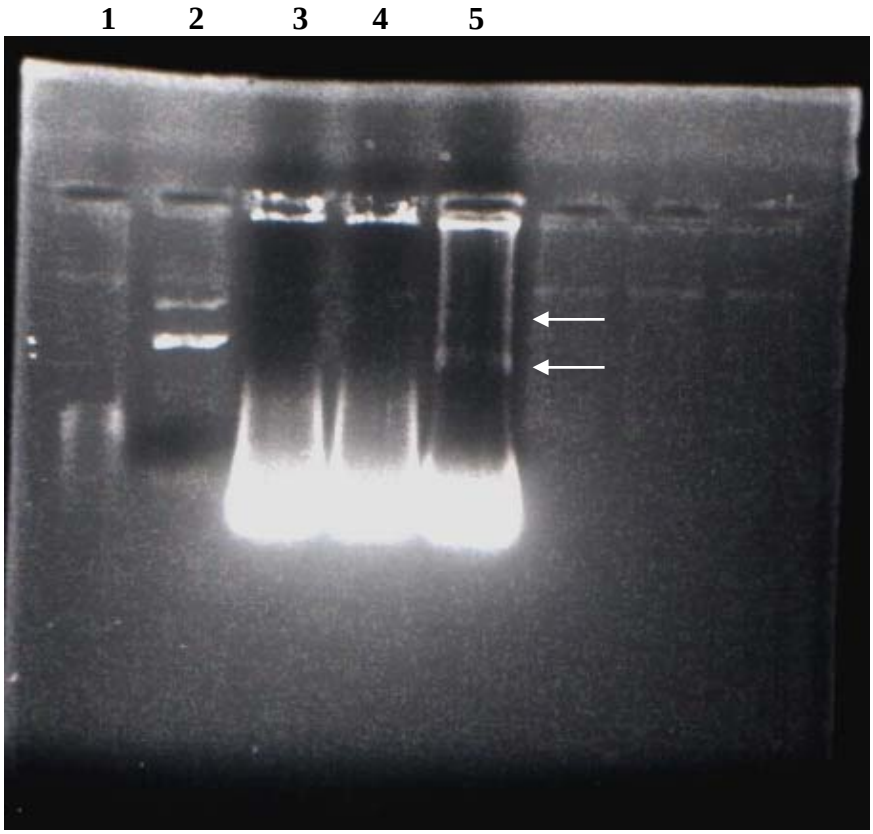

Figure 3.2. Agarose gel electrophoresis of isolated E. coli DNA from transformed competent cells.

Lane1: DNA ladder

Lane 2: pET42a

Lane 3 and 4: Not-transformed competent cells

Lane 5: Transformant

3.3. GST-$(His)_6$ Activity

Recombinant glutathione S-transferase (GST-$(His)_6$) activities in the fractions, prepared from cultured transformed bacteria cells, were determined spectrophotometrically using 1-chloro-2,4-dinitrobenzene (CDNB) as a substrate by monitoring the thioether formation at 340 nm as described by Habig and co-workers (Habig *et al*., 1974). Some kinetic properties of the recombinant GST were established.

The reaction mixture contained 0.05 mM GST-Assay Buffer, pH 6.9, 1 mM CDNB, 1 mM GSH, 1.7 µg GST-$(His)_6$ enzyme in the final volume of 1.0 ml. The reaction was initiated by addition of enzyme and followed for 300 seconds, as described under "Materials and Methods". The duplicate measurements were done at room temperature.

The average value of GST enzyme activity of bovine liver cytosols was calculated as 4.58 µ 0.25 (Mean µ S.E., n = 5) µmole/min/mg towards CDNB.

3.3.1. Reaction Time Course of GST-$(His)_6$

The reaction mixture was prepared with pH 6.9, 10xGST assay phosphate buffer containing 1 mM CDNB, 1 mM GSH. 1.7 µg GST-$(His)_6$ was added into 1 ml reaction mixture.

Figure 3.3 shows the reaction time course plot of GST-$(His)_6$ using CDNB as substrate. It was found that absorbance linearly increased during 300 seconds.

3.3.2. Effect of Enzyme Amount on GST-$(His)_6$ Activity

Effect of enzyme amount on the GST-$(His)_6$ activity was measured by changing the final protein concentration in the 1.0 ml reaction mixture between 0.85 µg and 17 µg protein. It was found that the activity was proportional with enzyme amount up to 1.7 µg protein in 1.0 ml reaction mixture.

Effect of protein amount on recombinant GST-$(His)_6$ enzyme activity is shown in Figure 3.4.

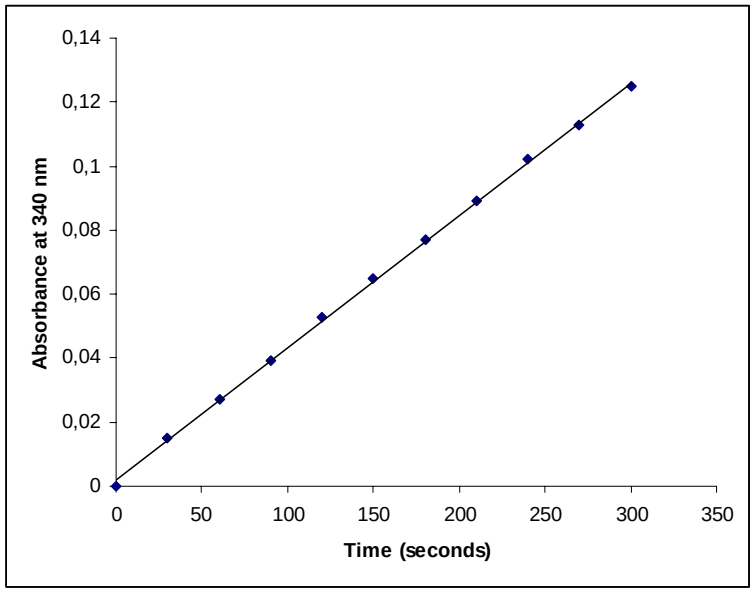

Figure 3.3. GST-$(His)_6$ reaction time course plot

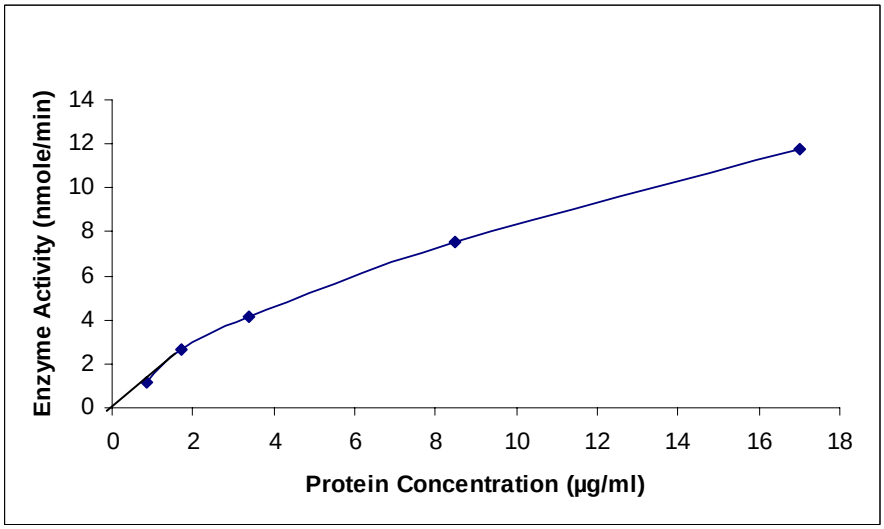

Figure 3.4. Effect of enzyme amount on GST-$(His)_6$ activity
(Values are expressed as mean ± S.E.M)

3.4. Thrombin Cleavage Standardization

Thrombin cleavage was done for cleavage and removal of the His tag-S-protein from GST-$(His)_6$ with 0.04, 0.02, 0.01 and 0.005 U thrombin/µl, incubated at 4, 8 and 16 hours at 22^{o}C, by using Novagen Thrombin Cleavage Capture kit. The extent of cleavage of the samples was determined by SDS-PAGE analysis given in Figure 3.5, 3.6 and 3.7. Protein bands on the gels were stained by rapid silver staining method.

After cleavage, non-cleaved recombinant protein band (MW of 34100 Da) was cleaved into GST-$(His)_6$ (MW of 26500) and S-protein (MW of 7500 Da).

As shown in Figure 3.7, the dissapearence of the uncleaved recombinant protein band and the increase in the density of the cleaved GST-$(His)_6$ band were considered as an indication of the complete cleavage. After standardization, 0.04 U/µl diluted thrombin was used at 16 hr incubation time for further cleavage procedures.

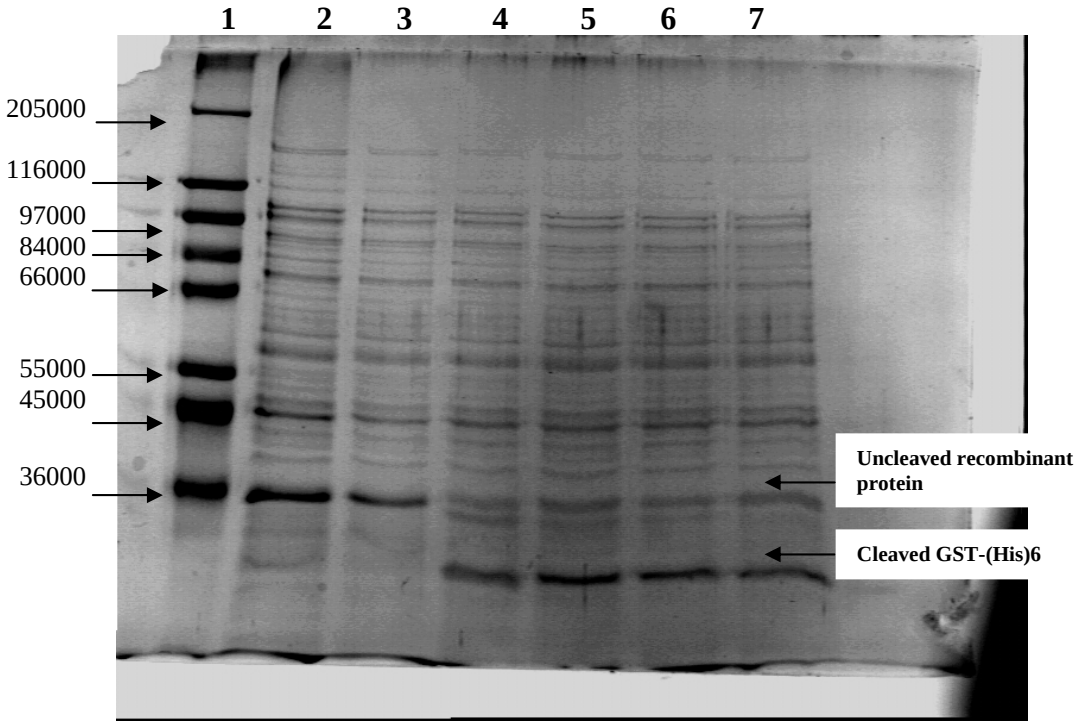

Figure 3.5. SDS-PAGE stained with silver (12%), of the cleaved fractions (4µg/µl) at 4 hours and high range molecular weight markers (36000 Da –205000 Da).

Lane 1: Molecular weight markers

Lane 2: Bacterial sonicate

Lane 3: GST-$(His)_6$-His tag-S protein (no thrombin)

Lane 4: 0.04 U/µl diluted thrombin

Lane 5: 0.02 U/µl diluted thrombin

Lane 6: 0.01 U/µl diluted thrombin

Lane 7: 0.005 U/µl diluted thrombin

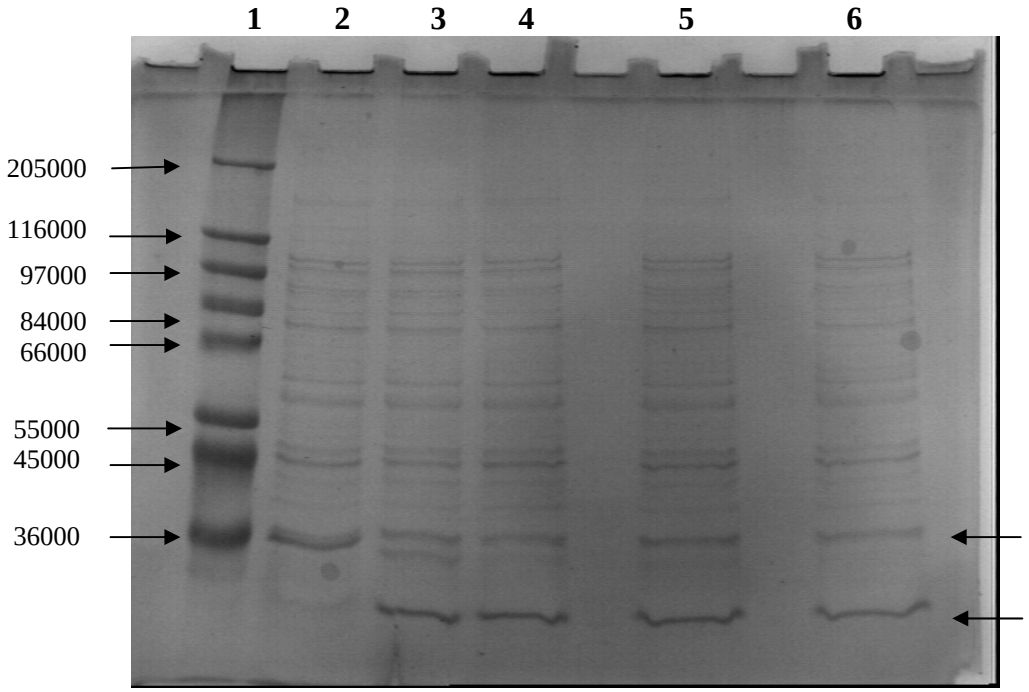

Figure 3.6. SDS-PAGE stained with silver (12%), of the cleaved fractions (4µg/µl) at 8 hours and high range molecular weight markers (36000 Da –205000 Da).

Lane 1: Molecular weight markers

Lane 2: GST-$(His)_6$-His tag-S protein (no thrombin)

Lane 3: 0.04 U/µl diluted thrombin

Lane 4: 0.02 U/µl diluted thrombin

Lane 5: 0.01 U/µl diluted thrombin

Lane 6: 0.005 U/µl diluted thrombin

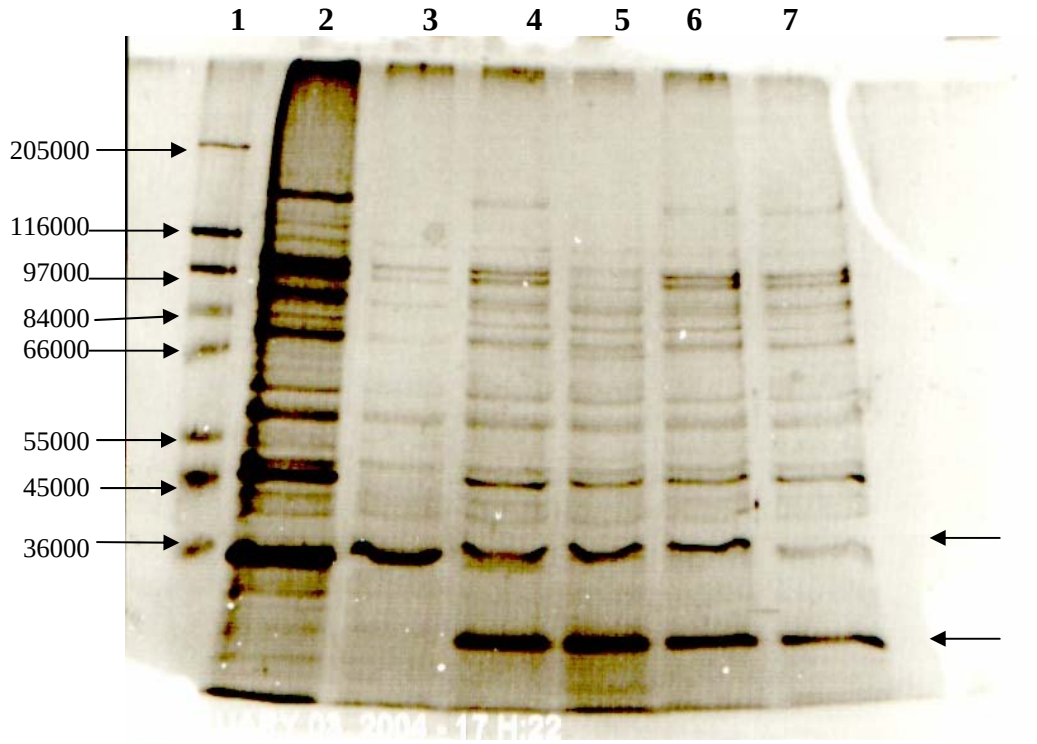

Figure 3.7. SDS-PAGE stained with silver (12%), of the cleaved fractions (4µg/µl) at 16 hours and high range molecular weight markers (36000 Da –205000 Da).

Lane 1: Molecular weight markers

Lane 2: Bacterial sonicate

Lane 3: GST-$(His)_6$-His tag-S protein (no thrombin)

Lane 4: 0.04 U/µl diluted thrombin

Lane 5: 0.02 U/µl diluted thrombin

Lane 6: 0.01 U/µl diluted thrombin

Lane 7: 0.005 U/µl diluted thrombin

3.5. GST-$(His)_6$ Purification

The purification of the GST-$(His)_6$ from bacterial sonicate (for batch purification 0.9 mg/ml and for column purification 3 mg/ml with 1566.5 unit/mg of GST enzyme activity towards CDNB) was carried out basically according to the Amersham Bulk GST and Qiagen Ni-NTA purfication protocols with some modifications. These methods included the sequential Glutathione Sepharose 4B affinity column and Ni-NTA column chromatography after specific protease (thrombin) cleavage procedure.

As described under "Methods", the protein solution after thrombin cleavage step was applied to preequilibrated Glutathione Sepharose 4B affinity column (1.0 cm X 4.5 cm). The cleaved fraction containing a total of 3 mg protein with 1667.5 unit/mg of GST enzyme activity towards CDNB was loaded to the column at a flow rate of 0.5 ml/hour. Afterwards, the column was washed with the equilibration buffer. The eluate containing a total of 0.0156 mg protein with 81472 unit/mg of GST enzyme activity towards CDNB was loaded to the preequilibrated Ni-NTA spin columns with 600 µl capacity and the spin columns were washed with the equilibration buffer containing imidazole. Elution was done with elution buffer containing 250 mM imidazole. Eluates were collected and dialysed against sonication buffer and stored as aliquats in -80^oC.

All of the purification process results are summarized in Table 3.1 for the purification of GST-$(His)_6$ from transformed bacterial cell culture

Table 3.1. Column Purification Table of GST-$(His)_6$ from Transformed Bacterial Cell Culture.

Fractions	*Volume of Fraction (ml)*	*Protein Concentration (mg/ml)*	*Total Amount (mg)*	*Activity (nmole/min)*	*Specific Activity (nmole/min/mg)*	*Total Activity (nmole/min)*	*Yield (%)*	*Purification Fold*
Bacterial Sonicate	0.882	3.4	3	5326	1566.5	4697.5	100	1.00
Thrombin Cleavage	15	0.2	3	333.5	1667.5	5002.5	106.5	1.06
GSH Sepharose 4B Affinity Column	2.02	0.0156	0.0315	1271	81472	2567.3	54.6	52.0
Ni-NTA Spin Column	0.6	0.084	0.0504	105	1250	63	1.34	0.8

3.6. Characterization of GST-$(His)_6$ Activity

Kinetic characterisation of GST-$(His)_6$ was achieved by using GSH Sepharose 4B affinity column eluate. Since the enzyme was eluted in 50 mM GSH containing Tris-HCl buffer at pH 8.0 as described under "Materials and Methods", GSH may interfere with the determination of kinetic constants, therefore, the fraction is subjected to dialysis in order to remove GSH.

The reaction mixture was prepared with pH 6.9, 10x GST assay phosphate buffer containing 1 mM CDNB, 1 mM GSH. 1.7 µg/ml GST enzymes were added into 1 ml reaction mixture. The duplicate measurements were done at room temperature.

3.6.1. Effect of pH on GST-$(His)_6$ Activity

Effect of pH on GST activity was measured by changing the pH of 10x GST assay phosphate buffer between 6 and 9 in the 1.0 ml reaction mixture. It was found that the activity increased from pH 6 through pH 7.4, then decreased linear until pH 9.0. Figure 3.8 shows the effect of pH on GST activity.

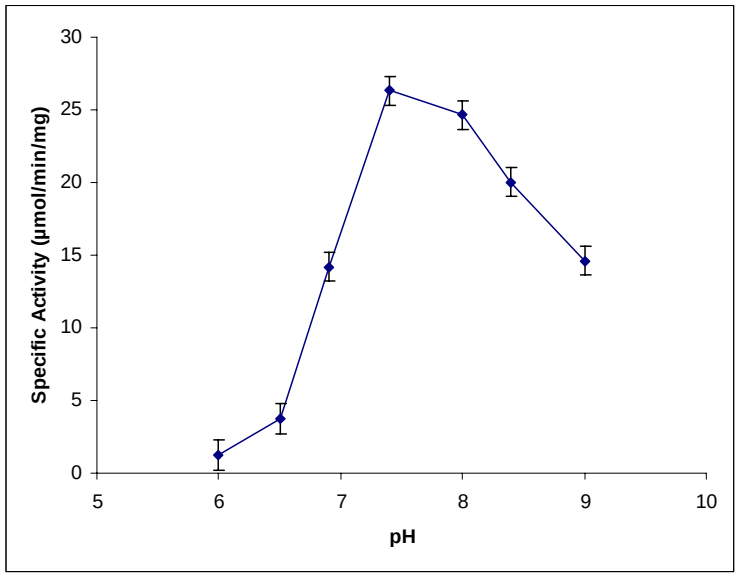

Figure 3.8. Effect of pH on GST-$(His)_6$ activity (Values are expressed as mean ± S.E.M).

3.6.2. Effect of Substrate (CDNB) Concentration on GST-$(His)_6$ Activity

The effect of substrate 1-chloro-2,4-dinitrobenzene (CDNB) concentration on GST activity was measured by changing CDNB concentrations in the 1.0 ml reaction mixture between 0.25 mM and 2 mM. The effect of substrate concentration is shown Figure 3.9. It was found that GST activity reached saturation at around 1,5 mM CDNB. In addition, GST-$(His)_6$ Km and Vmax were calculated for CDNB by constructing Lineweaver–Burk plot (Figure 3.10). With the help of Lineweaver–Burk plot GST Km (CDNB) and Vmax (CDNB) were calculated as 0.23 mM and 5.34 µmol/min/mg, respectively.

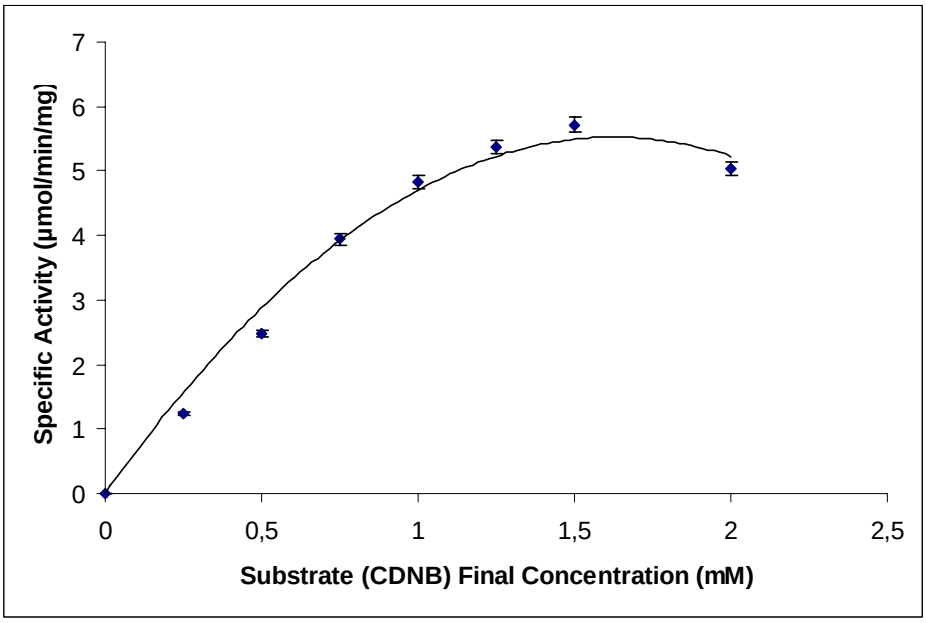

Figure 3.9. Effect of CDNB concentration on GST-$(His)_6$ activity at pH 6.9 (Values are expressed as mean ± S.E.M).

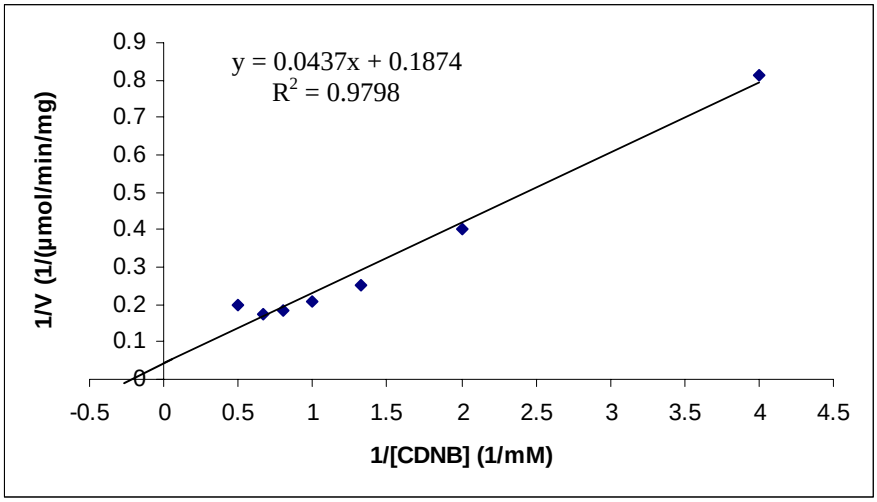

Figure 3.10. Lineweaver-Burk Plot of GST-$(His)_6$ activity against substrate (CDNB)

3.6.3. Effect of Cofactor Reduced Glutathione (GSH) Concentration on GST-$(His)_6$ Activity

The effect of reduced glutathione (GSH) concentration on GST-$(His)_6$ activity was measured by changing GSH concentrations in the 1.0 ml reaction mixture between 0.25 mM and 1.5 mM. The effect of GSH concentration is shown in Figure 3.11. It was found that GST activity was reached saturation at around 1 mM GSH. In addition, K_m and V_{max} were calculated for GSH by constructing Lineweaver–Burk (Figure 3.12). According to the Lineweaver–Burk GST K_m (GSH) and V_{max} (GSH) were found as 0.27 mM and 6.63 µmol/min/mg, respectively.

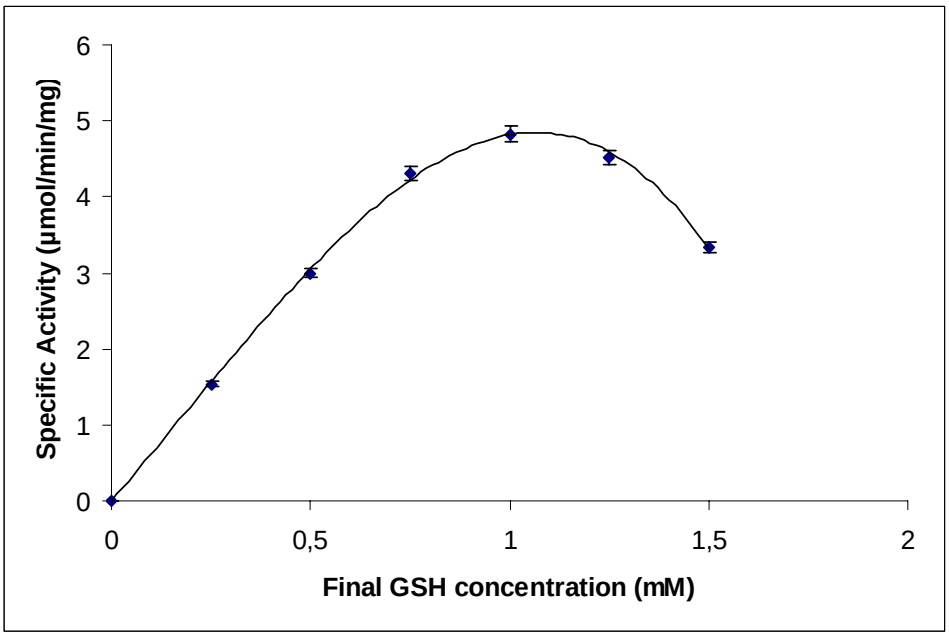

Figure 3.11. Effect of GSH concentration on GST-$(His)_6$ activity at pH 6.9 (Values are expressed as mean ± S.E.M).

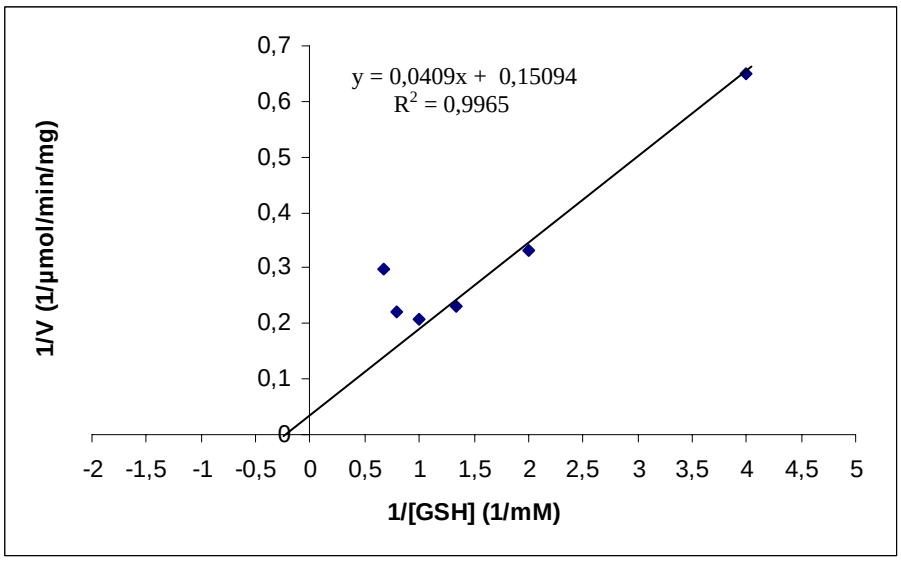

Figure 3.12. Lineweaver-Burk Plot of GST-$(His)_6$ activity against cofactor (GSH).

3.6.4. Imidazole Effect on GST-$(His)_6$ Activity

The presence effect of imidazole concentration on GST-$(His)_6$ activity was measured by changing imidazole concentrations in the 1.0 ml reaction mixture between 25 mM and 250 mM. The inhibition effect of imidazole concentration is shown in Figure 3.13.

The inhibition effect of imidazole concentrations on GST-$(His)_6$ activity was 67% at the final 250 mM imidazole concentration.

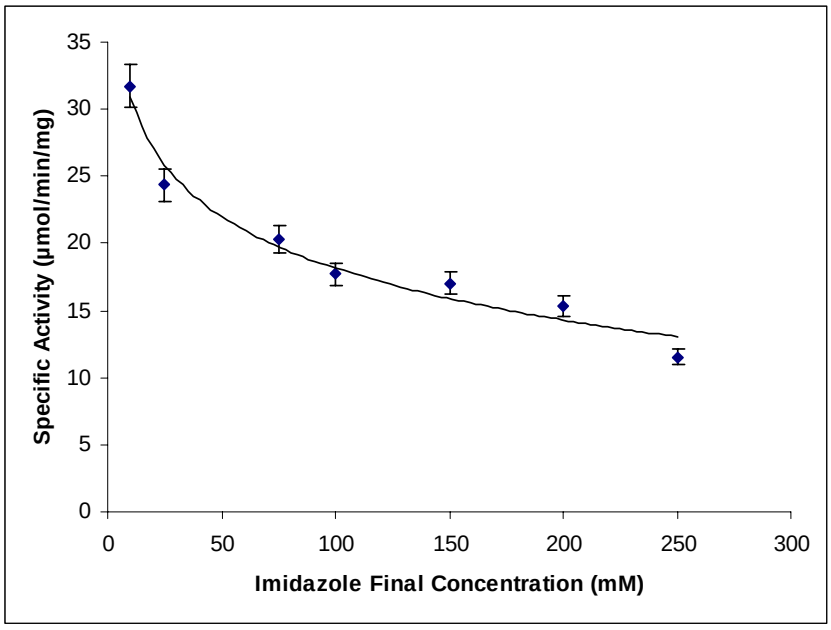

Figure 3.13. The inhibition effect of imidazole concentration on GST-$(His)_6$ activity (Values are expressed as mean ± S.E.M).

3.7. SDS-PAGE and Western Blotting Analysis of the Purified GST-$(His)_6$ Protein

After GST-(His_6) protein purification, fractions obtained from purification steps were analyzed with SDS-PAGE gel method. Protein bands were visualized with short silver staining method.

In the Figure 3.14, lanes contained molecular weight markers and protein fractions obtained from the column purification of the recombinant protein. The SDS-PAGE revealed that the GST-$(His)_6$ is a homodimer with a subunit molecular weight of about 26500 Da. This was also confirmed by the Western Blotting, where the gel obtained from the SDS-PAGE was electroblotted onto PVDF membrane and then immunostained with monoclonal Anti-GST antibody (Figure 3.15) and with monoclonal RGS-His antibody using the amplified alkaline phosphatase immunoblotting kit. Figure 3.16 shows the photograph of monoclonal His-tag antibody stained PVDF membrane of Ni-NTA elution fractions.

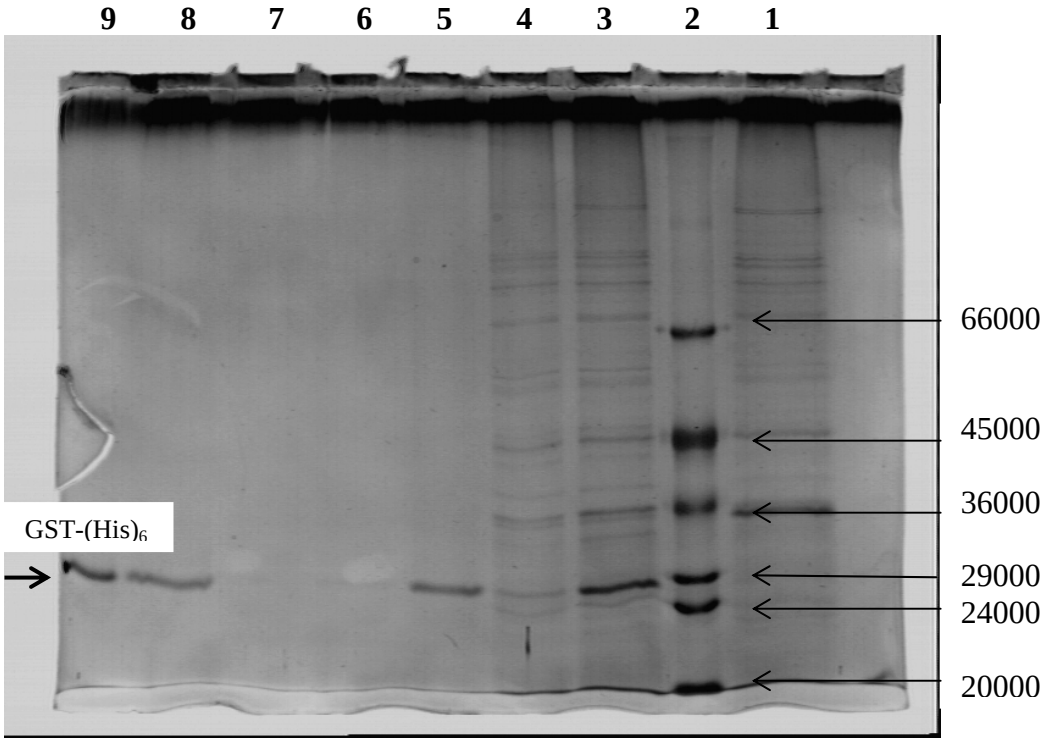

Figure 3.14. SDS-PAGE stained with silver (12%), of the protein fractions (each well containing 5 µg of protein) obtained from the each purification step and low range molecular weight markers (6500 Da –66000 Da).

Lane 1: Bacterial sonicate

Lane 2: Molecular weight markers

Lane 3: After thrombin cleavage

Lane 4: GSH Sepharose 4B flow through

Lane 5: GSH Sepharose 4B eluate

Lane 6: Ni-NTA Column Flow through

Lane 7: Ni-NTA Column Wash

Lane 8: Ni-NTA Eluate

Lane 9: GSH Sepharose 4B eluate after dialysis

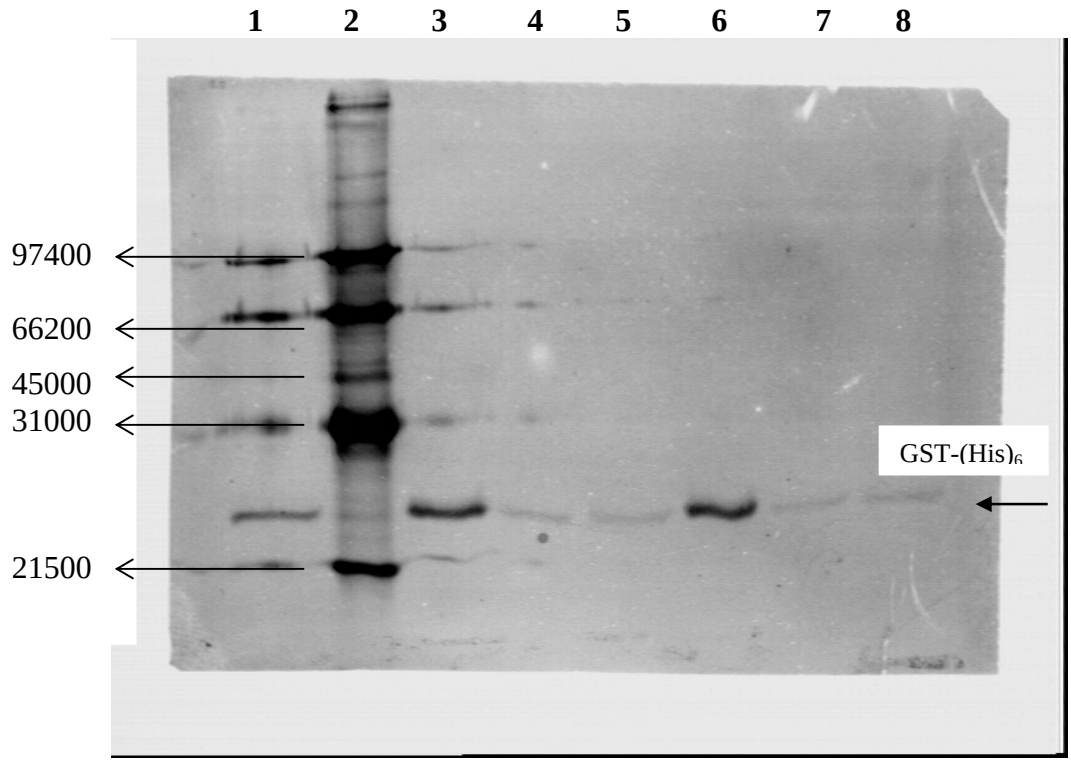

Figure 3.15. Western blotting of monoclonal Anti-GST antibody immunostained purification step fractions (each well containing 5 µg of protein) (PVDF membrane immunostained with monoclonal anti-GST) and biotinylated low range molecular weight marker (14400 Da-97400 Da)

Lane 1: Bacterial sonicate

Lane 2: Biotinylated molecular weight markers

Lane 3: After thrombin cleavage

Lane 4: GSH Sepharose 4B flow through

Lane 5: Ni-NTA Column Flow through

Lane 6: GSH Sepharose 4B eluate

Lane 7: Ni-NTA Eluate

Lane 8: GSH Sepharose 4B eluate after dialysis

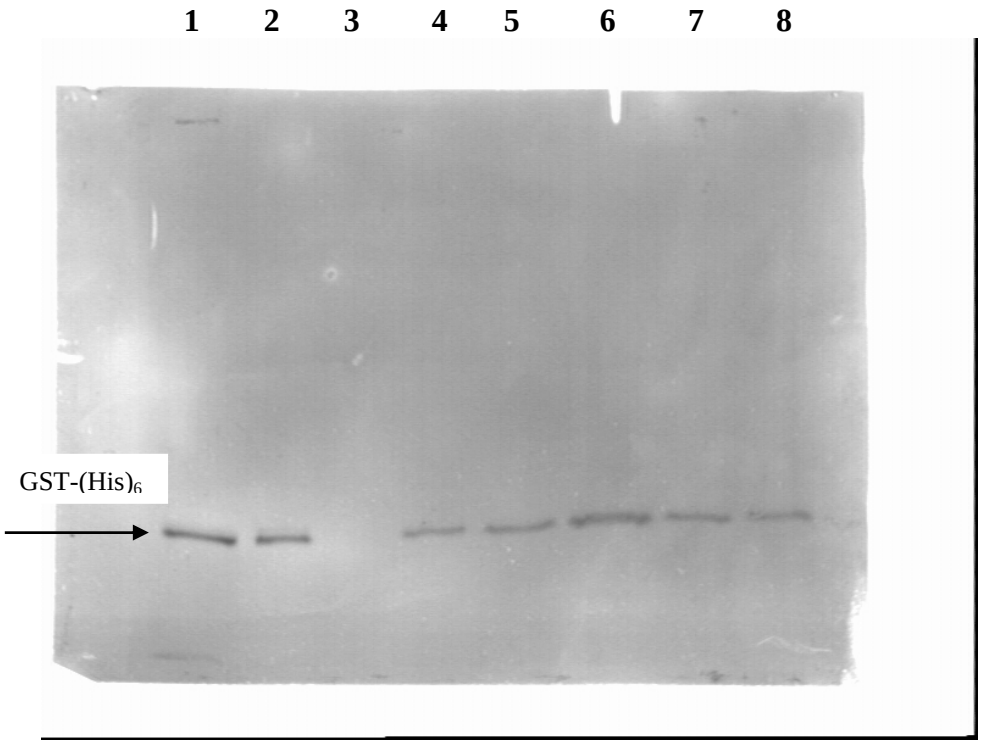

Figure 3.16. Western blotting of monoclonal RGS-His antibody immunostained Ni-NTA elution fractions (each well containing 5 µg of protein).

Lane 1: GSH Sepharose 4B eluation fraction

Lane 2: Ni-NTA Column eluation fraction

Lane 3: His-tag molecular weight markers

Lane 4: 90 mM Imidazole elution protein fraction

Lane 5: 100 mM Imidazole elution protein fraction

Lane 6: 150 mM Imidazole elution protein fraction

Lane 7: 200 mM Imidazole elution protein fraction

Lane 8: 250 mM Imidazole elution protein fraction

3.8. Preparation of Working Electrode

3.8.1. Cyclic Voltammograms

Modified gold electrode measurements were performed in 5 mM $K_3[Fe(CN)_6]$, 0.1 M KCl, with scan rate of 100 mV/s. An Ag/AgCl reference electrode was used. The complete insulation of gold electrode was shown in Figure 3.17.

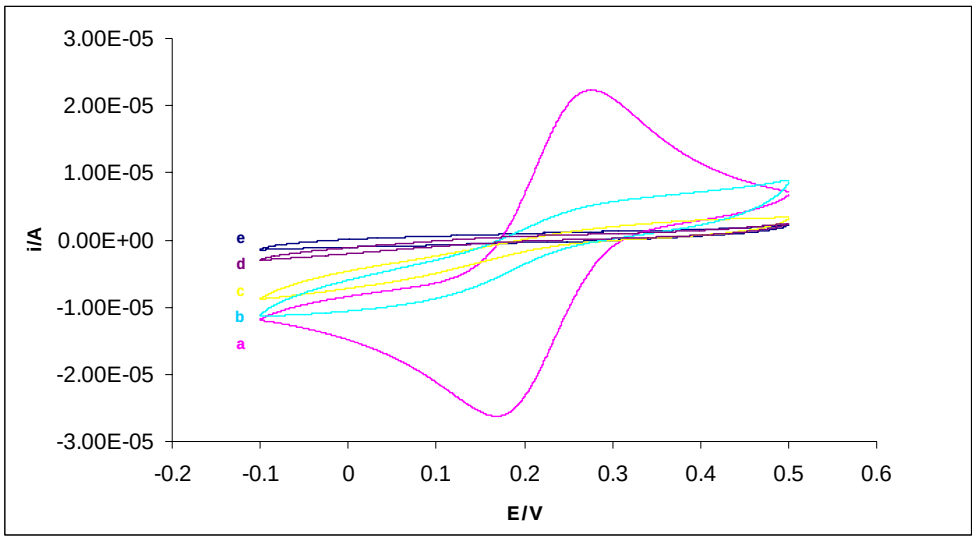

Figure 3.17. Cyclic voltammograms recorded for (a) clean gold electrode, (b) gold modified with thioctic acid, (c) gold modified with thioctic acid and EDC-immobilized GST-$(His)_6$ protein, (d) as in (c) but with additional 1-dodecanthiol treatment, (e) bare gold electrode (without $K_3[Fe(CN)_6]$).

3.9. Capacitance Measurements

The electrode which was decided to be appropriate by cyclic voltammetric measurements were placed into the electrochemical cell. The capacitance measurements were carried out under 0.01 M Tris-tricine buffer, pH 8.6, at a flow rate 0.25 mL/min, with the injection of 250 µL standard solutions, in four-electrode cell with a dead volume of 10 µl.

The heavy metal standards [$Cd(NO_3)_2.4H_2O$, $CuCl_2.2H_2O$, $ZnCl_2$, $HgCl_2$] were injected into the flow via a 250 µl sample loop in a range of 10 mM-1 fM. The carrier buffer (10 mM Tris-tricine, pH 8.6) was filtered through a 0.22 µm Millipore filter and degassed before using.

In order to optimize the capacitance measurement conditions, different buffer systems were tried. Capacitance changes of the GST-$(His)_6$ electrode to 1 nM Cd^{+2} and 1 nM Hg^{+2} standard solutions were studied by using 0.1 M Borate buffer at pH 8.75, 0.1 M Tris-HCl buffer at pH 8.2 and 0.1 M Tris-tricine buffer at pH 8.6 (Figure 3.18). The 0.1 M Tris-tricine buffer, pH 8.6 was used in measurements due to the regeneration problems with 0.1 M Borate buffer, pH 8.75.

In Figure 3.19 and 3.20, working electrode regenerations were shown by using different buffer compositions and EDTA concentrations. No regeneration was seen at the GST-$(His)_6$ electrode with 0.1 M borate buffer, pH 8.75 (Figure 3.19). Regeneration was seen at the GST-$(His)_6$ electrode with 0.1 M Tris-tricine buffer, pH 8.6 (Figure 3.20).

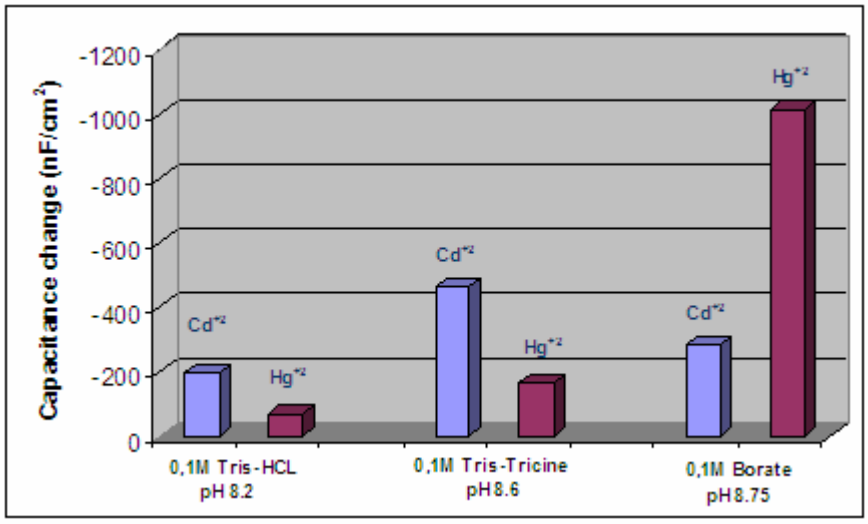

Figure 3.18. Capacitance changes of the GST-$(His)_6$ electrode to 1 nM Cd^{+2} and 1 nM Hg^{+2} at different buffer compositions and pH values.

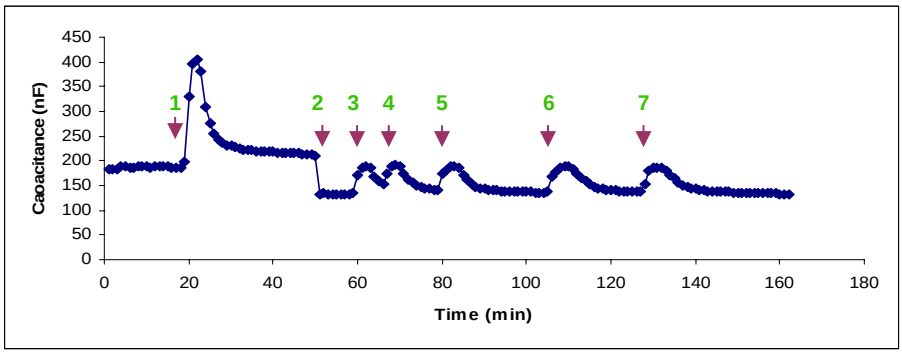

Figure 3.19. Regeneration graph for the GST-$(His)_6$ electrode under O.1 M Borate buffer pH 8.75, 0.25 ml/min, injection of 250 µl Cd^{+2} standard solution.
1) 10 mM EDTA, 2) 1 nM Cd^{+2}, 3) 10 mM EDTA, 4) 10 mM EDTA, 5) 20 mM EDTA, 6) 30 mM EDTA, 7) 50 mM EDTA injections.

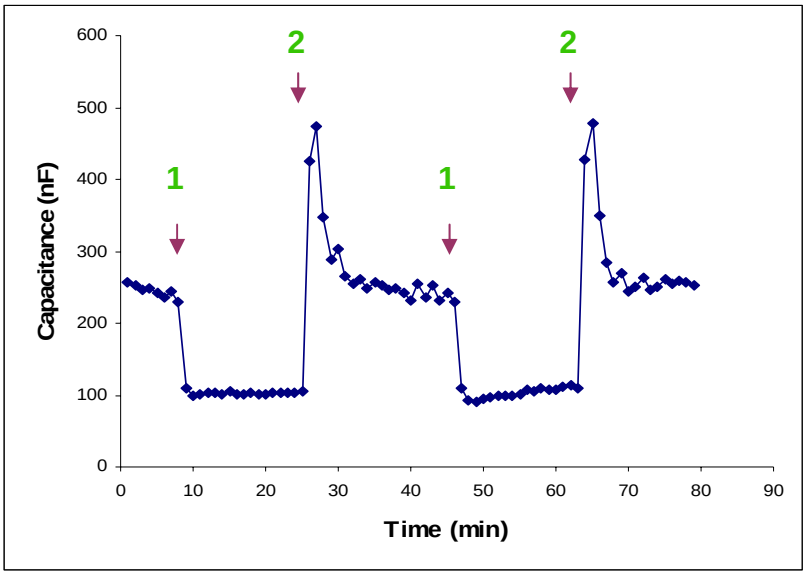

Figure 3.20. Regeneration graph for the GST-$(His)_6$ electrode under O.1 M Tris-tricine buffer pH 8.6, 0.25 ml/min, injection of 250 µl 100 Cd^{+2} standard solution 1)100 µM Cd^{+2} standard solution, 2) 20 mM EDTA regeneration buffer injections.

In Figure 3.21, the calibration curve of GST-$(His)_6$ electrode was given by using Cd^{+2} standard solution. 100 µM Cd^{+2} concentration was used in pH optimization measurements.

Effect of pH on the GST-$(His)_6$ electrode was measured by changing the pH of 0.1 M Tris-tricine buffer between 8.1 and 8.9 under 0.1 M Tris-tricine buffer, at a flow rate of 0.25 ml/min, injection of 250 µl, 100 µM Cd^{+2} standard solution.

It was found that the response increased from pH 8.1 through pH 8.7, then decreased until pH 8.9. Figure 3.22 shows the effect of pH on the heavy metal ion detection (100 µM Cd^{+2}) by GST-$(His)_6$ electrode.

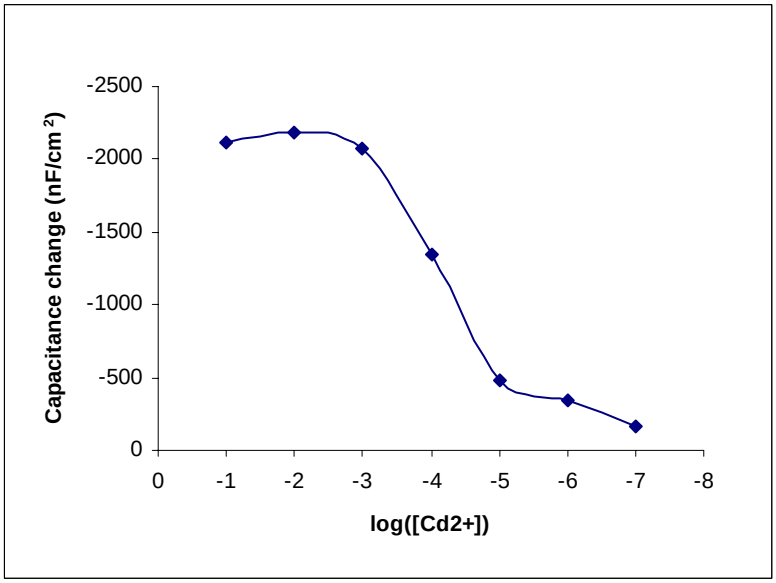

Figure 3.21. Calibration curve under 0.1 M Tris-tricine buffer pH 8.3, 0.25 ml/min, injection of 250 µL Cd^{+2} standard solutions.

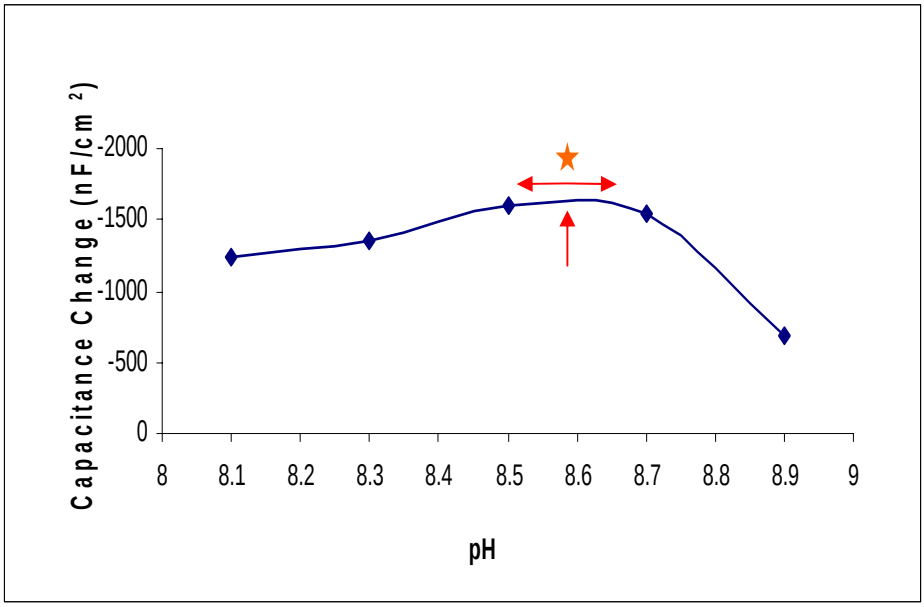

Figure 3.22. Capacitance changes of GST-$(His)_6$ electrode at pH 8.1-8.9 under 0.1 M Tris-tricine buffer, 0.25 ml/min, injection of 250 µl 100 µM Cd^{+2} standard solutions.

Storage stability of the GST-$(His)_6$ electrode was studied injection of 100 µM Cd^{2+} after regeneration with 20 mM EDTA, 0.1 M Tris-tricine buffer pH 8.6, 0.25 ml/min. The biosensor was stored overnight after sample injection at 4^oC in 0.1 mM Tris-tricine buffer, pH 8.6, between measurements, and it was regenerated by injecting 20 mM EDTA just before a new measurement. Figure 3.23 shows the storage stability of the GST-$(His)_6$ electrode. The sensor was stable for 14 days.

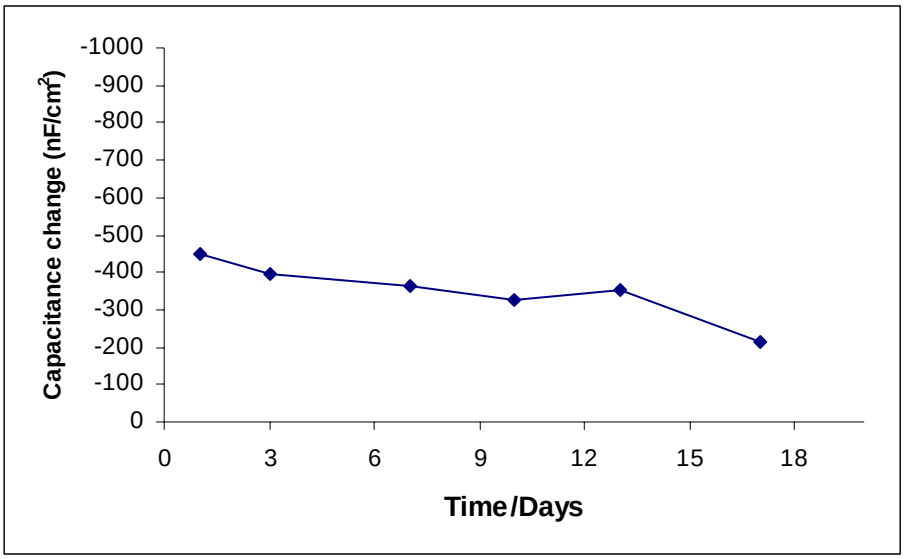

Figure 3.23. Storage stability of the GST-$(His)_6$ electrode. Injection of 100 µM Cd^{2+} after regeneration with 20 mM EDTA, O.1 M Tris-tricine buffer pH 8.6, 0.25 ml/min.

Figure 3.24 shows the reproducibility of the GST-$(His)_6$ electrode, prepared and stored under the same conditions: injection of 250 µl Cd^{2+} after regeneration with 20 mM EDTA, 0.1 M Tris-tricine buffer pH 8.6, 0.25 ml/min. Electrodes were stored after sample injection at 4^oC in 0.1 mM Tris-tricine buffer, pH 8.6, between measurements, and it was regenerated by injecting 20 mM EDTA just before a new measurement.

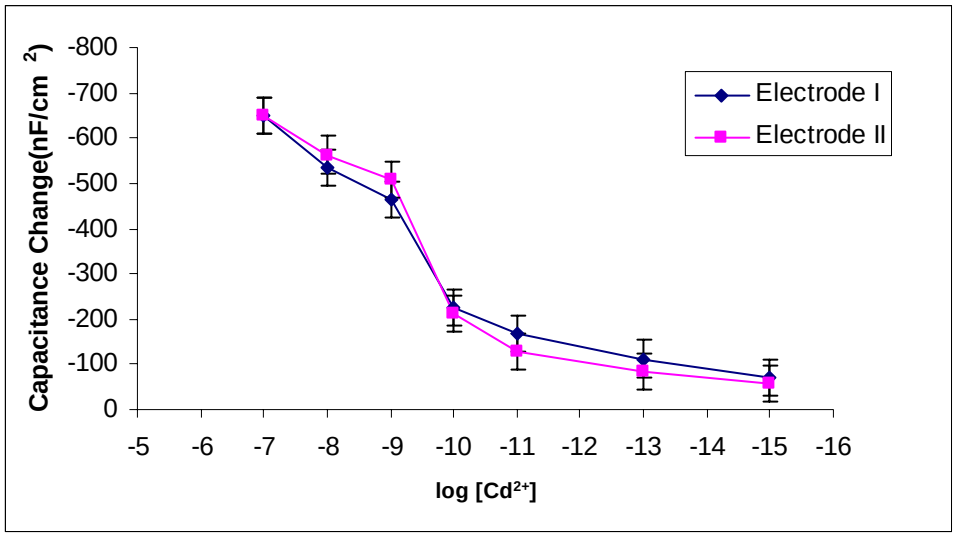

Figure 3.24. Calibration curves for Cd^{+2} recorded with two different biosensors prepared at different times under the same conditions reproducibility.

Figure 3.25 and 3.26 show the response of the GST-$(His)_6$ electrode under 0.1 M Tris-tricine buffer, pH 8.6, 0.25 mL/min flowrate, injection of 250 µL standard solutions to Cd^{+2}, Zn^{+2}, Cu^{+2} and Hg^{+2} for Figure 3.25, across the 10 mM - 1 fM and for Figure 3.26, across the 1nM - 1 fM concentration ranges tested.

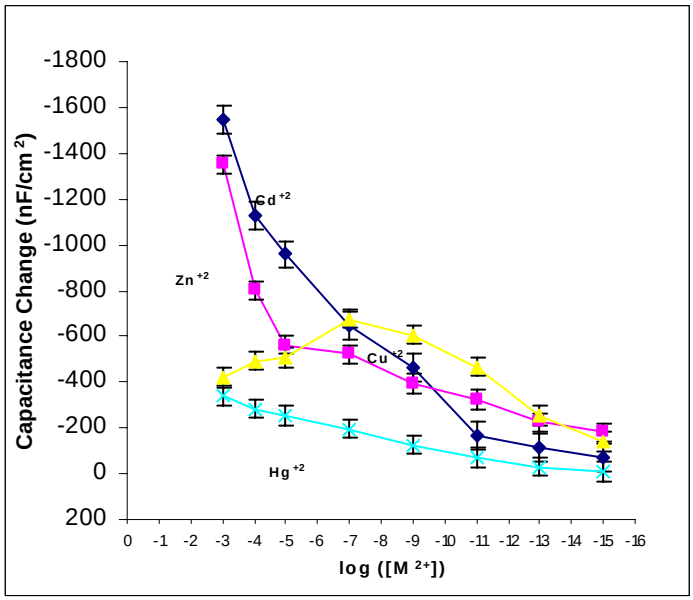

Figure 3.25. Calibration curves obtained for Cd^{+2}, Zn^{+2}, Cu^{+2} and Hg^{+2}, with the GST-$(His)_6$ electrode under 0.1 M Tris-tricine buffer, pH 8.6, 0.25 mL/min flowrate, injection of 250 µL standard solutions.

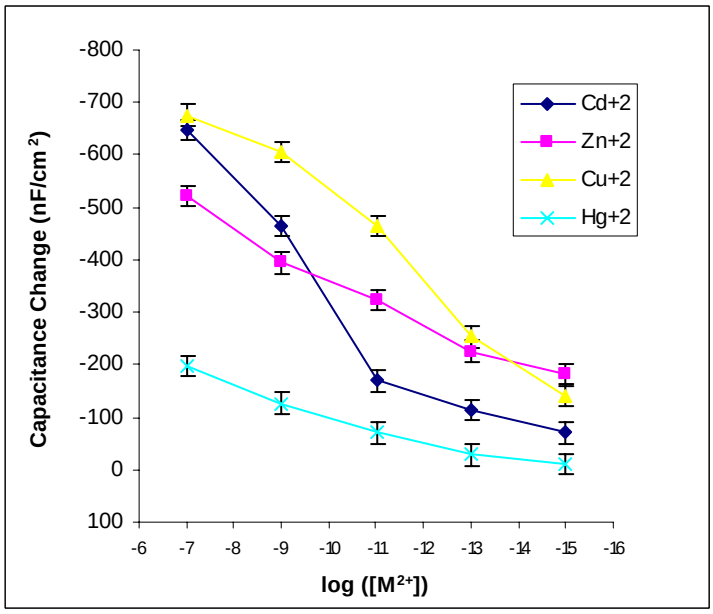

Figure 3.26. Calibration curves obtained for Cd^{+2}, Zn^{+2}, Cu^{+2} and Hg^{+2}, with the GST-$(His)_6$ electrode at low concentrations of heavy metals under 0.1 M Tris-tricine buffer, pH 8.6, 0.25 mL/min flowrate, injection of 250 µL standard solutions.

Figure 3.27 shows the control experiments. Measurements were done by Porcine Pancreatic Elastase (PPE): MW 25900 Da (Serva) and GST-$(His)_6$: MW 26500 Da under 0.1 M Tris-tricine buffer, pH 8.6, 0.25 mL/min flowrate, injection of 250 µL to Cd^{+2} and Zn^{+2} standard solutions. The comparison between two electrodes prepared with different type of proteins as recognition element shows the usable signals of GST-$(His)_6$ electrode for the detection heavy metal ions.

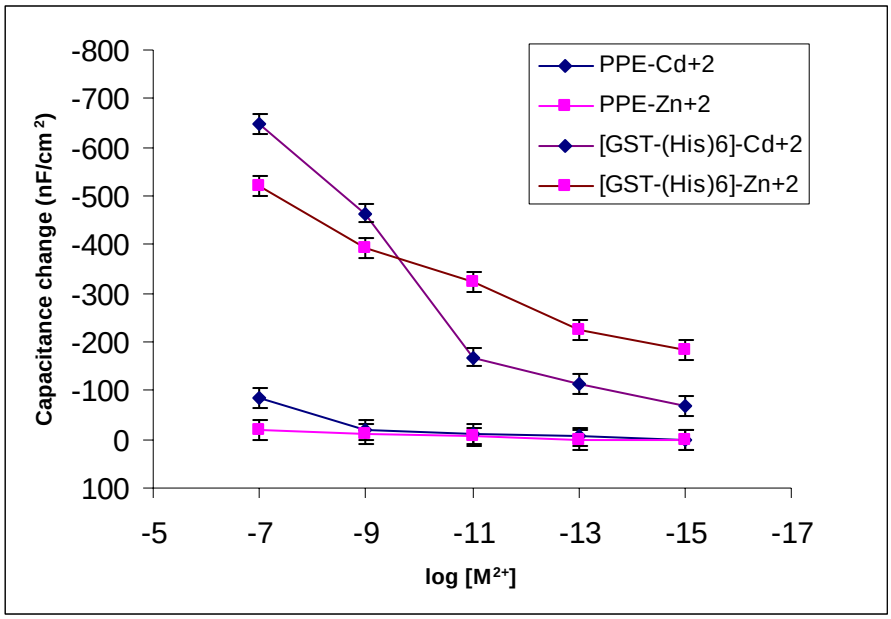

Figure 3.27. Control experiment graph. Measurements were done by Porcine Pancreatic Elastase (PPE): MW 25900 Da (Serva) and GST-$(His)_6$: MW 26500 Da under 0.1 M Tris-tricine buffer, pH 8.6, 0.25 mL/min flowrate, injection of 250 µL to Cd^{+2} and Zn^{+2} standard solutions.

CHAPTER IV

DISCUSSION

Biosensors are first mentioned as such in the literature in 1977 (Cammann and Fresenius, 1977). Before that, devices that contained a biological sensing element are simply referred to as electrodes with a description of the kind of sensing component, e.g. enzyme electrode. Today, according to the International Union of Pure and Applied Chemistry (IUPAC), an electrochemical biosensor is defined as a self-contained integrated device, which is capable of providing specific quantitative or semi-quantitative analytical information using a biological recognition element, which is retained in direct spatial contact with an electrochemical transduction element (Thevenot *et al*., 2001).

The diversity of the molecular recognition systems and of the electrochemical transducers incorporated in each biosensor is enormous. Since the development of the enzyme-based sensor for glucose, first described by Clark and Lyons in 1962, in which glucose was entrapped between two membranes, an impressive amount of literature on methods of immobilization and related biosensor development has appeared. Biological recognition elements, i.e. enzymes, antibodies, cells or tissues with high biological activity, are immobilized on the transducer (electrode) surface by using different procedures (O'Connell and Guilbalt, 2001).

Several different configurations on different types of biosensors have been described in the past for heavy metal detection. Sensors based on proteins (GST-SmtA, MerR, Mer P and EC20) (Bontidean *et al.*, 1998, 2003, Mortari *et al*., 2004) with distinct binding sites for heavy metal ions are developed. A capacitive signal transducer is used to measure the conformational change following binding of heavy metal ion to the Cys amino acids of the proteins. In these studies, the proteins are overexpressed in *Escherichia coli,* purified, and immobilized in different ways to a self-assembled thiol layer on a gold electrode placed as the working electrode in a potentiostatic arrangement in a flow analysis system.

Whole cell biosensors, based on bacteria, yeasts, fungi, lichens, mosses, and water plants as the recognition element (Corbisier *et al*., 1999), multienzyme electrochemical sensor arrays (Kukla *et al*., 1999, Starodub *et al*., 1999), microfabricated electrochemical sensors (Palchetti *et al*., 2001), fast amperometric FIA procedures (Compagnone *et al*., 2001) are used for heavy metal detection. Nevertheless, these biosensors could hardly attain a limit of detection in pM range. Design and development of new sensor types using specific proteins as the biorecognition elements to meet the high selectivity and sensitivity requirements is desirable for environmental protection.

Proteins can be very effective and often specific recognition molecules for a variety of metal ions. They contain a great number of potential donor atoms through the peptide backbone and amino acid side chains. The complexes formed exist in a variety of conformations that are sensitive to the pH environment of the complex (Gooding *et al.*, 2001). Conformational consequences of metal ion binding to proteins also have a critical impact on the peptide folding processes. Protein folding, and in particular hydrophobic effects, although receiving much attention, are only partly understood. Detailed studies on the relations between the peptide sequence, complex structure and thermodynamical stability are instrumental for the understanding of biological functions of peptides as well as the impact of metal ions on protein folding and conformation (Kozlowsky *et al*., 1999). With at least 20 amino acid combinations available in a protein sequence,

some with coordinating side chains, in any particular order and length, the number of sequences that can be synthesized using simple amino acids is practically infinite. Some of the amino acids have a strong binding capacity for heavy metals such as Cys (Bontidean, et al., 1998), Gly and His (Gooding *et al.*, 2001). The histidine residue possesses a very efficient nitrogen donor in its side chain imidazole ring. The cooperativity of all three donor groups of this amino acid in metal binding is made possible by the formation of two fused chelate rings (Gooding *et al.*, 2001). In a single amino acid, Gly, with a non-coordinating side chain, there are two donor atoms that complex the metal, the terminal amine and carbonyl oxygen or amide nitrogen. A study of Cu(II) complexation by Gly–Gly–Gly–His, tetra-peptide, shows a strong complex formation with heavy metals (Gooding *et al.*, 2001). This peptide sequence is also found in the original amino acid sequence of *Schistosomal* glutathione S-transferase.

Glutathione-S-transferases (GSTs) (E.C.2.5.1.18) are a group of multifunctional proteins involved in the detoxification of a broad spectrum of xenobiotics (Jackoby, 1978). The conjugation of toxic electrophiles with GSH not only decreases their ability to modify macromolecules but allows their elimination from the cell via the glutathione-S-conjugate efflux pumps (Ishikawa, 1988). Besides their catalytic functions, GSTs act as ligand binding proteins, thus lowering the intracellular concentration of a wide spectrum of hydrophobic non-substrate chemicals such as heme, billirubin and steroids (Mannervik and Danielson, 1988, Coles and Ketterer, 1990).

In this study, a protein-based biosensor was developed by expressing a C-terminally polyhistidine-tagged protein of *S. japonicum* GST (GST-$(His)_6$**)** for detection of heavy metal ions. The GST-$(His)_6$ biosensor were prepared by immobilizing the GST-$(His)_6$ on the thioctic acid self-assembled gold electrodes by coupling with 1-(3-dimethylaminopropyl)-3-ethyl-carbodiimide hydrochloride (EDC). After immobilization of the recombinant protein, the electrode was treated with 1-dodecanthiol to block any uncovered spots of the sensor surface. Cyclic

voltammetric measurements, which were performed in $K_3[Fe(CN)_6]$, shows that the electrode surface was totally blocked by treatments.

The biosensor was inserted as the working electrode in the constructed four-electrode flow cell. The conformational change resulting from the binding of the metal ion to the recombinant protein which caused in the capacitance proportional to the concentration of the metal ions was determined. Although biosensor response is an important parameter to indicate the signal and facilitate biosensor optimization in a given matrix, other biosensor specific, performance criteria are necessary to fully characterize the biosensor. Standard protocols for evaluation of performance criteria were defined in accordance with standard IUPAC protocols (Inczedy *et al*., 1998). The sensor calibration is generally performed by adding standard solutions of the analyte and by plotting steady-state responses corrected for a background versus the analyte concentration. The heavy metal salts $CuCl_2.2H_2O$, $ZnCl_2$, Hg Cl_2, and $Cd(NO_3)_2.4H_2O$ were used as standards. The sensitivity and linear concentration range are determined by plotting the steady-state response versus the analyte concentration. The sensitivity, not to confuse with detection limits, is defined as the slope of the calibration curve (Inczedy *et al*., 1998). It was found that the biosensor was sensitive to $Cd^{+2}>Zn^{+2}>Cu^{+2}>Hg^{+2}$ metal ions at high concentrations and $Cu^{+2}>Zn^{+2}>Cd^{+2}>Hg^{+2}$ metal ions at low concentrations. The GST-$(His)_6$ biosensor had a large operational range between 1 fM and 10 mM.

The heavy metal detection with the capacitance based biosensors generally employs basic buffer systems such as borate buffer, pH 8.75. However, using borate buffer has a drawback of metal precipitation at higher metal ion concentrations. For this reason, different buffer systems at varying pH values have been examined and Tris-tricine buffer system at pH 8.6 was choosen to overcome precipitation problem and due to better regeneration of electrode.

The stability of a biosensor is determined by the storage (shelf) lifetime or operational (use) lifetime necessary for the sensitivity, within the linear concentration range, to decrease by a factor 10% or 50% (Inczedy *et al*., 1998). In

our study, the biosensor was stored with sample at 4^{o}C in 100 mM tris-tricine buffer, pH 8.6, between measurements, and it was regenerated by injecting 20 mM EDTA just before a new measurement. Storage stability was found as approximately 2 weeks considering the decrease of response at the same concentration of standard solution by 10 %.

The response time is the time necessary to reach 90% of the steady-state response after adding the analyte into the measurement cell (Inczedy *et al*., 1998). In our measurements, the response time of our biosensor was found as 2 to 3 min which is short enough for routine measurements in comparison to the others of the same generation.

The reliability of biosensors for given samples depends both on their selectivity and reproducibility. The term reproducibility is either defined as the drift in a series of results performed over a period of time by the same electrode, as for any other analytical devices, or by comparison of responses of different electrodes prepared under the same conditions at different times. The reproducibility of the electrode preparations was tested and a perfect reproducibility was found between the electrodes, prepared under the same conditions at different times. Also perfect reproducibility was achieved by the measurement of the standart solution over a period of time by the same electrode.

In Table 4.1, the biological activities of metal sensing capacitance biosensors which are prepared by immobilizing different proteins are compared. As evident in the table, GST-SmtA biosensor is best for Cu^{2+} and Hg^{2+}. Mer R biosensor is best for Hg^{2+}, and EC20 biosensor is best for Zn^{2+}. The biosensor GST-$(His)_6$ as recognition element is perfectly sensitive for Cu^{2+}>Zn^{2+}>Cd^{2+}>Hg^{2+} heavy metal ions and can be selective for Cu^{2+} heavy metal ion. The sensitivity range of the biosensor is for Cu^{2+}: 100 nM-1 fM; for Zn^{2+}: 10 µM-1 fM; for Cd^{2+}: 10 µM-1 fM; for Hg^{2+}:10 mM-1 fM. The decrease in the slope of the Cu^{2+} heavy metal ion calibration curve, at high concentrations of the standard Cu^{2+}, depends on the precipitation of Cu^{2+} ions with tricine, in the buffer system.

Table 4.1. Comparison of the biological activities of metal sensing capacitance biosensors prepared by four different protein electrodes for the detection of heavy metal ions

Protein	**Preferential Biological Activity**	**Tested Heavy Metal Ions at 10 pM (Capacitance changes/nFcm^{-2})**			
		Cu^{2+}	Cd^{2+}	Zn^{2+}	Hg^{2+}
GST-SmtA*	$Cu^{+2} \geq Hg^{+2} > Cd^{+2} > Zn^{+2}$	-165	-150	-120	-160
Mer R*	$Hg^{+2} > Cu^{+2} > Zn^{+2} \geq Cd^{+2}$	-50	-30	-35	-90
EC20**	$Zn^{+2} > Cu^{+2} > Hg^{+2} > Cd^{+2}$	-75	-25	-145	-55
GST-(His)$_6$	$Cu^{+2} > Zn^{+2} > Cd^{+2} > Hg^{+2}$	-460	-170	-320	-70

* The values for GST-SmtA and Mer R were taken from Bontidean *et al*., 2000.
** The values for EC20 were taken from Bontidean *et al*., 2002.

In literature, Choi and his co-workers have developed an optical biosensor to detect captan (non-systemic fungicides) by using human placental GST as a biorecognition element (Choi, *et al*., 2003a and 2003b).

CHAPTER V

CONCLUSIONS

In conclusion, a biosensor specific for heavy metal detection, based on recombinant protein GST-$(His)_6$ as biorecognition element is developed with high reproducibility of measurement stability of the electrode measurements in Tris-tricine buffer, at pH 8.6 as working buffer of the GST-$(His)_6$ biosensor.

The developed heavy metal biosensor shows differential sensitivity for heavy metal ions as 100 nM-1 fM for Cu^{2+}; 10 µM-1 fM for Zn^{2+}; 10 µM-1 fM for Cd^{2+}; 10 mM-1 fM for Hg^{2+}. The GST-(His)6 biosensor has a large operational range between 10 mM and 1 fM

The response time of the system is found as 2 to 3 min, short enough for routine measurements in comparison to the others of the same generation.

A perfect reproducibility is found between the electrodes, prepared under the same conditions at different times and the measurement of the standart solution over a period of time by the same electrode.

The storage conditions are found as to keep the prepared electrodes in tris-tricine buffer, pH 8.6 at $4^{o}C$, between the measurements and 20 mM EDTA injection is determined for the best regeneration just before a new measurement.

GST-$(His)_6$ as recognition element is perfectly sensitive for $Cu^{2+}>Zn^{2+}>Cd^{2+}>Hg^{2+}$ heavy metal ions .

Future work targets modifying and testing of optimal electrode designs for mixture of metal ions and enviromental water and soil samples obtained from pollutant industrialized areas.

The future development of the biosensor will be in the area of Interdigitated-Electrode Capacitor biosensors.

REFERENCES

1. Abu-Hijleh, A.A., 1993. "Characterization and partial purification of sheep kidney and liver cytosolic glutathione S-transferases: A comparative study", *M.Sc. Thesis in Biochemistry*, Middle East Technical University - Ankara.

2. Abu-Hijleh, A.A., 1999. "Purification, and kinetic and Immunologic characterization of theta class glutathione S-transferase GSTT1-1 from normal and cancerous human breast tissues", *Ph.D. Thesis in Biochemistry*, Middle East Technical University – Ankara.

3. Akram, M., Stuart, M.C., Wong, D.K.Y., 2004. “Direct application strategy to immobilize a thioctic acid self-assembled monolayer on a gold electrode.”, *Anal. Chim. Acta*., Vol. 504(2), pp. 243-251.

4. Allocati, N., 1999. "Functional analysis of the evolutionarily conserved proline 53 residue in proteus mirabilis Glutathione-S-transferase B1-1”, *FEBBS lett*. Vol. 445, pp.347-350.

5. Andersson, C., Mosialou, E., Weinander, R., Morgenstern, R., 1994. "Enzymology of Glutathione S-transferase", *Adv.Pharmacol*., Vol. 27, pp.19-35.

6. Andreescu, S., Magearu, V., Lougarre, A., Fournier, D., and Marty, J.L., 2001. “Immobilization of enzymes on screen-printed sensors via a histidine tail. Application to the detection of pesticides using modified cholinesterase.”, *Anal.Lett*., Vol. 34(4), pp. 529-540.

7. Armstrong, R.N., 1991. "Glutathione S-transferases: reaction mechanism, structure, and function", *Chem.Res.Toxicol*., Vol. 4, pp. 131-140.

8. Armstrong, R.N., 1997. "Structure, catalytic mechanism, and evolution of the Glutathione transferases ", *Chem.Res Toxicol*., Vol. 10, pp. 2-18.

9. Asaoka, K., Ito, H. and Takahashi, K., 1977. "Monkey glutathione S-aryltransferases", *J.Biochem.*, Vol. 82, pp. 973-981.

10. Askelof, P., Guthenberg, C., Jakobson, I., and Mannervik, B., 1975. "Purification and characterization of two glutathione S-aryltransferase activities from rat liver", *Biochem.J*., Vol. 147, pp. 513-522.

11. Bain, C.D. and Whitesides G.M., 1988. “Molecular-level Control over Surface Order in Self-Assembled Monolayer Films of Thiols on Gold”. *Science*, Vol. 40, pp. 62-63.

12. Bain, C.D., Troughton, E.B., Tao, Y.T., Evall, J., Whitesides G.M., Nuzzo, R.G., 1989. “Formation of monolayer films by the spontaneous assembly of organic thiols from solution onto gold.”, *J. Am. Chem.Soc*., Vol. 111(1), pp. 321-335.

13. Barbas, C. F, Rosenblum, J. S. and Lerner, R. A., 1993. “Direct selection of antibodies that coordinate metals from semisynthetic combinatorial libraries.”, *Proc. Natl. Acad*. Sci. USA, Vol. 90, pp. 6385-6389.

14. Berggren, C. and Johansson, G., 1997. “Capacitance measurements of antibody-antigen interactions in a flow system.”, *Anal. Chem,*. Vol. 69, pp. 3651-3657.

15. Berggren, C., Bjarnason, B., Johansson, G., 2001. ”Capacitive biosensors”, *Electroanal.*, Vol. 13(3), pp. 173-180.

16. Berggren, C., Bjarnason, B., Johansson, G., 2001. ”Instrumentation for direct capacitive biosensors.”, *Inst. Science & Tech*., Vol. 27(2), 131-140.

17. Bertilsson, L. and Liedberg, B., 1993. “Infrared Study of thiol monolayer assemblies on gold: preparation, characterization, and functionalization of mixed monolayers.”, *Langmuir*, Vol. 9(1), pp.141-149.

18. Board, P.G., 1997. "Zeta, A novel class of glutathione transferases in a range of species from plants to humans", *Biochem.J*., Vol. 238, pp. 929-935.

19. Board, P.G., Coggan, M., Chelvavayagam, G., Easteal, S., et al., 2000. "Identification, characterization, and crystal structure of the omega class glutathione transferases", *J.Biol.Chem*., Vol. 275, pp. 24798-24806.

20. Bontidean I., Berggren C., Johansson G., Csöregi E. et al., 1998. ”Detection of heavy metal ions at femtomolar levels using protein-based biosensors”, *Anal. Chem*., Vol. 70, pp. 4162-4169.

21. Bontidean, B., Lloyd J.R., Hobman J.L., Wilson J.R., Csoregi E., Mattiasson B., Brown N.L., 2000. “Bacterial metal-resistance proteins and their use in biosensors for the detection of bioavailable heavy metals.”, *Journal of Inorganic Biochemistry*., Vol.79, pp. 225–229.

22. Bontidean, B., 2002. “Design, Development and Applications of Highly Sensitive Protein-based Capacitive Biosensors”, *Doctoral Dissertation*, Lund University- Lund.

23. Bontidean, B., Ahlqvist, J., Mulchhandani, A., Chen, W., Bae, W., Mehra R.K., Mortari, A., Csoregi, E., 2003. “Novel synthetic phytochelatin-based capacitive biosensor for heavy metal ion detection”, *Biosensors and Bioelectronics.*, Vol. 18, pp. 547-553.

24. Bontidean I., Mortari, A., Leth S., Brown N.L., Karlson, U., Larsen, M.M., Vangronsveld J., Corbisier, P., Csoregi, E., 2004. “Biosensors for detection of mercury in contaminated soils”, *Environmental Pollution*, Vol. 131, pp. 255-262

25. Brown, N. L., 1994. “Genes and proteins for detecting heavy metals: from molecular biology to practical solutions?”, *Proceedings of the Second International Symposium on Environmental Biotechnology*. Inst. Chem. Engineers, London, pp 1-3.

26. Bryant, M. A., Crooks, R. M., 1993. "Determination of Surface pK_a Values of Surface-Confined Molecules Derivitized with pH-Sensitive Pendant Groups", *Langmuir*, Vol. 9, pp. 388.

27. Buetler, T.M., and Eaton, D.L., 1992. "Glutathione S-transferases: amino acid sequence comparison, classification and phylogenetic relationship", *Environ.Carcinogen.Exotoxicol Revs.*, Vol. C10, pp. 181-203

28. Caccuri, A.M., Giovanni, A., 1999. "Proton release on binding of glutathione to alpha Mu and Delta class glutathione transferases", *Biochem.*, Vol. 344, pp. 419-425.

29. Caccuri, A.M., Antonini, G., Board, P.G., Flanagan, J., Parker, M.W., Paolesse, R., Turella, P., Chelvanayagam, G., and Ricci, G., 2001. "Human Glutathione Transferase T2-2 Discloses Some Evolutionary Strategies for Optimization of the Catalytic Activity of Glutathione Transferases.", *J. Biol. Chem.*, Vol. 276, pp. 5432-5437.

30. Cai, J.Y., Henion, J., 1995. "Capillary electrophoresis-mass spectrometry", *J. Chromatogr. A.*, Vol. 703, pp. 667–92.

31. Cammann, K., Fresenius Z., 1977. *Anal. Chem.*, Vol. 287, p. 1.

32. Campanella, L., De Luca, S., Sammartino, M. P., and Tomassetti, M., 1999. "A new organic phase enzyme electrode for the analysis of organophosphorus pesticides and carbamates", *Anal. Chim. Acta.*, Vol. 385, pp. 59-71.

33. Carter, P., Bedouelle, H. and Winter, G., 1985. "Improved oligonucleotide site-directed mutagenesis using M13 vectors", *Nucleic Acids Research*, Vol. 13(12), pp. 4431- 4443.

34. Cass, E. G., Davis, G., Francis, G. D., Hill, H. A. O., et al., 1984. "Ferrocene mediated enzyme electrode for amperometric determination of glucose", *Anal. Chem.*, Vol. 56, page 657.

35. Chang, L.H., Chuang, L.F., Tasi, C.P., Tu, C.P.D., and Tam, M.F., 1990. "Characterization of glutathione S-transferases from day-old chick livers", *Biochem.*, Vol. 29, pp.744-750.

36. Chen, W.J., Graminski, G.F., and Armstrong, R.N., 1988. "Dissection of the catalytic mechanism of isoenzyme 4-4 of glutathione S-transferases with alternative substrates", *Biochemistry,* Vol. 27, pp. 647-654.

37. Chen, H., Luo S., Chen, K., Lii, C., 1999. "Affinity purification of Schistosoma japonicum glutathione-S-transferase and its site-directed mutants with glutathione affinity chromatography and immobilized metal affinity chromatography", *J. Chromatogr. A.* Vol. 852, pp. 151-159.

38. Chen, H. and Chen K., 2000. "Production and characterization of glutathione-S-transferase fused with a poly-histidine tag", *Enzyme and Microbial Technology,* Vol. 27, pp. 219–226.

39. Cheng, Q. and Brajter-Toth, A., 1996. "Permselectivity, sensitivity, and amperometric pH sensing at thioctic acid monolayer electrodes", *Anal. Chem.*, Vol. 68(23), pp. 4180-4185.

40. Chidsey, C. E. D., and Loiacono, D. N., 1990. "Chemical Functionality in Self-Assembled Monolayers: Structural and Electrochemical Properties", *Langmuir*, Vol. 6, pp. 682-691.

41. Choi, J., Kim, Y., Oh, B., Song, S., Lee, W., 2003a. "Optical biosensor for simultaneous detection of captan and organophosphorus compounds", *Biosensors and Bioelectronics*, Vol. 18, pp. 591-597.

42. Choi, J., Kim, Y., Song, S., Lee, I., Lee, W., 2003b. "Optical biosensor consisting of glutathione-S-transferase for detection of captan", *Biosensors and Bioelectronics,* Vol. 18, pp. 1461-1466.

43. Clark, A.G., Smith, J.N., and Speir, T.W., 1973. "Cross specificity in some vertebrate and insect glutathione transferases with methylparathion (dimethyl p-nitro-phenyl phosphorothionate), 1-chloro-2,4-dinitro-benzene and S-crotonyl-N-acetylcysteamine as substrates", *Biochem.J.*, Vol. 135, pp. 385-392.

44. Clark, A.G., and Dauterman, W.C., 1982. "The characterization by affinity chromatography of glutathione S-transferases from different strains of housefly", *Pestic.Biochem.Physiol*., Vol. 17, pp. 307-314.

45. Clegg, R.S. and Hutchhison, J.E., 1996. “Hydrogen-bonding, self-assembled monolayers: ordered molecular films for study of through-peptide electron transfer”, *Langmuir*, Vol. 12(22), pp. 5239-5243.

46. Clemmitt, R. H. and Chase, H. A., 2000. “Facilitated downstream processing of a histidine-tagged protein from clarified E.coli homogenates using immobilized metal affinity expanded-bed adsorption”, *Biotech. Bioeng*., Vol. 67, pp. 206-216.

47. Coles, B., Ketterrer, B., 1990. "The role of glutathione and glutathione transferases in chemical carcinogenesis”, *CRC Crft. Rev. Biochem J.*, Vol.25, pp. 47-70.

48. Compagnone D., Lupu A. S., Ciucu A., Magearu V., Cremisini C., and Palleschi G., 2001. “Fast amperometric procedure for heavy metal detection using enzyme inhibition”, *Anal.Lett.*, Vol. 34(1), pp. 17-27.

49. Corbieser P., Van der Lelie D., Borremans B., Provoost A., Lorenzo V., Brown N.L., Brown N.L. and et al., 1999. “Whole cell- and protein-based biosensors for the detection of bioavailable heavy metals in environmental substance”, *Anal. Chim. Acta*., Vol. 387, pp. 235-244.

50. Crowe J., Masone B. S. and Ribbe J., 1996. “One-step purification of recombinant proteins with the 6xHis tag and Ni-NTA resin.” In: Harwood A. J.

(Ed). Basic DNA and RNA Protocols. London, UK: Humana Press Inc., pp. 491-510.

51. Daniel, V., 1993. "Glutathione S-transferases; Gene structure and Regulation of Expression", *Crit. Rev. Biochem and Mol. Biol*., Vol. 3, pp. 173-207.

52. Di Ilio, C., Polidoro, G., Arduini, A., and Federici, G., 1982. "Glutathione S-transferase activity from guinea pig brain- A comparison with hepatic multiple forms", *Gen. Pharmacol*., Vol. 13, pp. 485-490.

53. Dieckman, L., Gu, M., Stols, L., Donnelly, M. I. and Collart, F. R., 2002. "High Throughput Methods for Gene Cloning and Expression", *Protein Expression and Purification*, Vol. 25, pp. 1–7.

54. Dijksma, M., Kamp, B., Hoogvliet, J.C., van Bennekom, W.P., 2000. "Formation and electrochemical characterization of self-assembled monolayers of thioctic acid on polycrystalline gold electrodes in phosphate buffer pH 7.4", *Langmuir,* Vol. 16(8), pp. 3852-3857.

55. Dirr, H.W., Reinemer, P., 1994. "X-ray crystal structures of cytosolic glutathione S-transferases. Implications for protein architecture, substrate recognition and catalytic function", *Biochem.J*., Vol. 220, pp. 645-661.

56. Dubois, L.H. and Nuzzo, R.G., 1992. "Synthesis, structure, and properties of model organic surfaces", *Annual Review of Physical Chemistry*, Vol. 43, pp. 437-63.

57. Eaton, D.L., Bammler, T.K., 1999. "Concise review of the glutathione S-transferases and their significance to toxicology", *Toxicol.Sci*., Vol. 49, pp. 156-164.

58. Eggins B. R., 1996. "Biosensors an Introduction." New York, NY, USA: Jon Wiley and Sons, pp. 51-85

59. Edwards, R., Dixon, P.D., Walbot, V., 2000. "Plant glutathione s-transferases: Enzymes with multiple functions in sickness and health", *Trends in plant sci.,* Vol. 5, pp. 193-198.

60. Finklea, H.O. and Hanshew, D.D., 1992. “Electron-transfer kinetics in organized thiol monolayers with attached pentaammine(pyridine)ruthenium redox centers”, *J. Am. Chem. Soc*., Vol. 114(9), pp. 3173-3181.

61. Fishman, H.A., Greenwald, D.R., and Zare, R.N., 1998. “Biosensors in Chemical Separations”, *Annu. Rev. Biophys. Biomol. Struct.,* Vol. 27, pp. 165-198.

62. Flatgaard, T.E., Bauer, K.E., Kauvar, M.L., 1993. "Isozyme specificity of novel glutathione s-transferase inhibitors”, *Cancer Chemotherapy and Pharmacol.*, Vol. 33, pp.63-70.

63. Foureman, G.L., and Bend, J.R., 1984. "The hepatic glutathione transferases of the male little skate, Raja-Erinacea", *Chem.Biol.Interact*., Vol. 49, pp. 89-103.

64. Frangioni, J. V. and Neel, B. G., 1993. “Solubilization and purification of Enzymatically active Glutathione-S-transferase (pGEX) fusion proteins”, *Anal. Biochem.*, Vol. 210, pp. 179-187.

65. Geiger, O., 1997. “Biosensors: Principles and Practice.” In: Telefoncu A. (Ed) Enzimoloji. Kuşadası, Türkiye, pp. 400-423.

66. Gooding, J. J., Praig, V. G. and Hall E. A. H., 1998. “Platinum-Catalyzed Enzyme Electrodes Immobilized on Gold Using Self-Assembled Layers”, *Anal. Chem*., Vol. 70, pp. 2396-2402.

67. Gooding, J.J. and Hibbert, D. B., 1999. “The application of alkanethiol self assembled monolayers to enzyme electrodes”, *Trends in Analytical Chemistry,* Vol. 18(8), pp. 525-533.

68. Gooding, J.J. and Hibbert, D. B. and Yang, W., 2001. “Electrochemical Metal Ion Sensors Exploiting Amino Acids and Peptides as Recognition Elements”, *Sensors*, Vol. 1, pp. 75-90.

69. Graminski, G.F., Kubo, Y., and Armstrong, R.N., 1989. "Spectroscopic and kinetic evidence for the thiolate anion of glutathione at the active site of glutathione S-transferase", *Biochemistry*, Vol. 28, pp. 3562-3568.

70. Guiducci, C., Stagni, C., Zuccheri, G., Bogliolo, A., Benini, L., Samori, B., Ricco, B., 2002. “A Biosensor for Direct Detection of DNA Sequences Based on Capacitance Measurements”, *ESSDERC*, pp. 479-482.

71. Habig, W.H., Pabst, M.J., and Jakoby, W.B., 1974. "Glutathione S-transferases. The first enzymatic step in mercapturic acid formation", *J.Biol.Chem.*, Vol. 249(20), pp. 7130-7139.

72. Hales, B.F., Jaeger, V., and Neims, A.H., 1978. "Isoelectric focusing of glutathione S-transferases from rat liver and kidney", *Biochem.J.*, Vol. 175, pp. 937-943.

73. Häring, D., and Schreier, P., 1999. “Cross-linked enzyme crystals”, *Current Opinion in Chemical Biology*, Vol. 3, pp. 35–38

74. Hayes, J.D., and Chalmers, J., 1983. "Bile acid inhibition of basic and neutral glutathione S-transferases in rat liver", *Biochem.J.*, Vol. 215, pp. 581-588.

75. Hayes, J.D., and Pulford, D.J., 1995. "The Glutathione S-transferase supergene family: Regulation of GST and the contribution of the isoenzymes to cancer chemoprotection and drug resistance", *CRC Crit. Rev. Biochem. Mol. Biol.*, Vol. 30(6), pp. 445-600.

76. Hayes, J.D., and McLellan, L.I., 1999. "Glutathione and glutathione dependent enzymes represent a co-coordinately regulated defense against oxidative stress", *Free Radical Res.*, Vol. 31, pp. 273-300.

77. Hebert, H., Schmidt-Krey, I., Morgenstern, R., 1995. "The protein structure of glutathione transferase ", *EMBO J* , Vol. 14, pp. 3864-3869.

78. Hjelmeland, L.M., Nebert, D.W., and Chrambach, A., 1979. "Electrofocusing of integral membrane proteins in mixtures of zwitterionic and nonionic detergents", *Anal.Biochem*., Vol.95, pp.201-208.

79. Huskey, S.E., Huskey, W.P., and Lu, A.Y.H., 1991. "Contributions of thiolate “desolvation” to catalysis by glutathione S-transferase isoenzymes 1-1 and 2-2: evidence from kinetic solvent isotope effects", *J.Am.Chem.Soc*., Vol. 113, pp. 2283-2290.

80. Hussey, A.J. and Hayes, J.D., 1992. "Characterization of a human class theta glutathione S-transferase with activity towards 1-menaphthyl sulphate", *Biochem. J*., Vol. 286, pp. 929-935.

81. Igarashi, T., Tomihari, N., Ohmori, S., Ueno, K., Kitagawa, H., and Satoh, T., 1986. "Comparison of glutathione S-transferases in mouse, guinea pig, rabbit and hamster liver cytosol to those in rat liver", *Biochem. Internat*., Vol. 13(4), pp. 641-648.

82. Inczedy, J., Lengyel.T., Ure,A.M. (eds), 1998. IUPAC Compendium of Analytical Nomenclature, 3rd ed. Blackwell Science, Oxford.

83. Irwin, C., O'Brien, J.K., Chu, P., Townsend-Parchman, J.K., O'Hara, P., and Hunter, F.E., 1980. "Glutathione peroxidase-II of guinea pig liver cytosol-Relationship to glutathione S-transferases", *Arch.Biochem.Biophys*., Vol. 205, pp. 122-131.

84. Ishikawa, T., 1989. “ATP/Mg2+-dependent cardiac transport system for glutathione S-conjugates, A study using rat heart sarcolemma vesicles”, *J.Biol.Chem*., 264: pp.17343-17348.

85. İşgör, B., 2004. ” Isolation and Immunological Characterization of Theta Class Glutathione -S-transferase GSTT2-2 from Bovine Liver”. *Ph.D. Thesis in Biochemistry*, Middle East Technical University – Ankara.

86. Jakoby, W.B., 1978. "The glutathione S-transferases: a group of multifunctional detoxification proteins", *Adv. Enzymol*., Vol. 46, pp. 383-414.

87. Jemth, P., Mannervik, B.,1999. "Fast product formation and slow product release are important features in a Hysteretic Reaction mechanism of glutathione Transferase T2-2", *Biochem.*, Vol. 38 , pp. 9982-9991.

88. Jemth, P., Steinberg, G., 1996. "Heterologous expression, purification and characterization of rat class theta glutathione transferase T2-2", *Biochem.J*., Vol. 316 , pp. 131-136.

89. Ji, X., Zhang, P., Armstrong, R.N., and Gilliland, G.L., 1992. "The three-dimensional structure of a glutathione S-transferase from the Mu gene class. Structural analysis of the binary complex of isoenzyme 3-3 and glutathione at 2.2 A resolution", *Biochemistry*, Vol. 31, pp. 10169-10184.

90. Ji, X.H., von Rosenvinge, E.C., Johnson, W.W, Tomarev, S.I., Piatigorsky, J., Armstrong, R.N., and Gilliland, G.L., 1995. "Three-dimensional structure, catalytic properties and evolution of a sigma class glutathione transferase from squid, a progenitor of the lens S-crystallins of cephalopods", *Biochem.* Vol. 34, pp. 5317-5328.

91. Kamisaka, K., Habig, W.H., Ketley, J.N., Arias, M., and Jakoby, W.B., 1975. "Multiple forms of human glutathione S-transferase and their affinity for bilirubin", *Eur .J. Biochem*., Vol. 60, pp. 153-161.

92. Katti, S. K., LeMaster, D. M. and Eklund, H., 1990. "Crystal structure of thioredoxin from Escherichia coli at 1.68 AI resolution", *J. Mol. Biol*.,Vol.212, pp.167-184.

93. Kearns, P.R., Hall, A.G., 1998. "Glutathione and the response of malignant cells to chemotherapy ", *DDT.*, Vol. 3, pp. 113-121.

94. Kennedy, R.T., Oates, M.D., Cooper, B.R., Nickerson, B., Jorgenson JW., 1989. “Microcolumn separations and the analysis of single cells”, *Science*, Vol. 246, pp. 57–63.

95. Klibanov, A.M., 1997. “Why are enzymes less active in organic solvents than in water?” *Trends Biotechnol*., Vol. 15(3), pp. 97-101.

96. Kolm, R.H., Sroga, G.E., and Mannervik, B., 1992. "Participation of the phenolic hydroxyl group of Tyr-8 in the catalytic mechanism of human glutathione transferase P1-1", *Biochem.J.*, Vol. 285, pp. 537-540.

97. Kozlowski, H., Bal, W., Dyba, M., Kowalik-Jankowska T., 1999. “Specific structure–stability relations in metallopeptides”, *Coordination Chemistry Reviews.*, Vol. 184, pp. 319–346.

98. Kress-Rogers, E., 1997. “Biosensors and electronic noses for practical applications.” *In Handbook of Biosensors and Electronic Noses: Medicine, Food, and the Environment*. Ed. E Kress-Rogers, pp. 3–39. Boca Raton: CRC

99. Kubo, I., Sode, K. and Karube, I., 1991. ”Whole organism based biosensors and microbiosensors.” *In Advances in Biosensors*. Ed. APF Turner, pp. 1–32. London: JAI

100. Kukla, A. L., Kanjk, N. I., Stradub, N. F., and Shirshov, Y. M., 1999. “Multienzyme electrochemical sensor array for determination of heavy metal ions”, *Sensors and Actuators B.*, Vol. 57, pp. 213-218.

101. Kulp, T.J., Camins, I., Angel, S.M., Munkholm, C., Walt, D.R., 1987. “Polymer immobilized enzyme optrodes for the detection of penicillin”, *Anal. Chem.* Vol. 59, pp. 2849-2853.

102. Laemmli, U.K., 1970. "Cleavage of structural proteins during the assembly of the head of bacteriophage T4", *Nature*, Vol. 227, pp. 680-685.

103. Landi, S., 2000. "Mammalian class theta GST & differential susceptibility to carcinogens; a review", *Mutation research*, Vol. 463, pp. 247-283

104. Lee, C.Y., Johnson, L., Cox, R.H., McKinney, J.D., and Lee, S.M., 1981. "Mouse liver glutathione S-transferases. Biochemical and immunological characterization", *J.Biol.Chem.*, Vol. 256, pp. 8110-8116.

105. Lee, T.R., Laibinis, P.E., Folkers, J.P., and Whitesides, G.M., 1991. "Heterogeneous catalysis on platinum and selfassembled monolayers on metal and metal oxide surfaces (Note a)", *Pure & Appl. Chem.*, Vol. 63(69), pp. 821-828.

106. Lercel, M.J., Redinbo, G.F., Pardo, F.D., Rooks, M., Tiberio, R.C., Simpson, P., Sheen, C.W., Parikh A.N. and Allara, D.L., 1994. "Electron Beam Lithography with Monolayers of Alkylthiols and Alkylsiloxanes", *J. Vac. Sci. Technol.*, Vol. B12, pp. 3663-3667.

107. Lerner, RA, Benkovic, SJ, Schultz, PG., 1991. "At the crossroads of chemistry and immunology: catalytic antibodies", *Science*, Vol. 252(3), pp. 659-667.

108. Lesley, SA., 2001. "High throughput proteomics: protein expression and purification in the post-genomic world", *Prot. Expr. Purif.*, Vol. 22, pp. 159-164.

109. Lilius, G., Persson, M., Bulow, L. and Mosbach, K., 1991. "Metal affinity precipitation of proteins carrying genetically attached polyhistidine affinity tails", *European Journal of Biochemistry*, Vol. 198, pp. 499-504.

110. Lim, W.A. and Sauer, R.T., 1989. "Alternative Packing Arrangements in the Hydrophobic Core of l Repressor", *Nature*, Vol. 339, pp. 31-36.

111. Lin, D., Meyer, D.J., 1994. "Effects of human and rat glutathione-S transferases on the covalent DNA binding of the N-acetoxy derivatives of heterocyclic amine carcinogens in vitro a possible mechanism of organ specificity in their ", *Cancer Res.,* Vol. 54, pp. 4920-4926.

112. Lowry, O.H., Rosebrough, N.J., Farr, A.L., and Randal, R.J., 1951. "Protein measurement with the folin phenol reagent", *J.Biol.Chem.*, Vol. 248, pp. 265-275.

113. Lu, Q., Bauer, J. C. and Greener, A., 1997. "Using Schizosaccharomyces pompe as a host for expression and purification of eukaryotic proteins", *Gene,* Vol. 200, pp.135-144.

114. Mannervik, B., and Jensson, H., 1982. "Binary combination of four protein subunits with different catalytic specificities explain the relationship between six basic glutathione S-transferases in rat liver cytosol", *J. Biol. Chem.*, Vol. 257, pp. 9909-9912.

115. Mannervik, B., 1985(a). "The isoenzymes of glutathione transferase", *Adv. Enzymol. Rel. Areas Mol. Biol.*, Vol. 57, pp. 357-417.

116. Mannervik, B., Alin, P., Guthenberg, C., Jensson, H., Tahir, M.,K., Warholm, M., and Jornvall, H., 1985(b). "Identification of three classes of cytosolic glutathione transferase common to several mammalian species: correlation between structural data and enzymatic properties", *Proc. Natl. Acad. Sci. U.S.A.*, Vol. 82, pp. 7202-7206.

117. Mannervik, B., and Danielson, U.H., 1988. "Glutathione transferases-Structure and catalytic activity", *CRC Crit. Rev. Biochem. Mol. Biol.*, Vol. 23, pp. 283-337.

118. Mannervik, B., Awasthi, Y.C., Board, P.G., Hayes, J.D., Di Ilio, C., Ketterer, B., Listowsky, I., Morgenstern, R., Muramatsu, M., Pearson, W.R.,

Pickett, C.B., Sato, K., Widersten, M., and Wolf, C.R., 1992. "Nomenclature for human glutathione transferase", *Biochem. J*., Vol. 282, pp. 305-306.

119. Margolin, A.L., 1996. "Novel crystalline catalysts", *Trends Biotechnol*., Vol. 14, pp. 223-230.

120. Martin, J. L., 1995. "Thioredoxin - a fold for all reasons", *Structure*, Vol. 3, pp. 245-250.

121. McLellan, L.I., 1999. "Glutathione and glutathione dependent enzymes in cancer drug", *Drug Res. updates*, Vol. 2, pp. 153-164.

122. Meyer, D.J., Coles, B., Pemble, S.E., Gilmore, K.S., Fraser, G.M., and Ketterer, B., 1991. "Theta, a new class of glutathione transferases purified from rat and man", *Biochem. J*., Vol. 274, pp. 409-414.

123. Miller, C., Cuendet, P., Gratzel, M., 1991. "Adsorbed ω-hyroxythiol monolayers on gold electrodes: evidence for electron tunneling to redox species in solution", *J. Phys. Chem*., Vol. 95(2), pp. 877-886.

124. Montagne, M. and Marty, J., 1995. "Bi-enzyme amperometric D-lactate sensor using macromolecular NAD^+", *Anal. Chim. Acta*., Vol. 315, pp. 297-302.

125. Morgenstein, R., Guthenberg, C., and DePierre, J.C., 1982. "Microsomal glutathione S-transferase. Purification, initial characterization and demonstration that it is not identical to the cytosolic glutathione S-transferases A, B and C", *Eur. J. Biochem*., Vol. 128, pp. 243-248.

126. Mortari, A., 2004. "Protein-Based Capacitive Biosensor". *Licentiate Thesis*, Lund University- Lund, Sweden.

127. Mortari, A., Campo-Reales, N., Corda, G., Dorneanu, S.A., Brown, N.L., Csoregi, E., 2004. “Protein-based Capacitive Biosensors: a New Tool for Structure-Activity Related Studies”, *Anal. Chem*. Submitted.

128. Mozer, T.J., Tiemeier, D.C., and Jaworski, E.G., 1983. "Purification and characterization of corn glutathione S-transferase", *Biochemistry*, Vol. 22, pp. 1068-1072.

129. Myszka, D.G., 1997. “Kinetic analysis of macromolecular interactions using surface plasmon resonance biosensors”, *Current Opinion in Biotechnology*. Vol. 8(1), pp. 50-57. Review Article

130. Nelson, R. W., Jarvik, J. W., Taillon, B. E. and Tubbs K. A., 1999. “BIA/MS of Epitope-Tagged Peptides Directly from E. Coli Lysate: Multiplex Detection and Protein Identification at Low-Femtomole to Subfemtomole Levels”, *Anal. Chem*., Vol. 71, pp. 2858-286.

131. Niculescu, M., Nistor C., Frebort, I., Pec, P., Mattiasson, B., Csoregi, E., 2000. “Redox Hydrogel-Based Amperometric Bienzyme Electrodes for Fish Freshness Monitoring”, *Anal. Chem*., Vol. 72, pp. 1591-1597.

132. Niculescu, M., Erichsen, T., Sukharev, V., Kerenyi, Z., Csoregi, E., Schuhmann, W., 2002. “Quinohemoprotein alcohol dehydrogenase-based reagentless amperometric biosensor for ethanol monitoring during wine fermentation”, *Anal. Chim. Acta.*, Vol. 463, pp. 39-51.

133. Nimmo and Spalding, 1985. "The glutathione S-transferase activity in the kidney of rainbow trout (Salmo Gairdneri)", *Comp. Biochem. Physiol*., Vol. 82B(1), pp. 91-94.

134. Novagen, 2001. “pET System Manual”. USA. 9th Edition.

135. Nuzzo, R. G., Allara, D. L., 1983. “Adsorption of Bifunctional Organic Disulfides on Gold Surfaces”, *J. Am. Chem. Soc*., Vol. 105, pp. 4481-4483.

136. Nygren, P., Ståhl, S., and Uhlén, M., 1994. “Engineering proteins to facilitate bioprocessing”, *Trends in Biotechnology*, Vol. 12(5), pp. 184-188.

137. O’Connell, P. J. and Guilbalt, G. G., 2001. “Future trends in biosensor research”, *Anal. Lett*., Vol. 34(7), pp. 1063-1078.

138. Oshino, R., Kamei, K., Nishioka, M., and Shin, M., 1990. "Purification and characterization of glutathione S-transferases from guinea pig liver", *J. Biochem*., Vol. 107, pp. 105-110.

139. Pabst, M.J, Habig, W.H., and Jakoby, W.B., 1973. "Mercapturic acid formation: the several glutathione transferases of rat liver", *Biochem. Biophys. Res. Commun*., Vol. 52, pp. 1123-1128.

140. Palchetti, I., Marrazza, G., and Mascini, M., 2001. “New procedures to obtain electrochemical sensors for heavy metal detection” *Anal. Lett*., Vol. 34(6), pp. 813-824.

141. Panasyuk, T. L., Mirsky, V. M., Piletsky, S. A., and Wolfbeis, O., 1999. “Electropolymerized molecularly imprinted polymers as receptor layers in capacitive chemical sensors”, *Anal. Chem*., Vol. 71, pp. 4609-4613.

142. Pemble, S.E., and Taylor, J.B., 1992. "An evolutionary perspective on glutathione transferases inferred from class-Theta glutathione transferase cDNA sequences", *Biochem. J*., Vol. 287, pp. 957-963.

143. Pemble, S.E., Schroeder, K.R., Spencer, S.R., Meyer, D.J., Hallier, E.,Bolt, H.M., Ketterer, B., and Taylor, J.B., 1994. "Human glutathione S-transferase Theta (GSTT1): cDNA cloning and the characterization of a genetic polymorphism", *Biochem. J*., Vol. 300, pp. 271-276.

144. Pemble, S.E., Wordle, A.F., Taylor, J.B., 1996. "Glutathione S-transferase Kappa: characterization by the cloning of rat mitochondrial GST and identification of a human homologue ", *Biochem. J*., Vol. 319, pp. 349-754.

145. Persichetti, R.A., St. Clair, N.L., Griffith, J.P., Navia, M.A., Margolin, A.L., 1995. “Cross-Linked Enzyme Crystals (CLECs) of thermolysin in the synthesis of peptides”, *J. Am. Chem. Soc*., Vol. 117, pp. 2732-2737.

146. Pettytt, M., Tsibouklist, J., Davis, F., Hedges, P., Pettyt M.C. and Feast, W. J., 1992. “Pyroelectric Langmuir-Blodgett films prepared using preformed polymers”, *J. Phys. D: Appl. Phys*., Vol. 25, pp. 1032-1035.

147. Porter, M. D., Bright, T. B., Allara D. L. and Chidsey C. E. D., 1987. "Spontaneously Organized Molecular Assemblies. 4. Structural Characterization of n-Alkyl Thiol Monolayers on Gold by Optical Ellipsometry, Infrared Spectroscopy, and Electrochemistry", *J. Am. Chem. Soc*., Vol. 109, pp. 3559-3568.

148. Quinn, J., Patel, P., Fitzpatrick, B., Manning, B., Dillon, P., Daly, S., O’Kennedy, R., Alcocer, M., Lee, H., Morgan, M., Lang, K., 1999. “The use of regenerable, affinity ligand-based surfaces for immunosensor applications”. Biosensors & Bioelectronics, Vol. 14, pp. 587–595.

149. Quinn, J.G. and O’Kennedy, R., 2001. “Biosensor-Based Estimation of Kinetic and Equilibrium Constants”, *Anal. Biochem*., Vol. 290, pp. 36–46.

150. Reddy, C.C.,Burgess,J.R., et al., 1983. “Purification and characterization of the individual glutathione-s-transferases from sheep liver”, *Arch. of Biochem and Biophys*., Vol. 224, pp. 87-101.

151. Reinemer, P., Dirr, H.W., Ladenstein, R., Schaffer, J., Gallay, O., and Huber, R., 1991. "The three-dimensional structure of class π glutathione S-transferase in complex with glutathione sulfonate at 2.3 A resolution", *EMBO J.*, Vol. 10, pp. 1997-2005.

152. Reinemer, P., Prade, L. Holf, P. Neufiend, T., Huber, R., Zettl, R. Palme, K., Shell, J.,Koelln, I., Bartnnik, H. D. and Bieseler, B.,1996. “Three-

dimensional structure of GSTs from A. thaliana at 2.2 A° resolution", *J. Mol. Biol*., Vol. 255, pp. 289-305.

153. Robertson, E.F., Dannelly, H.K., Malloy, P.J., and Reevers, H.C., 1987. "Rapid isoelectric focusing in a vertical polyacrylamide minigel system", *Anal. Biochem.*, Vol. 167, pp. 290-294.

154. Roe, J.N., 1992. "Biosensor Development", *Pharmaceutical Research*, Vol. 9(7), pp. 835-844.

155. Ross, V.L., Board, P.G., and Webb, G.C., 1993. "Chromosomal mapping of the human mu class glutathione S-transferases to 1p13", *Genomics*, Vol. 18, pp. 87-91.

156. Rossjohn, J., McKinstry, W.J., Oakley, A.J., Verger, D., Flanagan, J., Chelvanayagam, G., Tan, K.L., Board, P.G., and Parker, M.W., 1998. "Human theta class glutathione transferase: the crystal structure reveals a sulfate-binding pocket within a buried active site", *Structure*, Vol. 6, pp. 309-322.

157. Rossjohn, J.,Feil, S.C., Wilce, M.CS, et.al., 1997. "Crystallization, structural determination and analysis of a novel parasitic vaccine candidate: Fasciola hepatica Glutathione-S-transferase", *J. Mol. Biol*., Vol. 273, pp. 857-872.

158. Rouimi, P., Anglade, P., Debrawuer, L. and Tulliez J., 1996. "Characterization of pig liver glutathione S-transferases using HPLC–electrospray-ionization mass spectrometry", *Biochem. J*., Vol. 317, pp. 879-884

159. Sagiv, J., 1980. "Organized monolayers by adsorption. 1. Formation and structure of oleophobic mixed monolayers on solid surfaces", *Journal of the American Chemical Society*, Vol. 102(1), pp. 92-98.

160. Sánchez, M. A., Jiménez, J., Vázquez, F., Vico, F., Artigas, A. C., Pérez, V. J., 2003. “Thermodynamics of glutathione binding to the tyrosine 7 to phenylalanine mutant of glutathione S-transferase from Schistosoma japonicum”, *International Journal of Biological Macromolecules*, Vol. 32, pp. 77–82.

161. Saneto, R.P., Awasthi, Y.C., and Srivastava, S.K., 1980. "Interrelationship between cationic and anionic forms of glutathione S-transferases of bovine ocular lens", *Biochem. J.*, Vol. 191, pp. 11-20.

162. Sassenfeld, H.M., 1990. “Engineering proteins for purification”, *Trends Biotechnol.*, Vol. 8, pp. 88–93.

163. Scheibler, L., Dumy, P., Starnot, D., Duschl, C., Voge, H. and Mutter, M., 1998. “Functionalization of Gold Surfaces via Topological Templates”, *Tetrahedron*, Vol. 54, pp. 3725-3734

164. Shea, T.C., et al.1990. "Glutathione transferase activity and isoenzyme composition in primary human breast cancer ", *Cancer Res.*, Vol. 50, pp. 6848-6853.

165. Sheehan, D., Meade, G., Foley, V.M and Dowd, C.A., 2001. “Structure, function and evolution of GSTs implications for classification of non-mammalian members of ancient enzyme superfamily”, *Biochem. J.*, Vol. 360, pp. 1-16.

166. Schmitke. J.L., Wescott, C.R., Klibanov, A.M., 1996. “The mechanistic dissection of the plunge in enzymatic activity upon transition from water to anhydrous solvents”, *J. Am. Chem. Soc.*, Vol. 118, pp. 3360-3365.

167. Simons, P.C., and Vander Jagt, P.L., 1977. "Purification of glutathione S-transferases from human liver by glutathione-affinity Chromatography", Anal. *Biochem.*, Vol. 82, pp. 334-341.

168. Smith, G.J., Ohl, V.S., and Litwack, G., 1980. "Purification and properties of hamster liver ligandings, Glutathione S-transferases", *Cancer Res*., Vol. 40, pp. 1787-1790.

169. Smith, D. B., Davern, K. M., Board, P. G., Tiu, W. U., Garcia, E. G. and. Mitchell, G. F., 1986. “Mr 26,000 antigen of Schistosoma japonicum recognized by resistant WEHI 129/J mice is a parasite glutathione S-transferase”, *Proc. Natl. Acad. Sci. USA*, Vol. 83, pp. 8703-8707.

170. Smith, D. B., Rubira, M. R., Simpson, R. J., Davern, K. M., Tiu, W. U., Board, P. G. and Mitchell, G. F., 1988. “Expression of an enzymatically active parasite molecule in Escherichia coli: Schistosoma japonicum glutathione S-transferase”, *Mol. Biochem. Parasitol*., Vol. 27, pp. 249-256.

171. Smith, R. K., Lewis, P. A. and Weiss P, S., 2004. “Patterning self-assembled monolayers”, *Progress in Surface Science*, Vol. 75, pp. 1–68.

172. Skoog, D.A., West, D.M., Holler, F.J., 1992. *Fundamentals of Analytical Chemistry*, p. 928. Fort Worth: Saunders.

173. Steinberg, S., Tor, Y., Shanzer, A., Rubinstein, I., 1995. “Ion-selective monolayer membranes based on self-assembling tetradentate ligand monolayers on gold electrodes: nature of the ionic selectivity”, *Thin Films*, Vol. 20, pp. 183-205.

174. Starodub, N.F., Kanjuk, N.I., Kukla A.L. and Shirshov, Yu. M., 1999. “Multi-enzymatic electrochemical sensor: field measurements and their optimization”, *Anal. Chim. Acta*., Vol. 385, pp. 461-466.

175. Sugiyama, Y., Yamada, T., and Kaplowitz, N., 1981. "Glutathione S-transferases in Elasmobranch liver- Molecular heterogeneity, catalytic and binding properties, and purification", *Biochem. J., Vol*. 199, pp.749-756.

176. Synder, L. and Champness, W., 1997. *Molecular Genetics of Bacteria*, Washington, DC, USA. ASM press, pp. 105-125.

177. Tahir, MK, Ozer, N, Mannervik, B., 1988. "Isoenzymes of glutathione transferase in rat small intestine", *Biochem. J.*, Vol. 253, pp. 759–764.

178. Tan, K.L., Webb, G.C., Baker, R.T., and Board, P.G., 1995. "Molecular cloning of a cDNA and chromosomal localization of a human theta-class glutathione S-transferase gene (GSTT2) to chromosome 22", *Genomics*, Vol. 25, pp. 381-387.

179. Telefoncu, A., 1999. *Biyosensörler*. Kuşadası, Türkiye, pp. 42-53.

180. Tew, K.D., 1994. "Glutathione-associated enzymes in anticancer drug resistance", *Cancer Research*, Vol. 54, pp. 4313-4320.

181. Thevenot, D. R., Toth K., Durst, R. A., and Wilson, G. S., 2001. "Electrochemical biosensors: Recommended definitions and classification", *Anal. Lett.*, Vol. 34(5), pp. 635-659.

182. Towbin, H., Staehelin, T., and Gordon, J., 1979. "Electrophoretic transfer of proteins from polyacrylamide gels to nitrocellulose sheets: Procedure and some applications", *Proc. Natl. Acad. Sci. U.S.A.*, Vol. 76, pp. 4350-4354.

183. Troughton, E.B., Bain, C.D., et al., 1988. "Monolayer films prepared by the spontaneous self-assembly of symmetrical and unsymmetrical dialkyl sulfides from solution onto gold substrates: structure, properties, and reactivity of constituent functional groups", *Langmiur*, Vol. 4, pp. 365-385.

184. Ulman, A., 1996. "Formation and structure of self-assembled monolayers", *Chem. Re.*, Vol. 96, pp. 1533-54.

185. Ünsal, I., and Öğüş, H., 1991. "Koyun karaciğeri glutatyon transferaz izozimlerinin saflaştırması", *Biyokimya Dergisi*, Vol. 16, pp. 27-42.

186. Vadgama, P. and Crump, P. W., 1992. “Biosensors: Recent Trends”, *Analyst*., Vol. 117, pp. 1657-1670. Review.Article.

187. Vo-Dinh, T., Alarie, J.P., Isola, N., Landis, D., Wintenberg, A.L., and Ericson, M.N., 1999. “DNA biochip using a phototransistor integrated circuit”, *Anal. Chem*., Vol. 71, pp. 358-363.

188. Walczak, M.M., Popenoe, D.D., Deinhammer, R.S., Lamp B.D., Chung, C., Porter M.D., 1991. “Reductive Desorption of Alkanethiolate Monolayers at Gold: A Measure of Surface Coverage”, *Langmuir*, Vol. 7, pp. 2687-2693.

189. Wang, J., 2000. “Chemically modified electrodes”, *Analytical Electrochemistry*. 2 nd Ed. Wiley and Sons, USA, pp. 118–120.

190. Walcerz I., Koncki R., Leszczynska E., Glap S., 1995. “Enzyme biosensors for urea determination based on an ionophore free pH membrane electrode”, *Anal. Chim. Acta*., Vol. 315, pp. 289-296.

191. Warburg, C., and Christian, W., 1941. *Biochem.Z.*, Vol. 310, pp. 402-408.

192. Ward, P.P., 1990. “Plasma Cleaning Techniques an Future Applications in Environmentally Concious Manufacturing”. Dept. 1812, Sandia National Laboratories Albuquerque, New Mexico.

193. Warholm, M., Guthenberg, C., Mannervik, B., and von Bahr, C., 1981. "Purification of a new glutathione S-transferase (transferase Mu) from human liver having high activity with benzo(a)pyrene-4,5-oxide", *Biochem. Biophys. Res. Commun*., Vol. 98, pp. 512-519.

194. Weber, K., Osborn M., 1969. "The reliability of molecular weight determinations by sodium dodecyl sulfate-polyacrylamide gel electrophoresis", *J. Biol. Chem*., Vol. 244, pp. 4406-4412.

195. Widersten, M., Kolm, R.H., Björnestedt, R., and Mannervik, B., 1992. "Contribution of five amino acid residues in the glutathione binding site to the

function of human glutathione transferase P1-1", *Biochem. J.*, Vol. 285, pp. 377-381.

196. Whittington, A. T., Vichai, V., Webb, G. C., Baker, R. T., Pearson, W. R., and Board, P. G.,1999. “Gene structure, expression, and chromosomal localization of murine theta class glutathione transferase mGSTT1-1”, *Biochem. J.*, Vol. 337, pp. 141-151.

197. Wilce, M.C.J., Board, P.G., Feil, S.C., and Parker, M.W., 1995. "Crystal structure of a theta-class glutathione transferase", *EMBO J.*, Vol. 14, pp. 2133-2143.

198. Wink, T., van Zuilen, S. J., Bult, A. and van Bennekom, W. P., 1997. ”Self-assembled Monolayers for Biosensors”, *Analyst*, Vol. 122, pp. 43R–50R.

199. Wise, G.E., and Lin, F., 1991. "Transfer of silver-stained proteins from polyacrylamide gels to polyvinylidene difluoride membranes", *J. Biochem. Biophys. Methods*, Vol. 22, pp. 223-231.

200. Wu, N., Peck, T.L., Webb, A.G., Magin, R.L., Sweedler, J.V., 1994. “H-1-NMR spectroscopy on the nanoliter scale for static and on-line measurements”, *Anal. Chem.*, Vol. 66, pp. 3849–57

201. Xiao, G., Liu, S., Ji, X., Johnson, W.W., Chen, J., Parsons, J.F., Stevens, W.W., Gilliland, G.L. and Armstrong, R.N., 1996. "First-Sphere and Second-Sphere Electrostatic Effects in the Active Site of a Class Mu Glutathione Transferase", *Biochemistry*, Vol. 35, pp. 4753-4765.

202. Yang, W., Gooding, J. J., Hibbert, D. B., 2001. “Characterization of gold electrodes modified with self-assembled monolayers of L-cysteine for the adsorptive stripping analysis of copper”, *Journal of Electroanalytical Chemistry*, Vol. 516, pp. 10–16.

203. Yeung, T.C., and Gidari, A.S., 1980. "Purification and properties of a chicken liver glutathione S-transferase", *Arch. Biochem. Biophys*., Vol. 205, pp. 404-411.

204. Zeigler, C. and Göpel, W., 1998. “Biosensor development”, *Current Opinion in Chemical Biology*, Vol. 2(1), pp. 585-591. Review Article.

205. Zhang S., Wright G. and Yang Y., 2000. “Materials and techniques for electrochemical biosensor design and construction”, *Biosensors and Bioelectronics*. Vol. 15, pp. 273-282.

206. Zhang, Y., Cho, C.-G.H. and Talalay, P., 1992. "Spectroscopic quantitation of organic isothiocyanates by cyclocondensation with vicinal dithiols”, *Anal. Biochem*, Vol. 205, pp. 100-107.

207. Zybin, A., Grunwald, C., Mirsky, V.M., Kuhlmann, J., Wolfbeis, O. S., and Niemax, K., 2005. “Double-Wavelength Technique for Surface Plasmon Resonance Measurements: Basic Concept and Applications for Single Sensors and Two-Dimensional Sensor Arrays”, *Anal. Chem*., Vol. 77, pp. 2393-2399.

APPENDIX A: Curriculum Vitae

PERSONAL INFORMATION

Surname, Name: Saatçi, Ebru
Nationality: Turkish (TC)
Date and Place of Birth: 12 December 1972, Erzurum
Marital Status: Single
Phone: +90 312 210 51 64
Fax: +90 312 210 12 89
email: ebru@metu.edu.tr

EDUCATION

Degree	Institution	Year of Graduation
MS	Erciyes University, Biochemistry	1997
BS	9 Eylül University, Medical Sciences	1994
High School	TED Kayseri College	1990

WORK EXPERIENCE

Year	Place	Enrollment
1999-Present	METU, Biology Department	Teaching Assistant
1996-1999	Erciyes University, Biology Department	Teaching Assistant

FOREIGN LANGUAGES

Advanced English, Fluent German

HOBBIES

Painting, basketbol, movies, music